From the Department of Clinical Science,
Intervention and Technology, Division of Radiology
Karolinska Institutet, Stockholm, Sweden

# PANCREATIC CANCER: PREVENTION THROUGH IMPROVED DIAGNOSTICS IN INDIVIDUALS AT RISK

Raffaella Pozzi Mucelli


Karolinska Institutet

Stockholm 2022

Published by Karolinska Institutet.
Printed by Universitetsservice US-AB, 2022

ISBN 978-91-8016-775-8
Cover illustration by Raffaella Pozzi Mucelli. Abstract flowers. Watercolour. Stockholm, 2022.

# Pancreatic cancer:
# Prevention through improved diagnostics in individuals at risk

THESIS FOR DOCTORAL DEGREE (Ph.D.)

By


## Raffaella Pozzi Mucelli


The thesis will be defended in public in lecture hall C1:87, Karolinska University Hospital, Huddinge, 16th December 2022 at 13:00.

*Principal Supervisor:*
Assoc. Prof. Nikolaos Kartalis
Karolinska Institutet
Department of Clinical Science, Intervention and Technology (CLINTEC)
Division of Radiology

*Co-supervisor(s):*
Prof. Marco del Chiaro
University of Colorado School of Medicine,
Department of Surgery
Division of Surgical Oncology

Prof. Caroline S. Verbeke
University of Oslo,
Department of Pathology

Prof. Lennart Blomqvist
Karolinska Institutet
Department of Molecular Medicine and Surgery
Division of Diagnostic Radiology

*Opponent:*
Prof. Miriam Klauß
Heidelberg University Hospital
Department of Diagnostic and Interventional Radiology
Division of Abdominal Radiology

*Examination Board:*
Assoc. Prof. Hanna Sartor
Malmö Lund University
Department of Translational Medicine
Division of Diagnostic Radiology

Prof. Paul Nikolaidis
Northwestern Memorial Hospital, Chicago
Department of Radiology

Prof. Bengt Isaksson
Uppsala University
Department of Surgical Sciences
Division of Upper Abdominal Surgery

*To Marco.*

*"A te che sei il mio grande amore*

*Ed il mio amore grande.*

*A te che hai preso la mia vita*

*E ne hai fatto molto di più".*

*(From A te. L. Cherubini, 2008)*

*To Chiara and Sofia. The loves of my life.*

“Keep Ithaka always in your mind.
Arriving there is what you are destined for.
But do not hurry the journey at all.
Better if it lasts for years,
so you are old by the time you reach the island,
wealthy with all you have gained on the way,
not expecting Ithaka to make you rich.
Ithaka gave you the marvelous journey.
Without her you would not have set out.
She has nothing left to give you now.

And if you find her poor, Ithaka won’t have fooled you.
Wise as you will have become, so full of experience,
you will have understood by then what these Ithakas mean.”

(From Ithaka, K.P. Kavafis)

# ABSTRACT

With the intent of timely detecting malignant precursors or pancreatic cancer (PC) in an early stage, current guidelines recommend surveillance for patients with pancreatic cystic neoplasms (PCNs), such as intraductal papillary mucinous neoplasms (IPMN), and individuals at risk (IAR) for familiar/hereditary pancreatic cancer (PC). This surveillance is mainly performed with magnetic resonance imaging (MRI). However, despite the associated examination time and costs, MRI is still suboptimal regarding its accuracy in predicting malignancy.

This thesis aims to contribute towards improved secondary prevention of PC through more efficient and accurate diagnostic methods in patients with IPMN and familiar/hereditary PC through (i) a shorter MRI protocol, (ii) new imaging features and radiomics models for the prediction of malignancy, (iii) a better understanding of the surveillance program for IAR.

In **Study I,** we compared a short (SP) and a comprehensive pancreatic MRI protocol (CP), with an acquisition time of approximately 8 and 35 minutes, respectively, in a cohort of 154 patients with PCNs. Our results showed that the SP provided equivalent clinical information in evaluating mural nodules, as well as cystic and main pancreatic duct diameters, compared to the more time-consuming and expensive CP in the surveillance of PCNs.

In **Study II**, we assessed whether two novel features, such as volumetry and elongation value (EV) and other routinely used resection criteria, could predict malignancy in a cohort of 106 patients operated for BD- and mixed-type IPMN. Cases with mass-forming PC were excluded as a possible cause of main pancreatic duct (MPD) dilatation. Our results showed that volumetry and EV were not predictive for malignancy. Only elevated serum levels of CA19-9, mural nodules and dilated MPD (in the absence of stricturing masses) were associated with malignancy.

In **Study III**, we evaluated the performance of MRI-based radiomics models in the preoperative prediction of malignancy in 130 patients operated for BD and mixed-type IPMN after exclusion of mass-forming PC. The radiomics models were internally cross-validated. Our results showed that a "pure" radiomics model outperformed a model including standard clinical and imaging features, suggesting that it might effectively predict malignancy in BD-IPMN even without standard clinical/imaging information.

In **Study IV**, we described the imaging findings and the performance of a mainly MRI-based surveillance program in a cohort of 278 individuals at risk (IAR) for familial/hereditary PC. Our results showed that focal pancreatic lesions were identified in over half of IAR, the vast majority being small cysts. No lesions with high-grade dysplasia were detected. Five patients had PC, with the same prevalence of stage I and stage IV. The sensitivity and positive predictive values for detecting PC and its precursors were low (60% and 37%, respectively).

**In conclusion**, a short pancreatic MRI protocol can be safely used in the surveillance of PCNs without losing relevant clinical information. Although novel imaging features cannot predict malignancy in IPMN, radiomics have shown its potentiality. In the context of

individuals at risk for familial or hereditary PC undergoing surveillance, the early diagnosis of PC is still challenging with “traditional” cross-imaging methods such as MRI.

# LIST OF SCIENTIFIC PAPERS

I. **Pancreatic MRI for the surveillance of cystic neoplasms: comparison of a short with a comprehensive imaging protocol.**
Pozzi Mucelli R, Rinta-Kiikka I, Wünsche K, Laukkarinen J, Labori KJ, Ånonsen K, Verbeke C, Del Chiaro M, Kartalis N.
Eur Radiol. 2017 Jan;27(1):41-50. doi: 10.1007/s00330-016-4377-4.

II. **Branch-duct intraductal papillary mucinous neoplasm (IPMN): Are cyst volumetry and other novel imaging features able to improve malignancy prediction compared to well-established resection criteria?**
Pozzi Mucelli R, Moro CF, Del Chiaro M, Valente R, Blomqvist L, Papanikolaou N, Löhr JM, Kartalis N.
Eur Radiol. 2022 Aug;32(8):5144-5155. doi: 10.1007/s00330-022-08650-5.

III. **MRI Radiomics as a tool for malignancy prediction in pancreatic branch-duct intraductal papillary mucinous neoplasms. A proof-of-concept study.**
Pozzi Mucelli R†, Rodrigues AC†, Moro CF, Papanikolaou N‡, Kartalis N‡
*(Manuscript)*

IV. **Imaging findings and performance of MRI-based screening for individuals at risk for pancreatic cancer.**
Pozzi Mucelli R, Vujasinovic M, Pettersson I, Farah-Mwais A, Del Chiaro M, Moro CF, Gustavsson P, Ghorbani P, Löhr JM†, Kartalis N†
*(Manuscript)*

†These authors contributed equally to the work.
‡ These authors contributed equally to the work.

# CONTENTS

# LIST OF ABBREVIATIONS

| | |
|---|---|
| ANOVA | Analysis of variance |
| BD-IPMN | Branch-duct IPMN |
| CA19-9 | Carbohydrate antigen 19-9 |
| CP | Comprehensive (MRI) protocol |
| CT | Computed tomography |
| DWI | Diffusion-weighted imaging |
| EG | European evidence-based guidelines |
| EUS | Endoscopic ultrasound |
| EV | Elongation value |
| FPC | Familial pancreatic cancer |
| HGD | High-grade dysplasia |
| HPC | Hereditary pancreatic cancer |
| IAR | Individuals at risk |
| ICC | Intraclass correlation coefficient |
| ICG | International consensus Fukuoka guidelines |
| IPMN | Intraductal papillary mucinous neoplasm |
| LGD | Low-grade dysplasia |
| MN | Mural nodule |
| MPD | Main pancreatic duct |
| MRCP | Magnetic resonance cholangio-pancreatography |
| MRI | Magnetic resonance imaging |
| MCN | Mucinous cystic neoplasm |
| NPV | Negative predictive value |
| PanIN | Pancreatic intraepithelial neoplasia |
| PC | Pancreatic cancer |
| PCN | Pancreatic cystic neoplasm |
| PDAC | Pancreatic adenocarcinoma |
| PPV | Positive predictive value |
| SP | Short (MRI) protocol |
| VIBE | Volume interpolated breath-hold examination |
| VOI | Volume of interest |

# 1 INTRODUCTION

Pancreatic cancer (PC) represents one of the deadliest malignant tumours, with a 5-year relative survival rate of 11% considering all stages combined [1]. In the United States, the number of newly diagnosed PCs is estimated to be around 62,210, with 49,830 deaths in 2022, with an increasing incidence rate of 1% per year since 2000 [2]. In Sweden, PC affects about 1500 individuals every year, with a slightly increasing trend over the last ten years [3].

Several reasons account for this dismal prognosis. Due to the anatomical location of the pancreatic gland (located deeply and posteriorly in the retroperitoneum), a pancreatic neoplastic lesion causes unspecific symptoms, thus leading to a delayed diagnosis. Further, due to the location mentioned above, PC infiltrates vital structures as mesenteric vessels, which poses technical challenges for surgical resection. Lastly, more than half of the patients with PC are diagnosed with metastatic disease, and the majority of those with a resectable tumour at diagnosis will develop metastases within four years from surgery [4, 5].

Several risk factors may play an essential role in the development of PC. They can be classified into "modifiable" and "inherited" risk factors. Obesity, type-2 diabetes, and smoke are encountered among the former, whereas all familial and hereditary cancer syndromes – responsible for 5-10% of all PC cases– are among the latter [4].

Moreover, some pancreatic lesions have been identified as non-invasive precursors: pancreatic intraepithelial neoplasia (PanIN), intraductal papillary mucinous neoplasms (IPMN) and mucinous cystic neoplasms (MCN).

While MCN are rare and PanIN are only microscopic findings, IPMN is nowadays very commonly detected at imaging as relatively small pancreatic cysts. Since they may harbour malignancy, surveillance is recommended by current guidelines [6, 7], which is mainly performed with magnetic resonance imaging (MRI). MRI surveillance is also recommended for individuals with familiar and hereditary pancreatic cancer.

The role of MRI is to identify features that may indicate malignancy, such as solid lesions, cystic size enlargement, or dilatation of the main pancreatic duct (MPD). In case of suspicious findings, the patient may be referred for pancreatic surgery.

However, there are drawbacks related to MRI surveillance. First, MRI is an expensive and time-consuming examination. Second, the imaging criteria recommended for early PC detection have low accuracy [8], which may lead to overtreatment. Furthermore, although MRI surveillance of patients with familiar and hereditary pancreatic cancer seems capable of detecting preneoplastic lesions or resectable PC, there is also a not negligible number of PC diagnosed in more advanced stages, which may be considered as a partial screening failure [9].

This thesis aims to explore new diagnostic features able to predict malignancy in patients at risk for PC more accurately and to optimize MRI surveillance.

# 2 BACKGROUND AND LITERATURE REVIEW

## 2.1 PRECURSORS OF PANCREATIC ADENOCARCINOMA

The vast majority of PCs (95%) arise from exocrine cells and most commonly are represented by pancreatic ductal adenocarcinomas (PDAC). A few non-invasive precursors have been identified: pancreatic intraepithelial neoplasia (PanIN), intraductal papillary mucinous neoplasms (IPMN) and mucinous cystic neoplasms (MCN). The 2019 WHO (World Health Organization) classification of tumours of the digestive system [10] has further subclassified these entities into low- and high-grade dysplasia. Lesions with low-grade dysplasia (LGD) have a lower risk of harbouring malignancy. Conversely, lesions with high-grade dysplasia (HGD) have a higher possibility of malignant transformation [4, 11]. The progression of these precursors from low-grade dysplasia to pancreatic ductal adenocarcinomas is characterized by stepwise mutations of genes. This process takes several years, similarly to the carcinogenetic mechanism of colorectal cancer.

### 2.1.1 Pancreatic intraepithelial neoplasia (PanIN)

PanIn is the most frequent precursor of PDAC. Histologically, it is a microscopic mucinous lesion with a diameter inferior to 5 mm that arises from small pancreatic ducts. PanIn is further subclassified into two classes: PanIn with low-grade and high-grade dysplasia [11]. The main difficulty with the diagnosis of PanIN is its small size, as it is not easily detectable at preoperative imaging [computed tomography (CT), MRI and/or endoscopic ultrasound (EUS)]. A few reports suggest that PanIN may be suspected at EUS when microcysts and/or hyperechoic foci are identified [12, 13]. At preoperative MRI, non-communicating cystic lesions less than 5 mm in diameter might be associated with the presence of histologically proven PanIN in patients with pancreatic lesions [14]. However, in these studies, it was not possible to correlate imaging to histopathological findings on a “lesion-per-lesion” basis, which represents a potential flaw and makes the characterization of these lesions impossible in daily clinical practice.

### 2.1.2 Intraductal papillary mucinous neoplasms (IPMN)

IPMN is the second most frequent precursor of PDAC. It is defined as a macroscopically and/or radiologically identifiable mucin-producing lesion. IPMN can affect the MPD, side branches or both. For this reason, IPMN is subclassified into main-duct type, branch-duct type (BD-IPMN) and mixed type. Depending on the epithelial morphological features, IPMN can be further distinguished into four categories: gastric, intestinal, pancreato-biliary and oncocytic. The grade of dysplasia is classified into low-grade and high-grade [11].

IPMN usually affects individuals of 60-70 years of age, with similar distribution among males and females. IPMN – together with other pancreatic cystic neoplasms (PCN) – is often incidentally detected at imaging and less often discovered in symptomatic patients. The prevalence of pancreatic cystic lesions identified in a normal and healthy population is as high as 49%, as shown in a population-based study [15]. Prevalence, number, and diameter tend to increase with the patient’s age [15]. Noteworthy, IPMN represents half of the pancreatic cystic lesions according to large surgical series [16].

At imaging (CT, MRI and EUS), the main-duct type IPMN may appear as a focal or diffuse dilatation of more than 5 mm of the main pancreatic duct [13]. In some cases, the overproduction of mucin causes protrusion of the papilla, a sign that can be easily identified at imaging and endoscopy as the "fish-eye ampulla". The BD-IPMN is a solitary or multifocal cystic lesion with a diameter larger than 5 mm, communicating with the MPD [6]. The mixed-type IPMN is represented by the combination of these findings, where both the MPD and side branches are affected.

The risk for harbouring malignancy varies depending on clinical, morphological, and histological features (where the pancreato-biliary type has a higher risk for malignant transformation than the gastric type).

During the last twenty years, various research groups worldwide have contributed to countless papers, identifying, and analysing the role of multiple preoperative factors associated with high-grade dysplasia and invasive carcinoma.

One significant finding is the striking difference between branch-duct and main-duct type (as well as mixed-type) in terms of risk of malignant transformation. The involvement of the MPD is an important predictive factor. Indeed, main-duct type and mixed-type IPMN have a higher risk of malignancy, while branch-duct IPMN has a lower risk. In published series of resected IPMN, branch-duct IPMN has a mean frequency of high-grade dysplasia and/or invasive cancer of 31%, while main-duct IPMN has a mean frequency of 61% [6]. When considering, on the contrary, studies including subjects under surveillance for BD-IPMN, the prevalence of PC is much lower (1.6%) for patients with so-called "*trivial*" BD-IPMN (i.e., those lesions without concerning features and stable for at least five years) [17].

The assessment of the MPD involvement is based on the detection of MPD dilatation at imaging. Despite the good agreement in the literature regarding the dilatation of MPD ≥ 10 mm as a strong predicting factor for malignancy, there is not a complete consensus in case of MPD dilatation of 5-9 mm and its relationship with the development of high-grade dysplasia/invasive cancer. In some papers, a MPD diameter of 5-9 mm seems to be associated with a higher risk of high-grade dysplasia and/or invasive cancer [18, 19], and it has been underlined that MPD dilatation appears to be the best single predictor of malignancy. However, other groups show that the only dilatation of the MPD 5-9 mm in patients under surveillance does not represent a risk factor for malignancy, suggesting instead that MPD dilation alone without other clinical or suspicious imaging findings should not be considered as a direct indication for surgery [20].

Besides the dilatation of the MPD, there are other imaging factors that may be associated with a higher risk of malignancy.

For instance, the BD-IPMN's diameter is another critical and debated parameter. Current guidelines propose cut-off diameters for the management of BD-IPMN since malignancy appears more frequently detected in larger cysts (e.g., larger than 3 cm) [6, 7, 21]. In Sahora et al. [21], the risk of high-grade dysplasia and/or invasive carcinoma results being two times with cysts larger than 3 cm. Cyst diameter has also been included in a nomogram for predicting malignancy in IPMN [22–24]. There are, however, studies where cyst size does not play a role in predicting malignancy [18] or appears associated with low specificity [25].

Moreover, high-grade dysplasia and invasive carcinoma may be present even in cysts smaller than the recommended cut-off diameters [26].

Progress in cyst size of IPMN is also encountered among factors associated with malignancy risk. Namely, an increase in size ≥ 2.5 mm/year seems associated with a higher risk of malignancy [17, 27]. However, although 45% of small BD-IPMN increase in size during surveillance, this progression is very discrete (1.2 mm/year) [27]. Furthermore, a drawback of these papers is represented by the method of assessing cyst size progression. Indeed, it has been calculated as the size difference between the first and last examination, divided by the number of years under surveillance [27]. This approach appears more suitable and applicable in the research setting rather than in daily practice [27].

The presence of contrast-enhancing mural nodules (MN) within a branch-duct IPMN is an important aid in predicting high-grade dysplasia and/or invasive carcinoma. This feature increases the risk of malignancy by 12-folds [25], although with sensitivity and a positive predictive value of 62% [28]. An issue may be represented by small MN, where the identification of contrast enhancement on cross-sectional imaging (CT and/or MRI) could be limited by their spatial resolution. In these cases, contrast enhancement EUS is recommended for a better delineation of the suspected MN [6, 7, 28].

Clinical features associated with malignancy in IPMN are represented by increased serum levels of carbohydrate antigen (CA) 19-9 [29]. For this reason, CA19-9 has been included in guidelines and nomograms [6, 7, 22]. Namely, CA19-9 serum levels higher than 37 U/mL are associated with a higher probability of malignant IPMN, particularly invasive cancer, although with sensitivity and positive predictive value of 41% and 45%, respectively [30]. Furthermore, elevated CA19-9 in patients with IPMN is associated with worse survival [30, 31].

### 2.1.3 Mucinous cystic neoplasms (MCN)

Mucinous cystic neoplasm is the third precursor of PDAC. Similar to IPMN, it is a mucin-producing cystic tumour, although without communication with the pancreatic ductal system. Furthermore, since the presence of ovarian-type stroma histopathologically characterizes it, it affects almost exclusively female patients in their fifties [11, 32]. Typically, MCN is located in the body or the tail of the pancreas. Similar to PanIN and IPMN, MCN can be classified into those with low-grade and high-grade dysplasia.

At imaging, MCN appears as a solitary cystic lesion, often with a thickened wall and internal septations. Calcifications may be present lining the outer wall or the internal septations. Contrast-enhancing solid nodules may also be present. MCNs are lesions with a low prevalence of high-grade dysplasia (5%) and/or invasive cancer (4%), as reported in surgical series [33]. For this reason, according to the European evidence-based guidelines (EG) [7], it is considered safe to follow-up lesions less than 4 cm in diameter without MN in asymptomatic subjects with low levels of tumoural markers.

## 2.2 INDIVIDUALS AT RISK FOR FAMILIAR AND HEREDITARY PANCREATIC CANCER

Most PCs are sporadic lesions. However, about 10% of the cases are represented by familial PC (FPC) among individuals with a strong familial history (approximately 7%) and hereditary PC (HPC) in the setting of well-defined germline mutations (circa 3%) [34]. These subjects are commonly defined as "individuals at risk" (IAR) or high-risk individuals. For being considered IAR, individuals should have a lifetime risk of PC higher than 5% (or a 5-fold increased relative risk), which is significantly higher than the general population's lifetime risk (about 1.5%) [35, 36].

IAR have a varying relative risk for developing PC depending on their familial history and/or germline mutation, reaching up to 132-fold risk for individuals with Peutz-Jeghers syndrome [37, 38]. More specifically, in the case of familial history, the risk increases with the number of affected relatives: with one first-degree relative (FDR), the risk is 4.6-fold; with two FDRs, 6.4-fold; with three FDRs, 32-fold risk, compared to "normal" population [39].

Regarding hereditary PC, the most frequent hereditary syndromes are Peutz-Jeghers syndrome (with mutation of STK11/LKB1), hereditary pancreatitis (with mutation of PRSS1, SPINK1, PRSS2, CTRC), familial atypical multiple mole melanoma (with mutation of P16/ CDKN2A), hereditary breast-ovarian cancer syndrome (with mutation of BRCA1, BRCA2, PALB2), familial adenomatous polyposis syndrome (with mutation of APC), Lynch syndrome (with mutation of MLH1, MSH2, MSH6, PMS2), Li-Fraumeni syndrome (with mutation of TP53), and cystic fibrosis (with mutation of CFTR) [36].

## 2.3 CURRENT GUIDELINES

### 2.3.1 IPMN guidelines

As already mentioned, understanding the malignancy potential of IPMN is a complicated matter. Most published articles are retrospective studies based on surgical series, with very heterogeneous patients' cohorts and low scientific evidence. Furthermore, twenty years ago, it was common practice to resect all PCNs, given the sparse knowledge about their natural history. This led to considerable variability in the management of patients with pancreatic cysts, with possibly profound effects not only on a "patient" level (due to relatively high comorbidity and mortality of pancreatic surgery), but even on a population level in terms of health costs. These issues have played a substantial role in developing several guidelines that focus on elaborating recommendations for the clinical management of patients affected by PCNs in general and IPMN in particular, thus, providing clear indications for surgery and surveillance.

The two most used and quoted guidelines are nowadays the *International consensus Fukuoka guidelines for the management of IPMN of the pancreas* (ICG), revised in 2017 [6] and the *European evidence-based guidelines on pancreatic cystic neoplasms* (EG), published in 2018 [7]. The two guidelines provide algorithms for the decision-making in the case of PCNs, which are essentially based on the detection of specific clinical and imaging findings characterized by a higher risk of high-grade dysplasia and invasive carcinoma. These features

are reported with slightly different terminology in the two guidelines. In the ICG, the concerning features are classified in so-called "high-risk stigmata" and "worrisome features", where high-risk stigmata pose an absolute indication for surgery [6]. In the EG, the suspicious features are distinguished into "absolute" and "relative indications" for surgery [7] (Table 1).

| International consensus Fukuoka guidelines | European evidence-based guidelines |
|---|---|
| **High-risk stigmata** | **Absolute indications** |
| Jaundice | Jaundice |
| Enhancing MN ≥ 5 mm | Enhancing MN ≥ 5 mm |
| MPD ≥ 10 mm | MPD ≥ 10 mm |
| **Worrisome features** | **Relative indications** |
| CA 19-9 >37 U/mL | CA 19-9 >37 U/mL |
| Enhancing MN < 5 mm | Enhancing MN < 5 mm |
| MPD 5-9 mm | MPD 5-9 mm |
| Acute pancreatitis | Acute pancreatitis |
| Cyst size ≥ 3 cm | Cyst size ≥ 4 cm |
| Cyst growth-rate > 5mm/2 years | Cyst growth-rate > 5mm/year |
| Thickened/enhancing cyst walls | Recent onset of diabetes (<1 year) |
| Abrupt change in MPD caliber and distal atrophy | |
| Lymphadenopathy | |
| Abbreviations: MN, mural nodules; MPD, main pancreatic duct | |

***Table 1.*** *Clinical and imaging features indicating risk for malignancy, as recommended by the International consensus Fukuoka Guidelines and the European evidence-based guidelines.*

In case of the presence of high-risk stigmata or absolute indications, surgery is strongly recommended by both guidelines if the patient is considered fit for surgery.

The approach is slightly different when encountering worrisome features or relative indications. The ICG are more prudent, recommending EUS for confirming the presence of such features before surgery. The EG recommend direct surgery in case of at least one relative indication in patients without significant comorbidities. EUS is only recommended if its results may change the patient's management.

The algorithms from the two guidelines are shown in Figures 1 and 2.

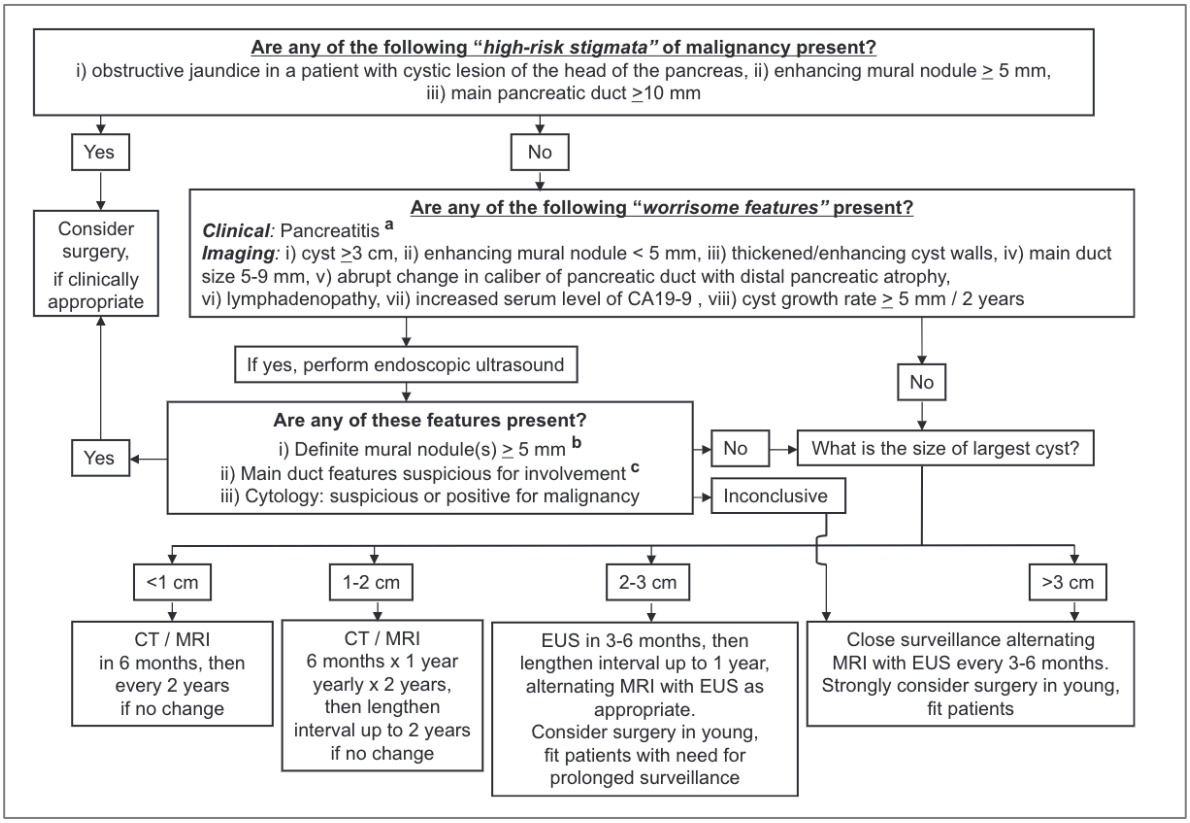


***Figure 1.*** *Algorithm for the management of IPMN proposed in the International consensus Fukuoka guidelines (reprinted with permission from Elsevier B.V.).*

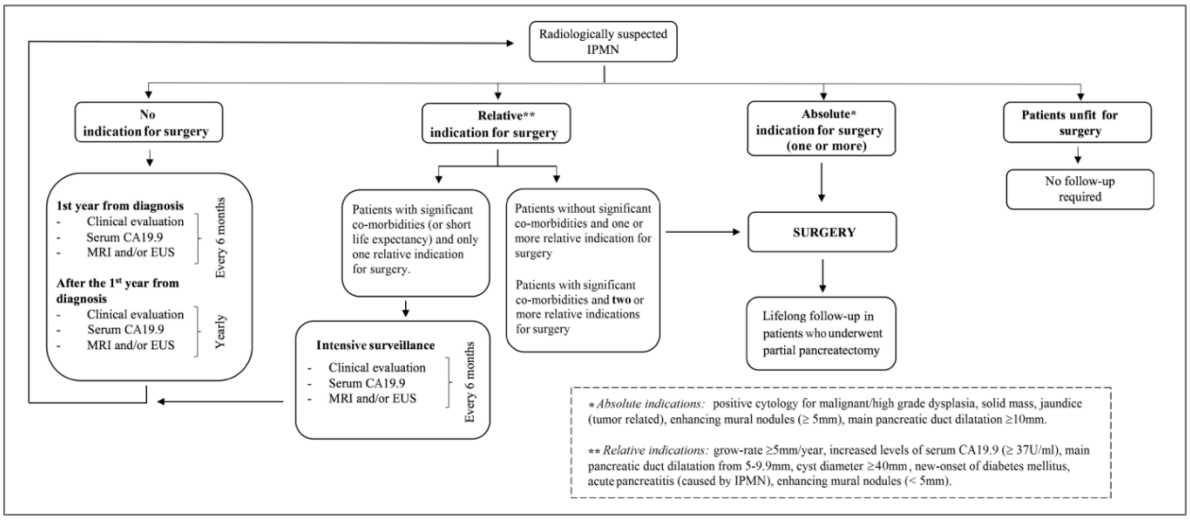


***Figure 2.*** *Algorithm for the management of IPMN proposed in the European evidence-based guidelines (source: European Study Group on Cystic Tumours of the Pancreas. Gut. 2018 May;67(5):789-804. doi: 10.1136/gutjnl-2018-316027. URL: https://gut.bmj.com/content/gutjnl/67/5/789/F1.large.jpg. Creative Commons CC BY-NC 4.0, https://creativecommons.org/licenses/by-nc/4.0/)*

According to both the EG and ICG, all the patients with lesions that do not fulfil the criteria for undergoing surgery should be closely followed-up by imaging (with MRI - if feasible - according to the EG; with CT/MRI and/or EUS according to the ICG) with slightly different intervals. Both the guidelines recommend not to dismiss the surveillance as long as the patient is considered fit for surgery since the incidence rate of PC increases over time [40, 41]. Surveillance should continue even in patients who have already been operated due to the risk of recurrence in the remnant pancreatic gland [42].

During surveillance, besides the onset of MPD dilatation or MN within a branch-duct IPMN, progression in size of any cystic lesion should also be assessed. Furthermore, since there is a certain risk for the development of a so-called "concomitant" cancer (i.e., arising distant from the "target" IPMN), great attention should be given to the detection of early parenchymal and/or ductal changes. Concomitant cancer is relatively rare, with a prevalence between 1% and 8% in surgical series [43, 44]. It can develop as a synchronous or metachronous tumour. The presence of these concomitant lesions strengthens the theory of "field cancerization", where in some patients the whole pancreatic epithelium is at risk of developing dysplastic changes, and concomitant cancer may arise from independent precursors [45]. Further, this hypothesis reminds us that IPMN is not the only precursor of PDAC since PanIN lesions may coexist.

Despite the great benefit of having clear tools for the identification of IPMN at risk of malignancy, such as the guidelines mentioned above, several issues remain with their application. As mentioned before, the guidelines aim to identify the highest number of patients at risk for high-grade dysplasia and/or invasive carcinoma. Thus, as shown in Table 2, they are characterized by high sensitivity and negative predictive value [8, 46, 47]. A direct consequence of this approach is represented by the low specificity and positive predictive value.

| | **Sharib JM et al. (2018)[a]** | **Jan IS et al. (2020)[b]** | **Crippa S et al. (2021)[c]** | |
|---|---|---|---|---|
| | **ICG** | **EG** | **ICG** | **EG** |
| **Sensitivity** | 98% | 94% | 83% | 99% |
| **Specificity** | 15% | 28% | 37% | 2% |
| **PPV** | 30% | 38% | 65% | 59% |
| **NPV** | 96% | 90% | 60% | 62% |
| **Accuracy** | n.a. | 49% | 64% | 59% |
| **Nr. included cases** | 251 | 158 | 627 | |
| **Low-grade dysplasia (%)** | 52% | 67% | 41% | |

Abbreviations: ICG, International Consensus Guidelines; EG, European evidence-based guidelines; PPV, positive predictive value; NPV, negative predictive value.
References: [a]Sharib JM et al. (2018) [46]. [b]Jan IS et al. (2020) [47]. [c]Crippa S et al. (2021) [8].

***Table 2.*** *Comparison of the diagnostic accuracy metrics of International (ICG) and European (EG) Guidelines in the identification of malignant IPMN*

The limited performance in the identification of patients at low risk contributes to a high number of unnecessary pancreatic surgery (41-67% in the papers reported in Table 2), which is a major flaw since the benefit of resecting lesions with low-grade dysplasia is uncertain for two main reasons. Firstly, pancreatic surgery is not risk-free, even in high-volume centres. Secondly, these patients would undergo surveillance anyhow due to the risk of recurrence or developing a concomitant tumour in the remnant pancreas.

Recently, it has also been developed and validated a nomogram for a better assessment of the risk of malignancy in patients with IPMN and personalization of the IPMN treatment [24]. This nomogram considers several parameters, for instance, the diameter of the cyst and the MPD, the presence of MN, and the level of CA19-9. Its validation showed promising results, with an area under the receiver operating characteristic (ROC) curve of 0.77 for the entire cohort [24].

Another way to overcome the low accuracy of the guidelines, which essentially base their decision on imaging criteria, would be to include molecular features besides the standard predictors. A fascinating and promising attempt (CompCyst) has been proposed. It consists in a machine-learning technique that analyses selected clinical, radiological, and molecular features and guides the management of patients with PCNs, being able to avoid surgery in 60% of the tested cases [48].

### 2.3.2 Guidelines for Individuals at Risk (IAR)

Regarding individuals at risk for familial/hereditary PC, there is nowadays a consensus on the necessity of surveillance. The International Cancer of the Pancreas Screening (CAPS) Consortium has recently provided updated recommendations defining which subjects should undergo surveillance, the age for the beginning of surveillance, follow-up intervals, screening methods, and indication for surgery [49].

As screening methods, the CAPS Consortium suggests pancreatic MRI at baseline, followed by yearly MRI alternating with EUS (although without consensus on this alternation) if there are no features of concern.

Imaging screening in IAR aims to detect precursor lesions, such as IPMN and/or PanIN with high-grade dysplasia, or PC in an early stage (stage I) [49], thus, to reduce mortality.

The CAPS Consortium has shown promising results in its series of papers that have analysed the findings and performance of the screening program on IAR [50–52]. Indeed, the latest published CAPS 5 study showed that among the 1461 enrolled patients with familial/hereditary PC, 78% (7/9) of the detected PC were diagnosed in a very early stage (stage I) [52]. The screening program also identified eight cystic lesions with concerning features, 37% (3/8) of whom were IPMN with high-grade dysplasia [52]. The same paper summarizes the experience from a single CAPS centre (John Hopkins) during 1998-2021 (CAPS 1-5 cohorts), showing that 58% of the surveillance-detected PC were diagnosed in stage I. Overall, patients with PC identified by the screening had a better 5-year median survival compared with patients whose PC was identified outside the screening (i.e., screening drop-out) (9.8 years versus 1.5 years), with a 5-year overall survival of 73% [52].

These data are apparently in contradiction with an - almost simultaneously - published article by Overbeek K. et al. [53] that analysed the data from 2552 IAR collected by 16 centres (most of them included in the CAPS Consortium). This paper shows that more than 70% of the resectable PC (21/27) were diagnosed at an advanced stage, and more than 30% of the detected PC (14/41) were unresectable at diagnosis. These results are in line with a systematic review and meta-analysis that showed that the cumulative incidence of advanced PC (i.e., with TNM T3-4, N0, M0; or with lymphnodes/distant metastases) was higher than the cumulative incidence of early detected PC or precursor lesions (i.e., T1N0M0 PC and lesions with high-grade dysplasia) (1.7 and 0.7 per 1000 patient-years, respectively), although the difference was not statistically significantly different [54]. The reasons for this delayed diagnosis are not easy to explain, as they appear unrelated to imaging and patients' characteristics. Further, most of the papers included in the meta-analysis did not report the

data regarding diagnostic errors [54]. Interestingly, these individuals appear more prone to rapidly developing solid lesions after less than one year since the previous negative examination, which shortens the window for prompt and early detection of a precursor lesion or an early PC [53]. It may be claimed that performing imaging controls every six months might be helpful. However, more frequent controls would increase patients' anxiety and healthcare costs without a clear benefit in improved detection rate [53].

For all the reasons above, imaging-based screening in IAR is still a field for improvement. All we have learned about it should not be considered a "*ceiling in the quest to improve early detection and reduce mortality from PC, but rather should be viewed as a floor upon which we must continue to build*" (cit. from Rosenthal M. et al. [9]).

## 2.4 ROLE OF IMAGING: ISSUES AND NEW DIRECTIONS WITH RADIOMICS

Imaging, in particular MRI and EUS, plays an essential role in the surveillance of patients with pancreatic cysts and the screening programs for individuals at risk. CT is only suggested in these settings when MRI or EUS cannot be performed. However, CT with a dedicated pancreatic examination protocol remains fundamental for the preoperative staging of PC.

MRI of the pancreas is suggested as the first-line imaging modality in the ICG, EG and CAPS recommendations [6, 7, 49]. Firstly, it does not use ionizing radiation, which is of the utmost importance in the lifelong surveillance of healthy subjects. Secondly, its inherent superior contrast resolution allows a more confident evaluation of cystic lesions' features such as the communication with the MPD, the presence of solid nodules, internal septations, and multifocality [55, 56]. MRI can also be performed without injecting a gadolinium-based contrast agent, without losing information in the surveillance of pancreatic cystic neoplasms [57]. This represents a significant advantage, considering patients with impaired renal function and the possible –still not fully understood– risk for cerebral gadolinium deposition [58], given the numerous MRI controls during a life span. Despite the absence of contrast agent, MRI can still be a valuable tool for the identification of PC, owing to the addition of a diffusion-weighted sequence (DWI), which is particularly helpful for the detection of lesions located in the end of the tail, where strictures of the MPD are not usually present [59, 60]. However, DWI has some issues, especially in pancreatic imaging, as it may be affected by artifacts, such as respiratory and susceptibility artifacts, as well as ghosting, due to the deep central location in the abdomen of the pancreatic gland and its proximity to bowel loops [61].

EUS is often used for the surveillance of PCNs, and in screening programs for IAR. Its indications vary depending on the guidelines, local availability, and expertise. For instance, the ICG recommend EUS for the follow-up of lesions larger the 2 cm alternating with MRI (or CT) [6]; while the EG suggest the use of EUS as an additional modality when the identified cystic lesion has suspicious features, and if contrast-enhanced EUS followed by fine-needle aspiration and/or biopsy may change the clinical management [7].

Interestingly, from an economic point of view, MRI alone seems the most cost-effective screening test in the setting of IAR surveillance compared to EUS. In comparison, alternating

MRI with EUS is associated with increased costs without improved effectiveness [62]. Conversely, EUS appears more cost-effective in IAR with a higher risk of developing PC (i.e., familial PC with ≥ 3 FDRs, hereditary pancreatitis and Peutz-Jeghers syndrome) [62].

Nevertheless, although imaging plays a crucial role in the follow-up of patients with PCNs and individuals with familial or hereditary PC, several considerations should be taken into account.

First, given the high prevalence of PCNs in the healthy population, MRI surveillance has an high impact on our healthcare systems since it is expensive and time-consuming. For instance, a pancreatic MRI that includes all the T2- and T1-weighted sequences before and after contrast agent, DWI and magnetic resonance cholangiopancreatography (MRCP) usually has an acquisition time of approximately 30-40 minutes, without considering the patient's preparation time outside the magnet.

Second, imaging methods are affected by a wide-ranging, "far-from-perfect" accuracy [63, 64]. Even in subspecialized multidisciplinary conferences, the accuracy of preoperative diagnosis is approximately 60% [65]. The main obstacles to imaging methods are encountered with the differential diagnosis of some cystic lesions, for instance, the differentiation between BD-IPMN and serous cystic neoplasia. The differentiation between main-duct type IPMN and chronic pancreatitis may also be challenging, especially considering that the two conditions may coexist.

Third, there are controversial data regarding the agreement between MRI and EUS in the surveillance of IPMN and IAR. For instance, some authors showed similar performance of EUS and MRI in the prediction of malignancy in IPMN [66], while others exhibited a substantial disagreement between MRI and EUS in the IPMN surveillance [67], which may have important clinical implications for the management of a given patient. In IAR, MRI and EUS agree in 90% of the cases in the overall detection of any kind of pancreatic lesion [50], while the agreement decreases to 62% in the evaluation of specific features (e.g., number of lesions, size difference, lesions' location) [68].

Last but not least, despite following meticulously the criteria for the identification of IPMN with "high-risk stigmata"/"absolute surgical indications" and "worrisome features"/"relative surgical indications", it is still complicated in practice to distinguish lesions with low-grade from high-grade dysplasia preoperatively. This issue is even more evident, considering the guidelines' low specificity and positive predictive values, as mentioned before.

For these reasons, the routinely used imaging-based features alone are not sufficient to predict malignancy. Other tools that may improve the accuracy of the preoperative diagnosis of PCNs may be the molecular and genetic analysis of the cyst fluid, especially in the differentiation between "no-touch lesions" (such as serous cystic neoplasms) and lesions where surveillance is indicated. However, cyst fluid analysis implies more invasive tests, such as EUS-guided fine-needle aspiration, which are affected by a not negligible - although low - risk for complications. Thus, to avoid invasive procedures, it might be valuable to assess new morphological features that might correlate with the amount of produced mucin and grade of dysplasia, such as cystic volume and elongation value (EV), the latter corresponding to the relationship between width and length [69].

However, there may be other approaches to overcome the issues mentioned above. Artificial intelligence and machine learning may represent the future direction for developing accurate diagnostic tools. Indeed, diagnostic images represent an enormous source of data that the human eyes can only partially explore. A way of exploiting data contained in medical images is represented by radiomics. Radiomics is a quantitative approach that mathematically analyses an extensive amount of data extracted from medical images using complex and non-intuitive algorithms, thus, extrapolating and enhancing the information that otherwise would not be accessible to clinicians. The "*omics*" suffix derives from the biological world, which usually refers to large sets of biological molecules [70], such as genomics, proteomics, or metabolomics.

Radiomics can be applied to any medical image, but it has mostly been tested on CT, MRI, and PET/CT, particularly in the oncologic field. A radiomics analysis includes several steps, such as the definition of a clinical question with the correct identification and selection of the study cohort; the choice of the imaging modality (with protocol's optimization/standardization); the segmentation of the target lesion on the images; the data extraction, followed by its dimensionality reduction; and, lastly, the training and validation of the radiomics model [71, 72].

Several research attempts have been made with radiomics in the pancreatic field, with almost 100 publications in PubMed only in the last five years. For instance, radiomics have been tested for differentiating pancreatic mucinous cystic neoplasms from serous cystic neoplasms [73]. Furthermore, it has also been applied in the preoperative prediction of IPMN malignancy, with some encouraging results [74–78]. However, most of these studies employed CT images, as the analysis of MRI images is more challenging due to the higher variability of MRI data [71, 72], even though most of the imaging surveillance on patients with IPMN is performed with MRI.

# 3 RESEARCH AIMS

This thesis aims to contribute towards improved secondary prevention of PC through more efficient and accurate diagnostic methods in patients with IPMN and familiar/hereditary pancreatic cancer.

In particular:

**Study I** aims to assess whether a short MRI protocol (SP) for the surveillance of pancreatic cystic neoplasms provides equivalent clinical information as a comprehensive protocol (CP) at a lower cost.

**Study II** aims to assess whether new imaging features, such as volumetry and elongation value, may improve the ability of MRI to predict malignancy in IPMN.

**Study III** aims to evaluate whether radiomics features may better predict the presence of malignancy in IPMN at preoperative MRI.

**Study IV** aims to describe the imaging findings and the performance of a mainly MRI-based surveillance program in the largest Scandinavian single-centre IAR cohort.

# 4 MATERIALS AND METHODS

## 4.1 ETHICAL CONSIDERATIONS

The regional ethical committee approved all four study parts (study part 1: DNR 2015/1544-31/4; study parts 2 and 3: DNR 2015/1544–31/4 and amendment DNR 2020/03657; study part 4: DNR 2020-00595 and amendment DNR 2022-02892-02). Written informed consent was waived.

All the studies were performed on retrospective cohorts collected from the Karolinska University Hospital's database. All the included patients had already completed one or more than one pancreatic MRI at the time of study inclusion.

Despite the intrinsic limitations of analysing retrospective material, from an ethical perspective, our studies minimize the risk of causing harm to our patients in keeping with the "*nonmaleficence*" principle as described by Beauchamp and Childress [79]. Moreover, we analysed MRI, an imaging modality that does not expose patients to ionizing radiation. However, MRI was performed with a gadolinium-based contrast agent to better identify and characterize pancreatic lesions in most cases. Like any injected drug, Gadolinium-based contrast agents may pose the patients at risk of allergic reactions (although rare). Since it is contraindicated in patients with renal impairment due to the risk of nephrogenic systemic fibrosis, the contrast agent was never administrated in such patients. In the last few years, it has been demonstrated that gadolinium may be retained in tissues (such as brain, skin, bones, and liver). However, it has not shown any correlation with patients' symptoms [58]. This risk has been minimized using macrocyclic, non-ionic contrast agents (i.e., gadoterate and gadobutrol).

## 4.2 STUDY DESIGN

Cross-sectional retrospective diagnostic studies, performed at one institution.

## 4.3 STUDY POPULATIONS

In study part 1, we included subjects from a database of patients under surveillance and/or operated for PCNs during the period September 2005 and January 2015. The patients were included if they had a suspected diagnosis of mucin-producing cystic pancreatic lesions after discussion at the multidisciplinary team conference and at least one pancreatic MRI (including MRCP). Patients with an MRI performed outside our institution or with only CT available were excluded.

In study parts 2 and 3, we included surgically resected patients with histopathological diagnosis of IPMN. The study period was 2008-2019 for study part 2 and 2008-2021 for study 3. The indication for surgery was decided after discussion at the multidisciplinary team conference, according to available guidelines at the time of diagnosis ("*Sendai criteria*" [80] until November 2012; "*European experts consensus statement on cystic tumours of the pancreas*" [81] from December 2012 until February 2018; EG [7] from March 2018). Only patients with at least one histopathologically proven BD-IPMN visible on a preoperative pancreatic MRI with an axial and coronal T2-weighted sequence were included. We excluded

patients with characteristic elements in keeping with main-duct IPMN (MPD diameter ≥ 5 mm and no visible BD-IPMN) and patients with a solid mass-forming PC (Figure 3).

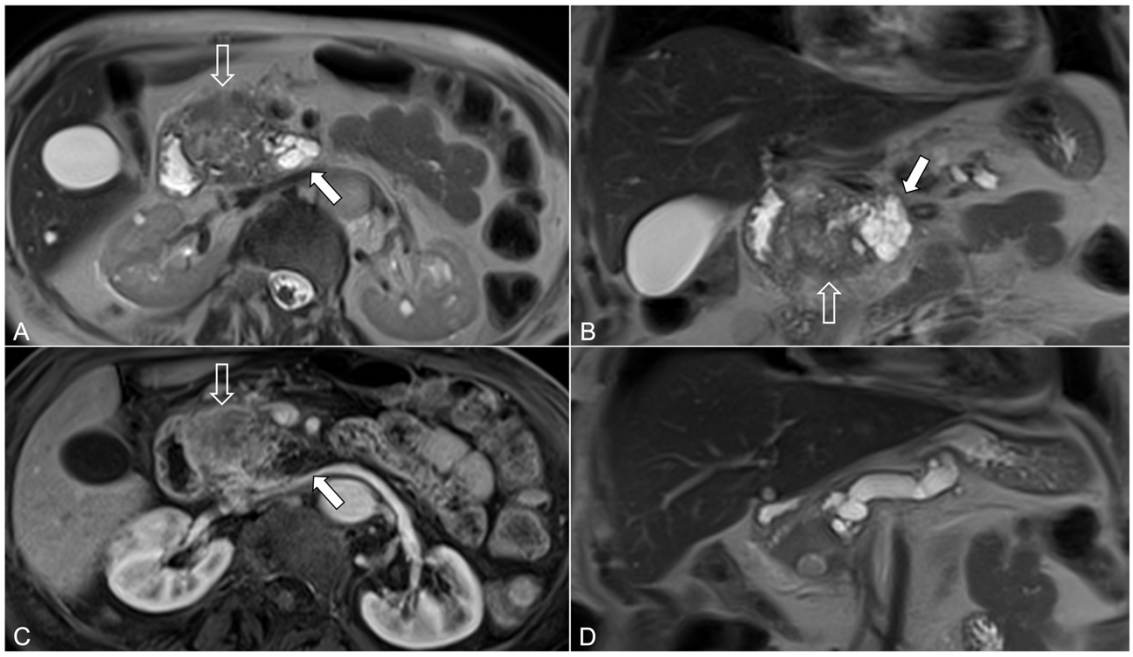


***Figure 3.*** *Example of a patient excluded from studies 2 and 3, due to the presence of a solid mass-forming pancreatic cancer (PC) (open arrows) contiguous to a BD-IPMN (white arrows) (a, b). The PC is hypovascular in the arterial phase (c) and causes a stricture of the main pancreatic duct MPD) (d). Such cases were excluded, as the upstream dilation of the MPD, consequent to a PC, may induce overestimation of the malignancy prediction capability for the finding "dilated MPD". Reprinted with permission [source: Pozzi Mucelli RM et al.* [82]*. Creative Commons CC BY 4.0, https://creativecommons.org/licenses/by/4.0/]*

Patients' selection for study parts 1, 2 and 3 is shown in Figure 4.

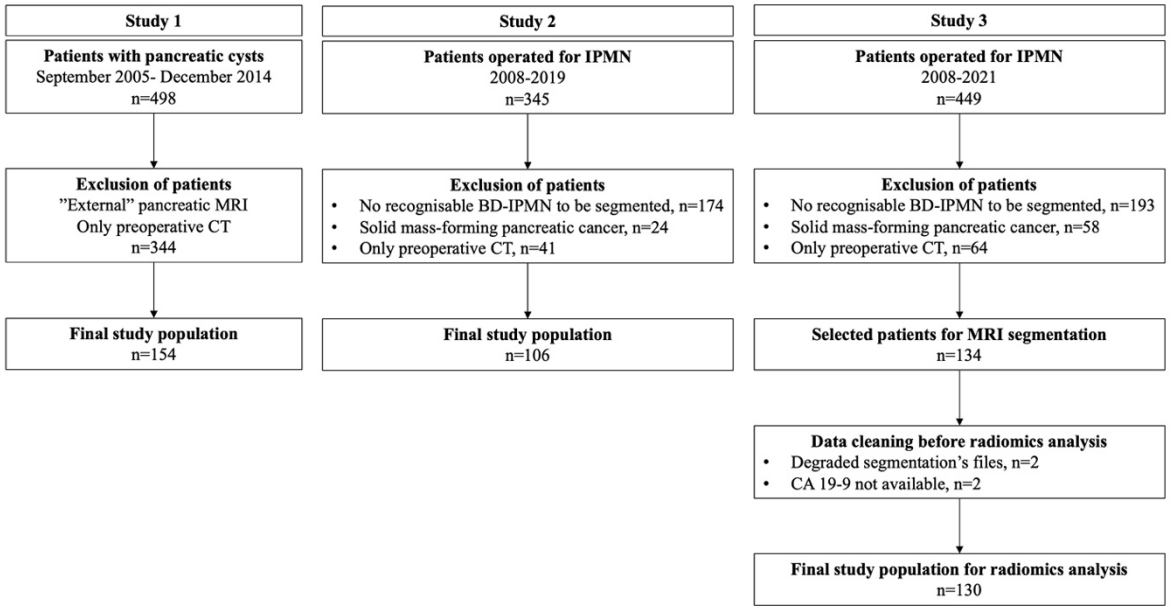


***Figure 4.*** *The flowcharts show the selection of study populations in study parts 1, 2 and 3. Reprinted and modified with permission from Springer Nature (flowchart study 1) and Pozzi Mucelli RM et al.* [82]*. Creative Commons CC BY 4.0, https://creativecommons.org/licenses/by/4.0/ (flowchart study 2).*

In study part 4, we included individuals at risk (IAR) for familial/hereditary PC undergoing imaging surveillance at the pancreatologists' outpatient unit during the period 2002-2021. According to the CAPS Consortium recommendations [49], patients were defined as:

a) familial PC (FPC), in case of at least one first-degree relative (FDR) and one second-degree relative (SDR) with PC in the same bloodline (unknown genetic mutation or genetic test not performed);
b) hereditary PC (HPC), if fullfilling causative germline mutations and family history criteria: LKB1/STK11 (Peutz-Jeghers syndrome); CDKN2A/p16 (familial atypical multiple mole melanoma); BRCA1, BRCA2, PALB2 (hereditary breast-ovarian cancer syndrome); MLH1, MSH2, MSH6 (Lynch syndrome); APC (familial adenomatous polyposis syndrome); TP53 (Li-Fraumeni syndrome); ATM (ataxia telangiectasia).

The relationship between the patients included in the four studies is shown in Figure 5.

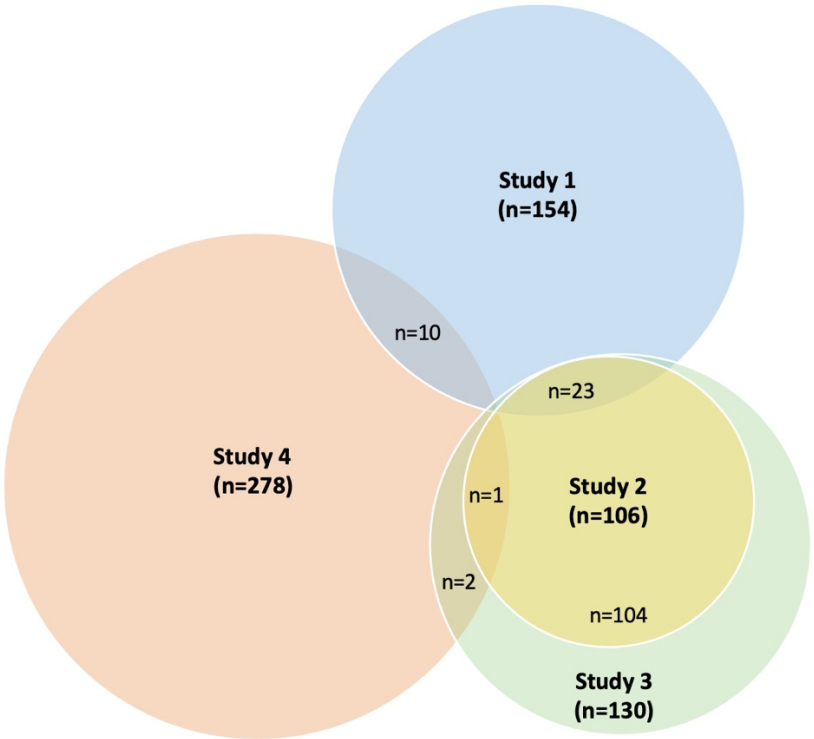


***Figure 5.*** *Venn diagram displaying the overlaps between the four studies' cohorts.*

## 4.4 IMAGING ACQUISITION AND ANALYSIS

### 4.4.1 Imaging acquisition

In study part 1, all the MRIs were performed with 1.5T scanners. The technical parameters are shown in detail in Table 3.

In studies parts 2 and 3, the MRIs were performed with 1.5 and 3T scanners from different vendors, with different sequences and technical parameters, as some patients with an MRI already performed outside our institution were referred to our high-volume pancreatic centre.

However, we accepted for inclusion "external" MRIs if performed with at least a 1.5T magnetic strength and comprehending a T2-weighted sequence (HASTE, SS-FSE, or SS-TSE) acquired in the axial and coronal plane (slice thickness ≤ 6 mm; interslice gap ≤ 20%).

For study part 4, IAR underwent imaging surveillance with pancreatic MRI or CT during the period 2002-2009. From 2010, all imaging controls were performed with MRI. CT was used as an alternative method in case of contraindications to MRI (e.g., claustrophobia, MRI-unsafe/unconditional active devices, such as pacemaker, etc.) or for local staging of an MRI-detected PC. Gadolinium-based contrast agent was not injected in patients having a glomerular filtration rate ≤ 30 mL/min. Imaging intervals were set at one MRI/year if patients did not show any findings; twice/year if a cystic lesion without concerning features was identified.

EUS was not routinely adopted in the IAR surveillance and was only used for selected cases (i.e., identification of MRI findings that would have changed the patient's management; or suspicious laboratory results not correlated to pathological findings at MRI/CT).

MRIs were acquired either on 1.5T or 3T scanners. The pancreatic MRI protocol corresponds to the comprehensive protocol (CP) as in study part 1 (Table 3). All CT consisted of a pancreatic arterial and portal-venous phase obtained after intravenous administration of iodinated contrast agent (contrast dose 0.75 g iodine/kg body weight of either iomeprol 400 mgI/mL or iodixanol 320 mgI/mL; fixed injection duration), with bolus tracking technique. Unenhanced CT scan was not mandatory.

| Sequence | Scan plane | Slice thickness/ gap | TE (ms) | TR (ms) | Scan time | Breathing technique | CP | SP |
|---|---|---|---|---|---|---|---|---|
| **T2-weighted HASTE** | Axial | 4 mm/ 0 | 76 | 1000 | 2-5 min | PACE | ✔ | ✔ |
| **T2-weighted HASTE** | Coronal | 4 mm/ 0-20%[a] | 76 | 1080 | 2-5 min | PACE | ✔ | ✔ |
| **T1-weighted 2D GRE in/opposed phase** | Axial | 4 mm | 5.04/2.4 | 126 | 1 min 11 s | Multi-BH | ✔ | |
| **or** | | | | | | | **or** | |
| **T1-weighted 3D VIBE DIXON** | Axial | 4 mm | 2.4-4.8 | 6.9 | 18 s | BH | ✔ | |
| **T2-weighted 3D SPACE MRCP** | Axial | 2.5 mm | 903 | 2500 | 3-5 min | PACE | ✔ | |
| **T2-weighted 3D SPACE MRCP** | Coronal | 1 mm | 904 | 2000 | 3-5 min | PACE | ✔ | |
| **T1-weighted 3D VIBE FS before contrast** | Axial | 1.8 - 2.5 mm | 1.9 | 4.3 | 17-22 s | BH | ✔ | ✔ |
| **T1-weighted 3D VIBE FS post-contrast[b]** | Axial | 1.8 - 2.5 mm | 1.9 | 4.3 | 5 min | BH | ✔ | |
| **DWI[c]** | Axial | 5 mm/ 0-20% | 77 | 5000 | 3-5 min | FB | ✔ | |

Abbreviations: PACE, Prospective Acquisition Correction Navigator-triggered; BH, breath-hold; FB, free-breathing. CP, comprehensive protocol; SP, short protocol; VIBE, Volume interpolated breath-hold examination; DWI, Diffusion Weighted Imaging.

Examinations were performed with a 6-/12- or 18-channel (Magnetom Avanto or Aera, Siemens Healthineers, Erlangen, Germany) body and spine matrix coil combination. Area of coverage: upper abdomen.

[a]Interslice gap until 2011: 20%; thereafter: 0

[b]0.1 mmol/kg of gadoterate meglumine (Dotarem, Guerbet) or gadobenate dimeglumine (MultiHance, Bracco); injection rate 2 mL/sec followed by a bolus of 20 mL saline flush. The CARE (Combined Applications to Reduce Exposure) bolus technique was used to acquire the late arterial phase. The portal venous phase was acquired 50 sec after the initiation of the arterial phase. The venous and late venous phases at 3 and 5 min, respectively.

[c]DWI was introduced in 2007. B-values /interslice gap for the period 2007-2009: 0 and 500 s/mm$^2$ /20%; thereafter: 50, 400, 800 and 1000 s/mm$^2$ /0.

***Table 3.*** *Technical parameters of the MRI imaging protocol and sequences included in the imaging data sets of comprehensive (CP) and short (SP) protocols in study 1 (reprinted and modified with permission from Springer Nature).*

### 4.4.2 Imaging evaluation and analysis

*Study I*

In study part 1, two imaging datasets derived from the same MRI examination were obtained (Figure 6): a) one comprehensive protocol (CP), which included all the sequences shown in Table 3; b) one short protocol (SP), that only consisted of one T2-weighted axial and coronal sequence, and one unenhanced 3D GRE (VIBE) T1-weighted fat-saturated sequence. The most recent MRI was used for the analysis if more than one MRI were performed.

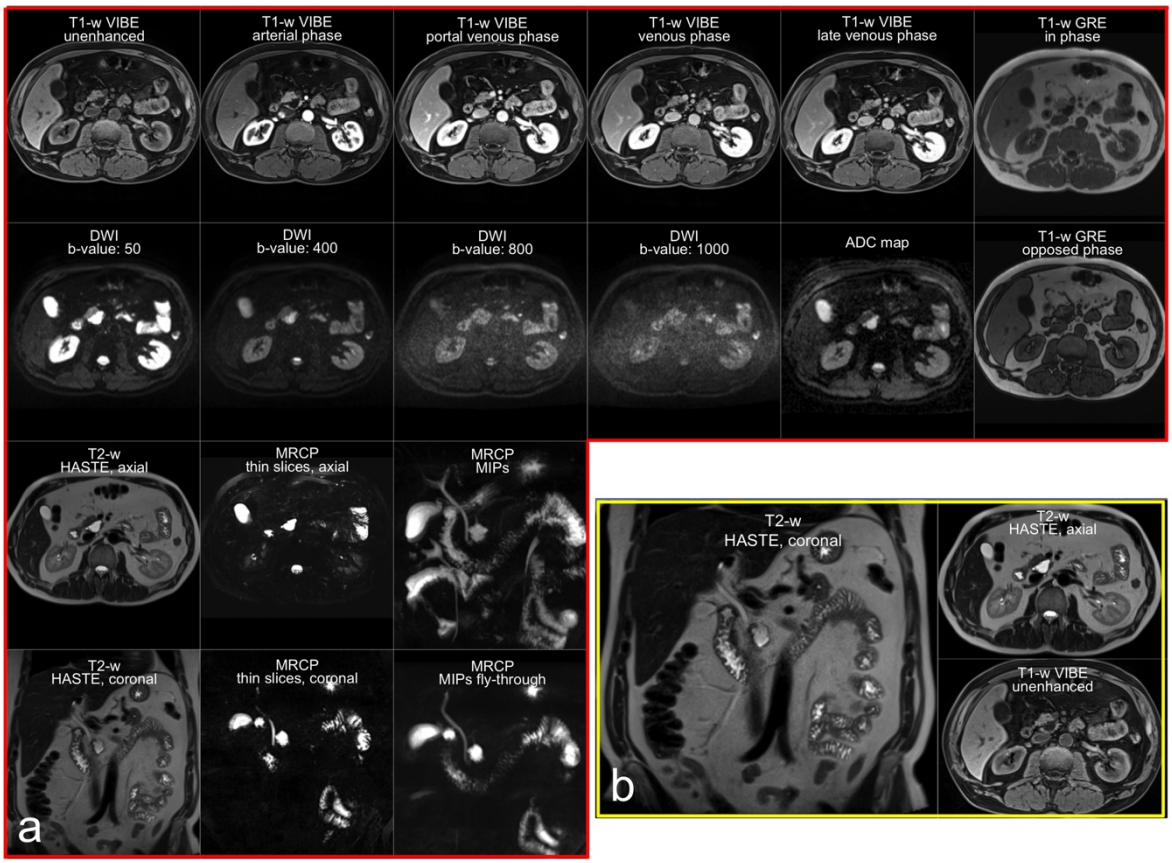


***Figure 6.*** *MRI imaging datasets (a, b) derived from the same examination performed in a 65-year-old patient under follow-up for a pancreatic cystic neoplasm in the uncinate process. The comprehensive protocol imaging data set is displayed with red edges (a); the short protocol data set with yellow edges (b). Reprinted with permission from Springer Nature.*

Three experienced radiologists (IRK, KW and RPM; 14, 10 and 10 years of experience at the time of analysis, respectively), were asked to randomly assess the two imaging datasets in one week. The three radiologists were informed of the study's aims and that some of the included patients were undergoing follow-up for a previous resected PCN. However, the readers were unaware of the patient's symptoms and histopathological diagnosis.

The three radiologists collected the following imaging parameters:

a) maximum diameter of the MPD ($D_{MPD}$) and the largest pancreatic cyst ($D_C$). In case of multiple cysts, up to two more lesions with imaging concerning features were allowed for assessment.

b) presence of MN within the MPD ($MN_{MPD}$) and/or the cyst ($MN_C$) (or in up to two cysts with concerning features). The readers were asked to grade their suspicion with a four-point scale (0=definitely absent, 1=probably absent, 2=probably present, and 3=definitely present)

Thereafter, we calculated the total number of described lesions, the mean $D_C$ and $D_{MPD}$ overall and for every reader. Their values were compared among the two imaging datasets. Regarding the parameters $MN_{MPD}$ and $MN_C$, the agreement was assessed between the two datasets overall and for every reader. The four-point scale analysis was dichotomized into two categories: "absent" MN with values 0 and 1; "present" MN with values 2 and 3. In case of discordant evaluation for an additional cyst with MN recorded in one imaging dataset for one patient, but not at all recorded in the other dataset for the same patient, the $D_C$ of this additional lesion was excluded from the comparative analysis.

*Study II and III*

In study part 2, we chose the closest MRI to the surgery date for the imaging analysis. Two radiologists with similar experience in pancreatic imaging (RPM and NK, 15 and 12 years of experience in abdominal imaging, respectively) evaluated the MR-images in consensus on a picture archiving and communication system (Sectra Workstation, IDS7 version 23.1, Sectra AB), choosing one BD-IPMN per patient (i.e., the largest or the most suspicious). The imaging features collected for the analysis in study 2 are shown in Table 4.

| Imaging parameters | Description |
|---|---|
| **Diameter 1 (Diam1)** | maximum cyst diameter on axial T2-weighted sequence (mm) |
| **Diameter 2 (Diam2)** | maximum cranio-caudal cyst diameter on coronal T2-weighted sequence (mm) |
| **Cyst maximum diameter** | either Diam1 or Diam2, depending on which was largest (mm) |
| **Elongation value (EV)** | defined as [1-(width/length)] according to previous publication [69], where length was represented by the maximum diameter irrespective of the plane, and width as the maximum diameter perpendicular to the length |
| **Maximum MPD diameter** | expressed in mm |
| **Mural nodules (MN)** | presence of contrast-enhancing mural nodules within the cyst |
| **Cystic wall thickening** | present when cystic wall thickness ≥ 2 mm |
| **Progress in size during follow-up** | ≥5 mm/year according to EG [7] |
| **Solitary/multifocal BD-IPMN** | |
| **Lesion localization** | head/uncinate process or body/tail |
| **Cyst volume (Vsegm)** | calculated on axial T2-w images after file export to a free DICOM medical imaging viewer (Horos v2.1.1). A region of interest (ROI) was drawn along the edge of the BD-IPMN at multiple levels using the tool "ROI volume" available in the semi-automatic three-dimensional segmentation software implemented in the viewer. The common bile duct and the MPD were excluded from the segmentation. Thereafter, the volume was automatically calculated by the software |
| Abbreviations: MPD: main pancreatic duct; EG: European evidence-based guidelines; BD-IPMN: branch-duct IPMN. | |

***Table 4.*** *Imaging features collected in study part 2 [reprinted and modified with permission. Source: Pozzi Mucelli RM et al.* [82]*. Creative Commons CC BY 4.0, https://creativecommons.org/licenses/by/4.0/]*

For study part 3, only the maximum cystic diameter, cyst location, presence of contrast-enhancing MN, and multifocality were collected. The cystic segmentation required for the Radiomics analysis was performed independently by the same two radiologists as in study part 2, with an open-source volume segmentation tool (MedSeg [83], available at https://www.medseg.ai/), after uploading previously anonymized T2-weighted axial DICOM images. The radiologists traced the selected BD-IPMN using the brush tool, including cystic wall and avoiding the bile duct and/or the MPD from the volume of interest (VOI). The MedSeg tool also provided the volume (in $cm^3$) for the segmented lesion that was saved and collected.

*Study IV*

For study part 4, the same two radiologists as in studies 2 and 3 reviewed in consensus the radiological reports and the images, and collected the following imaging parameters:

1) type of detected lesion (cystic lesions– including dilatation of the MPD-; solid lesions; coexistence of cystic and solid changes);
2) features of solid lesions (size, location, vascular pattern);
3) features of cystic lesions:
   a) size, location, uni/multifocality and number of cystic lesions;
   b) presence of imaging risk factors, such as contrast-enhancing MN, size progression (≥ 5 mm/year), dilated MPD (≥ 5 mm);

c) hypothetical working diagnosis:
    i) BD-/main-duct/mixed-type IPMN (BD-IPMN defined as a cystic lesion ≥5 mm with communication with the MPD; main-duct IPMN: diffuse or focal MPD dilatation ≥5 mm, without visible causes of obstruction; mixed-type IPMN: a combination of BD- and main-duct type)
    ii) unspecific cyst if size <5 mm;
    iii) other cysts, such as serous cystic neoplasm or mucinous cystic neoplasm;
4) diameter of the MPD.

Moreover, we categorized all the patients in ten different clinical scenarios (Table 5).

## 4.5 CLINICAL AND HISTOPATHOLOGICAL FEATURES

*Clinical features*

Demographic information (age, gender) was collected. Regarding the patient's age, in study part 1, we collected the age the patient had at the examination date. For patients included in studies 2 and 3, we considered the age at pancreatic surgery. For study part 4, we recorded the age at the imaging baseline.

In study 1, we collected whether the examinations were either performed within the framework of surveillance or in the preoperative setting. The type of surgery was also documented. For studies 2 and 3, we recorded the presence of symptoms (acute pancreatitis, weight loss, jaundice, abdominal pain, and new-onset diabetes) and serum levels of CA19-9, as well as the familial/hereditary status of PC. Furthermore, for study 4, detailed data regarding the familial history (number of FDR and SDR), the results from genetic testing – if performed-, gender, body mass index, history of alcohol overconsumption, smoking, chronic pancreatitis, and diabetes mellitus were also recorded. Finally, pancreatic surgery or biopsy, adjuvant or palliative chemotherapy, and TNM were documented in the database of IAR patients.

*Histopathological features*

In case of pancreatic surgery, histopathological data were recorded. For studies 2 and 3, histopathological features were reviewed side-by-side by a pathologist with experience in pancreatic pathology (CFM) in consensus with a dedicated radiologist (RPM), if the information provided in the histopathological report was deemed insufficient (histotype, grade of dysplasia and its location within the cyst or the MPD). If pancreatic surgery was not performed (e.g., metastatic disease), the result from liver biopsy and/or endoscopic biopsy was reported.

***Table 5.*** *Individuals at risk for familial/hereditary PC were categorized in ten clinical scenarios in study 4.*

| Scenario | Imaging findings at baseline | Imaging findings at follow-up | Interventions/actions |
|---|---|---|---|
| 1 | No findings | No findings | Ordinary surveillance |
| 2 | No findings | Onset of a solid lesion (i.e., PC, pNET, benign lesion) | - surgery ±(neo)adjuvant chemotherapy<br>- palliation or best supportive<br>- back to surveillance (if benign finding) |
| 3 | No findings | Onset of a cystic lesion with iRF | Surgery |
| 4 | No findings | Onset of a cystic lesion(s) without iRF<br>→ F/U → onset of iRF or solid lesion | Surgery |
| 5 | No findings | Onset of a cystic lesion(s) without iRF<br>→ F/U<br>→ unchanged (or regress) during F/U | Ordinary surveillance |
| 6 | Solid lesion | - | - surgery ±(neo)adjuvant chemotherapy<br>- palliation or best supportive<br>back to surveillance (if benign finding) |
| 7 | Cystic lesion without iRF | Onset of iRF or solid lesion | - surgery<br>- further controls or stop screening due to age/comorbidity/patient's refusal |
| 8 | Cystic lesion without iRF | Unchanged (or regress) during F/U | Ordinary surveillance |
| 9 | No findings or presence of cystic lesion(s) without iRF | No findings or unchanged cystic lesion(s) without iRF<br>→ onset of interval cancer, defined as:<br>- onset of symptoms: CT/MRI→ PC<br>- detection of a suspicious mass at CT/MRI performed for other reasons in between screening | - surgery ±(neo)adjuvant chemotherapy<br>- palliation or best supportive<br>back to surveillance (if benign finding) |
| 10 | Cystic lesion(s) with iRF (relative/absolute indication for surgery) | - | - surgery<br>- further controls or stop screening due to age/comorbidity/patient's refusal |

Abbreviations: PC, pancreatic cancer. pNET, pancreatic neuroendocrine tumour. iRF, imaging Risk Factors. F/U, follow-up

## 4.6 COST ANALYSIS

In study 1, we estimated the cost reduction from replacing the CP with the SP in the surveillance of patients with pancreatic cystic lesions through three different paths.

First, we calculated the approximate cost of the SP based on the cost of the CP, as reported in the 2015 invoice policy of Karolinska University Hospital. The estimation of the SP cost kept into consideration the removal of the injected contrast agent, the shorter MRI-technologist time for preparation, as well as a shorter MRI examination and reading.

Second, we calculated the cost for the surveillance of a hypothetical individual, at the age of 45, after incidental identification of a suspected IPMN. Following the guidelines available at the time this study was performed [81], we determined the total number of MRIs this individual patient ($MRI_{totalIP}$) would perform during his/her life until the age of 80, presuming that the patient would not need pancreatic surgery due to malignant transformation. The age limit of 80 years was set in keeping with the estimated life expectancy in Sweden in 2014 [84]. The cost reduction for this hypothetical individual patient ($CR_{IP}$) was calculated as follows:

$$CR_{IP} = (\text{Cost CP - cost SP}) \times MRI_{totalIP}$$

Third, we estimated the cost reduction for the entire study cohort. We determined the length of the follow-up for every included patient, with starting point set at the date the patient was first discussed at the multidisciplinary conference and an endpoint set at one of the following: a) arbitrary date of 1 May 2015 (if the patient was still deemed fit for surgery); b) the date the patient turned 80; c) the date, when the patient was considered no fit for surgery; d) the date of decease (regardless the cause). According to the previously available guidelines [81], we calculated the total number of MRI ($MRI_{totalCohort}$) all the patients would perform, assuming the guidelines were already in place in 2005 and full compliance with the surveillance protocol from the patients. The cohort's cost reduction ($CR_{Cohort}$) was determined with the following formula:

$$CR_{Cohort} = (\text{Cost CP - cost SP}) \times MRI_{totalCohort}$$

## 4.7 STATISTICAL ANALYSIS

For all the studies, numerical and categorical data were reported as means/medians and proportions, as appropriate. A two-side p-value $< 0.05$ was considered statistically significant for all four study parts.

*Study I*

Differences among readers of continuous variables ($D_C$ and $D_{MPD}$) were tested with analysis of variance (ANOVA). Thereafter, a post-hoc test by means of multiple comparisons was used in case of statistically significant results at ANOVA. The Student's t-test for paired data was applied to test variables' differences between the CP and SP for each reader. The results

were controlled with the Wilcoxon signed-rank (corrigendum of the published version of study 1). For the evaluation of internal consistency among readers with continuous variables (cyst number, $D_C$ and $D_{MPD}$), the intraclass correlation coefficient (ICC) was calculated with the Cronbachs' Alpha standardized test [85, 86]. Yule's Q test was used to assess the inter-observer agreement with categorical variables (presence/absence of $MN_C$ and $MN_{MPD}$) [87, 88]. All the analyses were performed with SAS software (SAS version 9.4, SAS Institute Inc., Cary, NC, USA).

*Study II*

For evaluating the presence of an association between the outcome "high-grade dysplasia/invasive cancer" (HGD/INV), the Wilcoxon rank sum test and Pearson's chi-squared test were used for numerical and categorical variables, respectively. In case of < 5 expected frequencies, the Fisher's exact test was applied instead of the Pearson's chi-squared test. Univariable logistic regression was performed to assess the strength of association between variables and the outcome HGD/INV, with the calculation of odds ratios (OR) and 95% confidence intervals (CI). The features MPD diameter and serum levels of CA19-9 were dichotomized in two categorical variables [MPD ≥ 5 mm (yes/no); CA19-9 >37 U/mL (yes/no), respectively] for the logistic regression analysis, according to the cut-off values proposed by guidelines [7]. The variables that resulted statistically significant at univariable logistic regression were assessed with multivariable logistic regression ("enter" method), adjusted for age and gender. Thereafter, we derived from the logistic model the predicted probabilities for the outcome HGD/INV in a hypothetical male at age ≥ 70, with and without the statistically significant variables entered in the multivariable regression analysis. We also calculated the observed probabilities for the outcome HGD/INV in relation to the sum of the variables above. Thereafter, we calculated the diagnostic sensitivity, specificity, positive and negative predictive values for the clinical and imaging concerning features, taken alone. Stata16 (StataCorp. 2019, Stata Statistical Software: Release 16, StataCorp LLC) was used for the analyses.

*Study III*

The complex mathematical and statistical radiomics analysis for this study part is described in detail in section 4.8.

*Study IV*

Pearson's chi-squared test and Fisher's exact test were used for analysing associations between categorical variables. Parametric tests such as Student's t-test for independent data and ANOVA were used to compare normally distributed variables, after testing for normality with the Shapiro-Wilk test. For non-normally distributed variables, the non-parametric analogue tests (Wilcoxon rank-sum and Kruskal-Wallis, respectively) were applied. Univariable logistic regression analysis was performed to assess the strength of association between binary outcomes (i.e., presence of malignancy, solid and cystic lesions) and clinical and imaging features. Diagnostic accuracy metrics for the screening program were calculated by setting: a) the true positive, as patients with malignant lesions (PC and/or high-grade dysplasia) correctly identified by imaging; b) false positive, as those that underwent surgery due to a suspicious finding with a final benign diagnosis at histopathology; c) false negative,

as those with interval cancer (regardless of the cause); d) true negative, as patients with a follow-up of at least 12 months, without suspicious lesions at imaging and histopathology. Stata17 (StataCorp. 2019. Stata Statistical Software: Release 17. StataCorp LLC) was used for the statistical analysis.

## 4.8 RADIOMICS ANALYSIS

The radiomics analysis consisted of several steps that are summarized in Figure 7. Images with degraded segmentations or unavailable CA19-9 values were not included in the radiomics analysis (Figure 4).

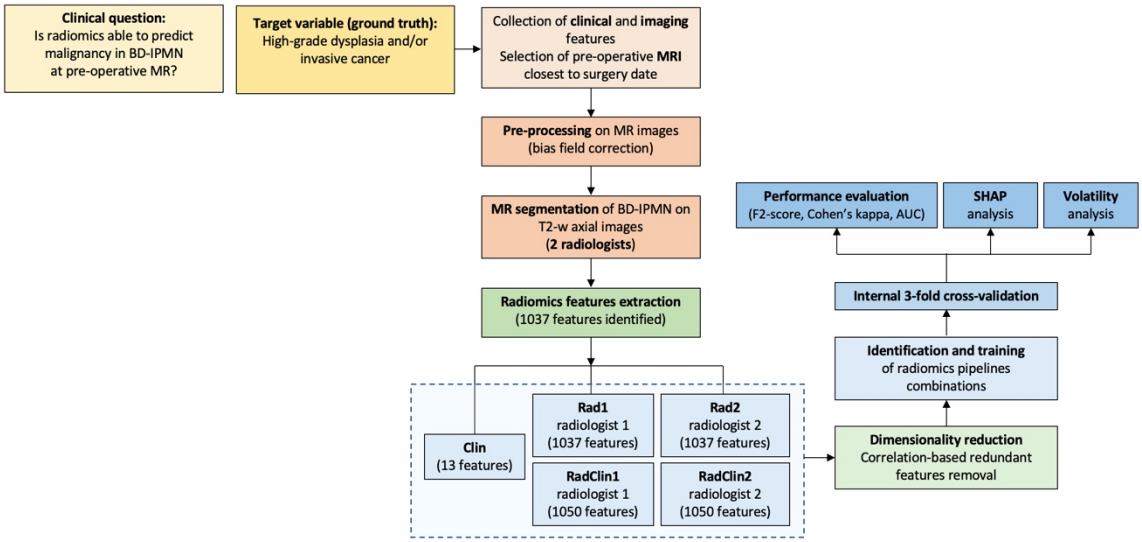


***Figure 7.*** *Radiomics pipeline for study 3.*

*Imaging pre-processing and radiomics features extraction*

The *N4 Bias Field Correction Image Filter* function of the Python package Simple ITK (version 2.0.0; available at https://simpleitk.org/) was used to remove from the images the bias field signal. Each image's x-, y-, and z-spacing was checked for discrepancies. Thereafter, feature extraction was performed in a 2D manner, as the x- and y-spacings differed from z-spacing. Additionally, since images' x- and y-spacings differed within and among patients, x- and y-spacings were resampled to the highest value of 1.6797. For all image filters, except for local binary pattern, a bin width of 25 was selected to produce between 30 and 130 bins. For the local binary pattern filter, a binwidth of 7 was used, which was the only way to achieve informative features even though it resulted in a histogram with over 130 bins. Finally, image intensities were normalized.

We extracted the radiomics features from the segmented BD-IPMN using the package Pyradiomics (version 3.0) in Python (v. 3.7.9; available at https://www.python.org/) [89]. All the pre-processing steps mentioned before were performed as parameters of the extractor function, except for bias field correction, which was performed before the extraction. All the image filters and feature classes were enabled, resulting in a total of 1037 extracted features. All the mathematical expressions and semantic meanings of the features extracted are explained at https://pyradiomics.readthedocs.io/en/latest/ [89].

*Spatial and cross-vendor stability of radiomics features*

The stability of the predictors depends on the segmentation margins, which in turn depends on each radiologist's segmentation manner. For this reason, the spatial stability of radiomics features was assessed. A two-way, single-rater, absolute agreement ICC [model (ICC 2.1)] was used for comparing the extracted features from the VOIs created by each radiologist [86]. Features with ICC > 0.75 were considered spatially stable and robust to segmentation. We assessed the cross-vendor stability by comparing the features extracted from each of the three available vendors with the Kruskal-Wallis test. Features without significant differences were considered stable across vendors and robust. Spatial and cross-vendor stability analyses were performed in Python (v. 3.7.9; https://www.python.org/), applying the package *icc* (https://pypi.org/project/icc/) and the *kruskal* function of the Python scipy package (version 1.7.3 https://scipy.org/).

*Dataset construction*

Different types of training data were compared in a binary outcome (LGD versus HGD/INV). The clinical dataset (Clin) consisted of 13 variables: volume ($cm^3$), maximum cystic diameter (mm), symptoms (such as jaundice, weight loss, abdominal pain, acute pancreatitis, steatorrhea, new-onset diabetes, expressed as binary categorical variables), serum levels of CA19.9 (U/mL), CA19.9>37 U/mL, age at surgery and gender (male set as 1). For each radiologist, one radiomics dataset (Rad) was generated (Rad1 and Rad2), including 1037 extracted radiomics features each. Thereafter, two "hybrid" datasets were created, derived from the combination of the clinical dataset and the two radiomics datasets (RadClin), with 1050 radiomics and clinical features for each (RadClin1 and RadClin2).

*Model development*

The first step consisted in removing redundant and correlated features. Features pairs were considered correlated if their Spearman correlation coefficient was > 0.75. Out of the two, the feature with the highest average correlation across all features was eliminated.

Thereafter, different pipeline combinations were trained. The removal of unstable features was optional so as not to permanently exclude potentially predictive variables. Specifically, two versions of each pipeline were trained: one including only stable features and the other including the full set of stable and unstable features. The pipelines with the highest performance were selected.

Due to the high dimensional feature space, we explored a computationally "light" tree-based feature selection algorithm, where the features with the highest tree importance were selected. The number of features selected was a hyperparameter optimized during model training. Finally, the scikit learn implementation of 6 machine learning algorithms was compared (Random Forest Classifier, Logistic Regression with L1 or L2 regularization, K-nearest Neighbours Classifier, Gaussian Process Classifier, AdaBoost Classifier, Gradient Boosting Classifier). Hyperparameter tuning was performed for each algorithm in a nested cross-validation fashion with an exhaustive grid search.

The different combinations resulted in 384 pipelines trained with:

- full dataset (stable and unstable features) or only stable features
- feature selection of 10, 15, 20, 25, 30, 35 or 40 features or no feature selection
- six machine learning algorithms
- two radiologists
- two data types: Rad dataset or RadClin dataset

The classifiers were internally validated through 3-fold cross-validation, and the performance was evaluated employing F2-score, Cohen's Kappa, and area under the receiver operating characteristic curve (AUC). For each of the five datasets (Clin, Rad1, RadClin1, Rad2 and RadClin2), the pipeline with the highest performance was selected. Dummy classifiers were also trained for comparison purposes. A flowchart summarizing the whole process is provided in Figure 7.

*Model assessment*

We compared the AUC of selected classifiers against a dummy classifier (trained to identify the majority class, i.e., LGD) and against each other using the DeLong test [90], corrected for multiple comparisons with the False Discovery Rate (FDR) correction [91, 92]. We performed a SHapley Additive exPlanations (SHAP) analysis [93] to identify which variables had the largest impact in predicting the outcome. Finally, we conduct a volatility analysis to assess the overfitting degree. The dataset was randomly split into a train and a test set with 100 different iterations. All the train and test sets partitions' performances were calculated, and their distribution was compared. The volatility analysis was performed with the Probatus package (https://ing-bank.github.io/probatus/).

# 5 RESULTS

## 5.1 STUDY I

The final population comprised 154 patients (52% males) with a median age of 66 years (IQR 58-72 years). Most of the MRIs (75%, 116/154) were performed for the surveillance of a pancreatic cystic lesion. The remaining MRIs were acquired either as a preoperative examination or during the postoperative follow-up of IPMN (Table 6).

| **Study population (study 1)** | | | | |
|---|---|---|---|---|
| N. patients | 154 | | | |
| Gender | 75 females (48%) | | 81 males (52%) | |
| Age | median 66 years (IQR 58-72) | | | |
| **Indication for MRI** | | | | |
| **Surveillance** | **Preoperative MRI** | | **Postoperative MRI follow-up** | |
| 116/154 | 14/154 | | 24/154 | |
| | **Type of surgery** | | | |
| | Pancreaticoduodenectomy | 7/14 | Pancreaticoduodenectomy | 11/24 |
| | Distal pancreatectomy (DP) | 1/14 | DP | 2/24 |
| | DP + splenectomy | 3/14 | DP + splenectomy | 7/24 |
| | Total pancreatectomy (TP) | 2/14 | Cystic enucleation | 3/24 |
| | TP + splenectomy | 1/14 | Central pancreatectomy | 1/24 |
| | **Histopathological diagnosis** | | | |
| | Mixed type IPMN | 8 (7 LGD; 1 HGD) | Mixed type IPMN | 13 (11 LGD; 2 HGD) |
| | BD-IPMN | 1 (LGD) | BD-IPMN | 10 (9 LGD; 1 INV) |
| | PDAC+BD-IPMN | 1 | | |
| | PDAC+mixed type IPMN | 1 | | |
| | SCN | 1 | MCN | 1 |
| | Retention cyst | 1 | | |
| | Chronic pancreatitis | 1 | | |

Abbreviations: DP, distal pancreatectomy; TP, total pancreatectomy; LGD, low-grade dysplasia; HGD, high-grade dysplasia; INV, invasive cancer; PDAC, pancreatic adenocarcinoma; SCN, serous cystic neoplasm; MCN, mucinous cystic neoplasm

***Table 6.*** *Demographic of the study population (study 1). Reprinted and modified with permission from Springer Nature.*

In the datasets evaluation, the three readers identified 157, 156 and 155 cystic lesions (reader 1, reader 2 and reader 3, respectively) with the largest diameter and/or concerning imaging features, for a total of 468 cysts. In most of the cases, the three readers described only one lesion (144, 129, 137 in readers 1, 2 and 3, respectively); two lesions were recorded in 5, 12 and 6 cases by readers 1, 2 and 3, respectively; three lesions were recorded in 1, 1 and 2 cases by reader 1, 2 and 3; cases without any lesions were reported in 4, 12 and 9 cases by reader 1, 2, and 3 respectively (corrigendum of the published version of study 1).

To analyse the mean cystic largest diameter $D_C$, 435 cysts were included (152, 143 and 140 from reader 1, reader 2 and reader 3, respectively). Overall, the mean $D_C$ corresponded to 21.4±14 mm for the SP and 21.7±14 mm for the CP, with a statistically significant difference of 0.3 mm (p=0.02). The overall mean $D_{MPD}$ was 3.52±2.7 mm for the SP and 3.58±2.6 mm

for the CP, with a not statistically significant difference of 0.06 mm (p=0.12). Table 7 shows the overall and per reader results for the $D_C$ and $D_{MPD}$ analysis.

For the analysis of the variable $MN_C$, 443 cysts were included (154, 147 and 142 from readers 1, 2 and 3 respectively). The SP and CP showed an overall agreement for the presence/absence of $MN_C$ and $MN_{MPD}$ of 93% and 98%, respectively (Table 7).

| Variable | Overall | | | Reader 1 | | | Reader 2 | | | Reader 3 | | |
|---|---|---|---|---|---|---|---|---|---|---|---|---|
| | CP | SP | Diff. | CP | SP | Diff. | CP | SP | Diff. | CP | SP | Diff. |
| **$D_C$ (mm)[a]** | 21.7 | 21.4 | 0.3* | 21.1 | 20.9 | 0.2 | 22.3 | 21.5 | 0.8* | 21.71 | 21.73 | 0.02 |
| **$D_{MPD}$ (mm)[a]** | 3.58 | 3.52 | 0.06 | 3.81 | 3.73 | 0.08 | 3.27 | 3.24 | 0.03 | 3.64 | 3.58 | 0.06 |
| **$MN_C$** | 93% | | | 90% | | | 93% | | | 97% | | |
| **Nr of cases** | 412/443 | | | 138/154 | | | 136/147 | | | 138/142 | | |
| **$MN_{MPD}$** | 98% | | | 98% | | | 98% | | | 99% | | |
| **Nr of cases** | 451/460[b] | | | 150/154 | | | 149/152[b] | | | 152/154 | | |

Abbreviations: CP, comprehensive protocol; SP, short protocol; Diff., differences in mean value between CP and SP
[a]Mean value; [b]data were missing in 2 cases. *Statistically significant difference.

***Table 7.*** *Results for the comparison between comprehensive (CP) and short protocol (SP) in the evaluation of the cystic diameter (DC) and MPD diameter, expresses as means, as well as for the presence/absence of MN within the cyst and the MPD. Reprinted and modified with permission from Springer Nature.*

The interobserver agreement was at least very strong for the $D_C$ and $D_{MPD}$ (Table 8). Similarly, the pairwise concordances among readers for the variables $MN_C$ and $MN_{MPD}$ were also strong (Table 8).

| Variable | ICC[a] | | Reader 1 vs 2[b] | | Reader 1 vs 3[b] | | Reader 2 vs 3[b] | |
|---|---|---|---|---|---|---|---|---|
| | CP | SP | CP | SP | CP | SP | CP | SP |
| **Nr of cysts** | 0.89 | 0.86 | | | | | | |
| **$D_C$** | 0.96 | 0.97 | | | | | | |
| **$D_{MPD}$** | 0.95 | 0.95 | | | | | | |
| **$MN_C$** | | | 0.83 | 0.89 | 0.94 | 0.93 | 0.75 | 0.85 |
| **$MN_{MPD}$** | | | 0.90 | 0.88 | 1 | 1 | 1 | 1 |

Abbreviations: ICC, intra-class correlation coefficient; CP, comprehensive protocol; SP, short protocol.
[a] ICC was calculated with Cronbach's alpha standardized test; ICC ≥ 0.8 indicates a very high level of agreement.
[b] Pairwise comparisons among users were performed with Yule's Q test; a value ≥ 0.75 indicates a strong relationship.

***Table 8.*** *Interobserver agreement for the evaluation of the total cyst number, the diameter of the largest cyst ($D_C$) and main pancreatic duct ($D_{MPD}$), as well as the presence/absence of mural nodules (MN) in the cyst and in the MPD. Reprinted and modified with permission from Springer Nature.*

## *Cost analysis*

The estimated cost of the SP was set at 25% of the CP. Since the CP in 2015 cost 1043 EUR at our institution, the cost of the SP corresponded to 260 EUR. The calculated number of MRIs for the hypothetical individual patient was 64; the cost reduction for the individual patient was $CR_{IP}$= (cost CP - cost SP) x $MRItotal_{IP}$ = (1043-260) x 64 = 50,112 EUR. For the entire cohort, the number of examinations ($MRI_{totalCohort}$) corresponded to 711 (521 MRIs for the 116 not resected individuals; 190 MRIs for the operated patients). Thus, the $CR_{Cohort}$ = (Cost CP - cost SP) x $MRI_{totalCohort}$ = (1043-260) x 711 = 556,713 EUR.

## 5.2 STUDY II

The final study cohort included 106 patients. As shown in the flowchart for study II (Figure 4), we excluded 24 patients because of the presence of a mass-forming PC as a cause of a MPD stricture. The demographic characteristics of the included patients are displayed in Table 9. Twenty-five (27/106) patients had HGD/INV at final histopathology (8 with invasive cancer and 19 HGD). Mixed-type IPMN and gastric histological cell subtype were the most prevalent types (74% and 70%, respectively) (Table 9).

Contrast-enhancing MNs were detected in 14 patients (13%) with a mean size of 12 mm (range, 4-32 mm). Half of the MN were identified in patients with HGD/INV (3 HGD and 4 INV) (Table 9). Although contrast-enhancing MNs were associated with the presence of HGD/INV (p=0.043), their size was not statistically significantly different among patients with LGD or HGD/INV (p= 0.3).

The BD-IPMN's volume was neither statistically significantly different depending on the grade of dysplasia (p=0.19), nor associated with malignancy (HGD/INV) in univariable logistic regression (alone or combined with the EV) (Table 10).

The mean EV was 0.36±0.16. The highest EV was 0.67, and its interquartile range 0.25- 0.5, showing that none of the BD-IPMN had a perfect spheric appearance. We observed a trend towards an inverse association between EV and HGD/INV, although not statistically significant (OR=0.38, 95% 0.02-5.93, p=0.49). Similarly, the predicted probabilities for having HGD/INV slightly diminished by incrementing the EV (Figure 8). Other morphological variables (maximum cystic diameter, wall thickening, multifocality, size progression) were not associated with HGD/INV at univariable logistic regression (Table 10).

We observed that only two morphological variables (contrast-enhancing MN, diameter of the MPD ≥ 5mm) and one laboratory variable (CA19-9 >37 U/mL) resulted correlated to HGD/INV at univariable logistic regression (Table 10), which was corroborated even in the subsequent multivariable logistic regression model adjusted for age and gender (Table 10).

The predicted probabilities for HGD/INV in a hypothetical 70-year-old man gradually increased from 0.08 if none of the previous variables was present (MN, MPD ≥5mm and CA19-9 >37 U/mL), to 0.92 when all the three variables were added (Figure 9). The observed probabilities for developing LGD or HGD/INV with none/one/more than one of the aforementioned features are shown in Table 11.

The diagnostic metrics for the individual resection criteria (according to the EG) are reported in Table 12. Noteworthy, the dilated MPD (≥ 5 mm) was the only resection criterion in 15 cases, of whom three had HGD/INV at final histopathology (20%). The sensitivity and positive predictive value (PPV) were 11% and 20 %, respectively (95% CI: 2-29%; and 43-48%).

| Variable | N (%) | Low-grade dysplasia (N, %) | High-grade dysplasia /Invasive cancer (N, %) |
|---|---|---|---|
| **Males** | 45/106 (42%) | 31/45 (69%) | 14/45 (31%) |
| **Age (years)** | median 70 (IQR 64-74)<br>(min 43, max 86) | median 70 (IQR 64-73)<br>(min 43, max 86) | median 70 (IQR 62-74)<br>(min 48, max 86) |
| **Individuals at risk** | 3/106 (3%)<br>(2 FPC; 1 Peutz-Jeghers) | 3/3 (100%) | 0 |
| **Histology** | | | |
| LGD | 79/106 (75%) | | |
| HGD/INV | 27/106 (25%) | | 8/106 (7.5%) INV<br>8/27 (29%) INV |
| *Mixed-type IPMN* | 78/106 (74%) | 53/79 (67%) | 25/27 (93%) |
| – BD-IPMN at pre-op MRI | 25/78 (32%) | 21/53 (40%) | 4/25 (16%) |
| – Mixed-type IPMN at pre-op MRI | 53/78 (68%) | 32/53 (60%) | 21/25 (84%) |
| *Histological cell subtypes* | | | |
| – Gastric | 75/106 (70%) | 63/79 (80%) | 12/27 (44.5%) |
| – Pancreato-biliary (PB) | 5/106 (5%) | 2/79 (2.5%) | 3/27 (11%) |
| – PB + gastric | 4/106 (4%) | 3/79 (4%) | 1/27 (4%) |
| – Intestinal | 7/106 (7%) | 2/79 (2.5%) | 5/27 (18.5%) |
| – Intestinal + gastric | 14/106 (13%) | 8/79 (10%) | 6/27 (22%) |
| – PB + gastric + intestinal | 1/106 (1%) | 1/79 (1%) | 0/27(0%) |
| **Symptoms**[a] | 32/106 (30%) | 21/79 (27%) | 11/27 (41%) |
| Jaundice | 3/106 (3%) | 1/79 (1%) | 2/27 (7%) |
| Weight loss | 3/106 (3%) | 2/79 (2%) | 1/27 (4%) |
| Abdominal pain | 13/106 (12%) | 9/79 (11%) | 4/27 (15%) |
| Acute pancreatitis | 15/106 (14%) | 9/78 (11%) | 6/27 (22%) |
| Diabetes (recent onset <1 year) | 0/53 (0%) | | |
| **Serum CA 19-9 (U/mL)**[b] | median 11 (IQR 6-29)<br>min 0.3, max 30359 | median 8.8 (IQR 4.8-21)<br>min 0.3, max 60 | median 29 (IQR 10-74)<br>min 1, max 30359 |
| CA 19-9 >37 U/mL[b] | 18/104 (17%) | 9/77 (12%) | 9/27 (33%) |
| **IPMN localization** | | | |
| Head/uncinate process | 59/106 (56%) | 42/79 (53%) | 17/27 (63%) |
| **Imaging features IPMN** | | | |
| BD-IPMN at pre-op MRI | 47/106 (44%) | 41/79 (52%) | 6/27 (22%) |
| Mixed-type IPMN at pre-op MRI | 59/106 (56%) | 38/79 (48%) | 21/27 (78%) |
| Cyst max diameter (mm) | median 33 (IQR 24-42)<br>min 9, max 100 | median 32 (IQR 24-41)<br>min 10, max 77 | median 36 (IQR 24-47)<br>min 9, max 100 |
| Diameter ≥ 30 mm | 65/106 (61%) | 47/79 (59%) | 18/27 (67%) |
| Diameter ≥ 40 mm | 37/106 (35%) | 25/79 (32%) | 12/27 (44%) |
| Elongation value[c] | mean 0.36±0.16 | mean 0.37±0.16 | mean 0.34±0.16 |
| Volume ($cm^3$) | median 9.7 (IQR 4-19)<br>min 0.3, max 424.2 | median 9.4 (IQR 3-17)<br>min 0.3, max 125.8) | median 11.4 (IQR 5-22)<br>min 0.5, max 424.2 |
| **MPD max diameter (mm)** | mean 5.8±3.3<br>median 5.1 (IQR 3.1-7.4)<br>min 1.5, max 19 | mean 5.3±2.9<br>median 4.9 (IQR 3-6.8)<br>min 2, max 15 | mean 7.2±4.1<br>median 6.6 (IQR 5.1-9.1)<br>min 1.5, max 19 |
| MPD ≥ 5 mm | 59/106 (56%) | 38/79 (48%) | 21/27 (78%) |
| – MPD 5-9.9 mm | 48/106 (45%) | 32/79 (40%) | 16/27 (59%) |
| – MPD ≥ 10 mm | 11/106 (10%) | 6/79 (8%) | 5/27 (18%) |
| **Contrast-enhancing mural nodules** | 14/106 (13.2%) | 7/79 (8.9%) | 7/27 (25.9%) |
| Size mural nodules (mm) | 12.1±7.6 (min-max 4-32) | 9.2±3.9 (min-max 5.3-17) | 15±9.6 (min-max 4-32) |
| Wall thickness ≥ 2mm | 6/106 (6%) | 3/79 (4%) | 3/27 (11%) |
| Solitary lesion | 39/106 (37%) | 30/79 (38%) | 9/27 (33%) |
| Progress in size (>5mm/year) | 29/106 (27%) | 24/79 (30%) | 5/27 (18%) |

Abbreviations: FPC, familial pancreatic cancer; LGD, low-grade dysplasia; HGD/INV, high-grade dysplasia/invasive cancer; pre-op, preoperative; MPD, main pancreatic duct; MN, mural nodules

[a]Four patients had ≥2 symptoms. [b]Preoperative CA19-9 was not available in 2 patients. [c]Elongation value=[1-(width/length)].

***Table 9.*** *Characteristics of the 106 patients included in study 2 [reprinted and modified with permission. Source: Pozzi Mucelli RM et al.* [82]*. Creative Commons CC BY 4.0, https://creativecommons.org/licenses/by/4.0/]*

| Patients' features | Univariable logistic regression analysis | | | |
|---|---|---|---|---|
| | **Nr. observations** | **Odds ratio** | **95% C.I.** | ***p*-value** |
| ***Demographic and clinical features*** | | | | |
| Age (years) | 106 | 1.01 | 0.96-1.06 | 0.63 |
| - Age ≥70 (cohort's median age) | 106 | 1.05 | 0.44-2.51 | 0.91 |
| - Age <70 | 106 | 0.95 | 0.39-2.28 | 0.91 |
| Gender (male) | 106 | 1.67 | 0,69-4.01 | 0.26 |
| Localization (head/uncinate) | 106 | 1.50 | 0.61-3.67 | 0.38 |
| Mixed-type IPMN | 106 | 6.13 | 1.34-27.89 | 0.02 |
| Symptoms | 106 | 1.90 | 0.76-4.74 | 0.17 |
| - Abdominal pain | 106 | 1.35 | 0.38-4.81 | 0.64 |
| - Acute pancreatitis | 106 | 2.22 | 0.71-6.97 | 0.17 |
| - Jaundice[a] | 106 | 6.24 | 0.54-71.76 | 0.14 |
| - Weight loss | 106 | 1.48 | 0.13-17.01 | 0.75 |
| Serum CA19-9 (U/mL) | 104 | 1.04 | 1.01-1.06 | **0.002** |
| CA19-9 >37 U/mL | 104 | 3,77 | 1.30-10.9 | **0.014** |
| ***Imaging-related features*** | | | | |
| Volume ($cm^3$) | 106 | 1.01 | 0.99-1.02 | 0.12 |
| Cyst max diameter (mm) | 106 | 1.02 | 0.99-1.04 | 0.18 |
| Diameter ≥ 30 mm | 106 | 1.36 | 0.54-3.4 | 0.51 |
| Diameter ≥ 40 mm | 106 | 1.72 | 0.7-4.22 | 0.23 |
| Elongation value | 106 | 0.38 | 0.02-5.93 | 0.49 |
| MPD max diameter (mm) | 106 | 1.17 | 1.02-1.33 | **0.02** |
| MPD ≥ 5 mm | 106 | 3.97 | 1.45-10.89 | **0.007** |
| - MPD 5-9.9 mm | 106 | 2.13 | 0.87-5.19 | 0.09 |
| - MPD ≥10 mm | 106 | 2.76 | 0.77-9.93 | 0.12 |
| Mural nodules | 106 | 3.6 | 1.13-11.47 | **0.03** |
| Wall thickness ≥ 2mm | 106 | 3.16 | 0.59-16.73 | 0.17 |
| Solitary lesion | 106 | 0.81 | 0.32-2.05 | 0.66 |
| Multifocal lesions | 106 | 1.23 | 0.49-3.07 | 0.66 |
| Progress in size (≥5mm/year)[b] | 67 | 1.01 | 0.36-2.8 | 0.98 |
| **Multivariable logistic regression analysis** | | | | |
| Mural nodules | 104 | 4.32 | 1.18-15.76 | **0.02** |
| MPD ≥ 5 mm | 104 | 4.2 | 1.34-13.1 | **0.01** |
| CA19-9 >37 U/mL | 104 | 6.72 | 1.89-23.89 | **0.003** |
| Age at surgery (years) | 104 | 1.01 | 0.95-1.07 | 0.61 |
| Gender (male) | 104 | 1.97 | 0.69-5.67 | 0.20 |

Abbreviations: C.I., confidence interval; MPD, main pancreatic duct

[a]No association was found between jaundice and elevated CA19-9 (Fisher's exact test, p=0.56)

[b]Calculated on 67 observations (39 subjects had no previous examinations)

***Table 10.*** *Uni- and multivariable logistic regression analysis (study 2) [reprinted and modified with permission. Source: Pozzi Mucelli RM et al.* [82]*. Creative Commons CC BY 4.0, https://creativecommons.org/licenses/by/4.0/*

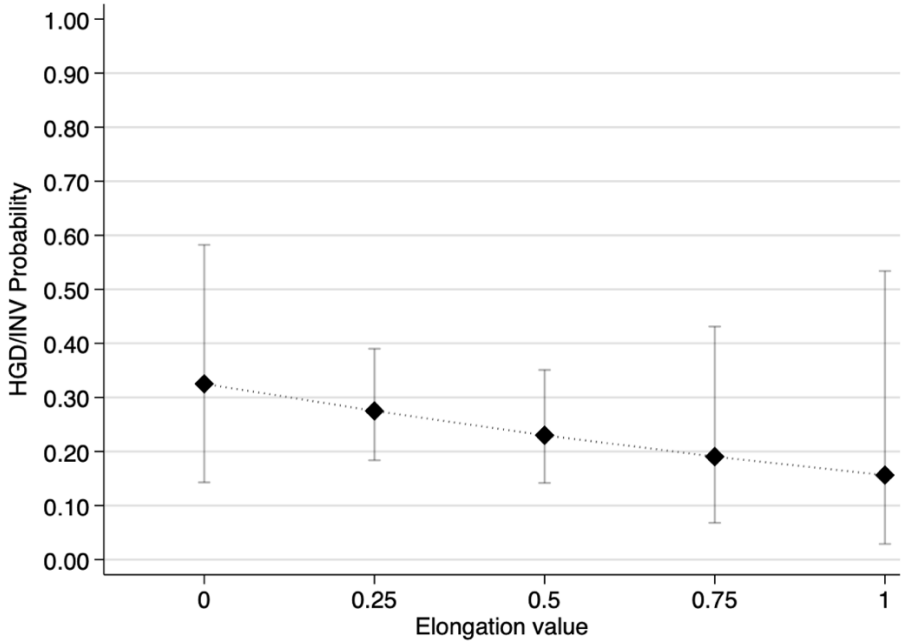


***Figure 8***. *Two-way graph displaying on the y-axis the predicted probabilities (with 95% CI) for the outcome high-grade dysplasia/invasive cancer (HGD/INV) in relation to the elongation value on the x-axis. The probability of malignancy is higher with lower values of EV (i.e., more spheric shape), although not statistically significant at logistic regression analysis. Reprinted with permission [source: Pozzi Mucelli RM et al.* [82]. *Creative Commons CC BY 4.0, https://creativecommons.org/licenses/by/4.0/]*

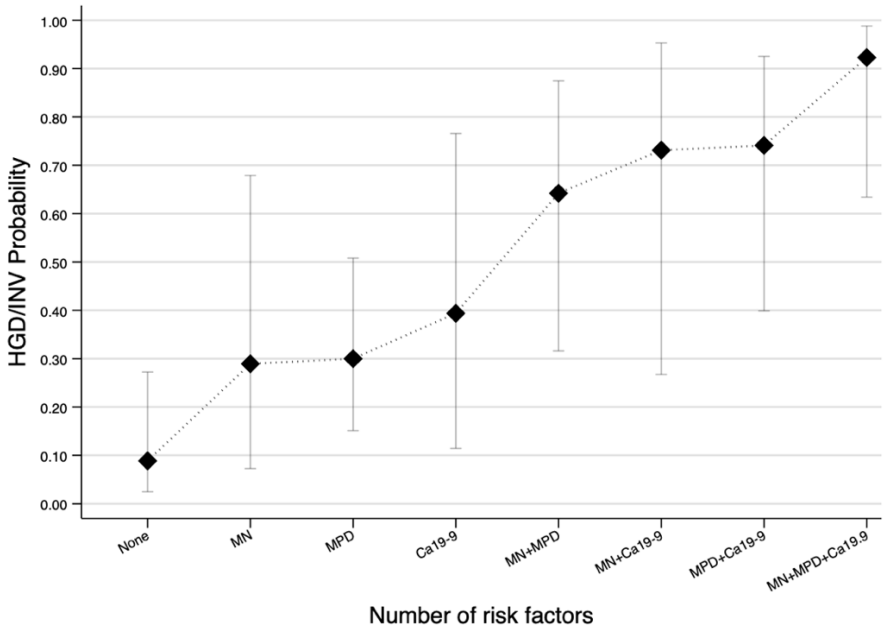


***Figure 9.*** *Two-way graph of the predicted probabilities (with 95% CI) for the outcome high-grade dysplasia/invasive cancer (HGD/INV) in a hypothetical 70 years-old man, in relation to the three risk factors [i.e., presence of mural nodules (MN); dilated main pancreatic duct (MDP) ≥5 mm; elevated tumoral marker CA19-9 >37 U/mL] significantly associated to malignancy in multivariable logistic regression analysis. Reprinted with permission [source: Pozzi Mucelli RM et al.* [82]. *Creative Commons CC BY 4.0, https://creativecommons.org/licenses/by/4.0/].*

| LGD versus HGD/INV | Sum of the observed risk factors (MN, MPD, CA19-9) % (n) | | | | |
|---|---|---|---|---|---|
| | **0** | **1** | **2** | **3** | **Total** |
| **LGD** | 91% (32/35) | 77% (41/53) | 35% (6/17) | 0 | 75% (79/106) |
| **HGD/INV** | 9% (3/35) | 23% (12/53) | 65% (11/17) | 100% (1) | 25% (27/106) |

Abbreviations: LGD, low-grade dysplasia; HGD/INV, high-grade dysplasia/invasive cancer; MN, mural nodules; MPD, main pancreatic duct;
Risk factors: contrast enhancing MN; MPD ≥ 5 mm; CA19-9 >37 U/mL.

***Table 11.*** *Observed probabilities for low-grade and high-grade dysplasia/invasive cancer by adding the risk factors identified at multivariable logistic regression analysis. Reprinted and modified with permission [source: Pozzi Mucelli RM et al.* [82]*. Creative Commons CC BY 4.0, https://creativecommons.org/licenses/by/4.0/]*

| Surgical indications | Sensitivity % [95%CI], (n) | Specificity % [95%CI], (n) | PPV % [95%CI], (n) | NPV % [95%CI], (n) | Accuracy % [95%CI], (n) |
|---|---|---|---|---|---|
| **Clinical features** | | | | | |
| Symptoms | 4 [0.1-19] (1/27) | 95 [87.5-99] (75/79) | 20 [0.5-72] (1/5) | 74 [64.5-82] (75/101) | 72 [62-80] (76/106) |
| - Acute pancreatitis | 0 (0/27)[a] | 97.5 [91-99] (70/79) | 0 (0/2)[a] | 74 [64.5-82] (77/104) | 73 [63-81] (77/106) |
| - Jaundice | 4 [0.1-19] (1/27) | 100 [95-100] (79/79) | 100 [2.5-100] (1/1) | 75 [66-83] (79/105) | 75.5 [66-83] (80/106) |
| - Diabetes (recent onset)[b] | n.a. | n.a. | n.a. | n.a. | n.a. |
| CA19-9 >37 U/mL* | n.a. | n.a. | n.a. | n.a. | n.a. |
| **Imaging features** | | | | | |
| Diameter ≥ 40 mm | 4 [0.1-19] (1/27) | 92 [84-97] (73/79) | 14 [0.4-58] (1/7) | 74 [64-82] (73/99) | 70 [60-78] (74/106) |
| MPD 5-9.9 mm | 11 [2-29] (3/27) | 85 [75-92] (67/79) | 20 [4-48 (3/15) | 74 [63-82] (67/91) | 66 [56-75] (70/106) |
| MPD ≥ 10 mm* | n.a. | n.a. | n.a. | n.a. | n.a. |
| Contrast-enhancing MN | 0 (0/27)[c] | 96 [89-99] (76/79) | 0 (0/3)[c] | 74 [64-82] (76/103) | 72 [62-80] (76/106) |
| Size progress (≥5mm/year) | 0 (0/27)[d] | 87 [78-94] (69/79) | 0 (0/10)[d] | 72 [62-81] (69/96) | 65 [55-74] (69/106) |

Abbreviations: CI, confidence intervals; PPV, positive predictive value; NPV, negative predictive value; MPD, main pancreatic duct; MN, mural nodules.
[a]Only 2 patients had acute pancreatitis as the only surgical indication; none of them had malignant IPMN.
[b]Recent onset of diabetes was never encountered in the study cohort.
[c]Only 3 patients had MN as the only surgical indication; none had malignancy.
[d]Ten patients had size progression as only resection criteria; none had malignancy.
*CA19-9 >37 U/mL and MPD ≥ 10 mm were never identified as only indications for surgery.

***Table 12.*** *Performance of imaging and clinical features, taken individually, according to the European Evidence-based Guidelines* [7]*. Reprinted and modified with permission [source: Pozzi Mucelli RM et al.* [82]*. Creative Commons CC BY 4.0, https://creativecommons.org/licenses/by/4.0/]*

## 5.3 STUDY III

The final study included 130 patients (Figure 4), with a median age of 71 years old (Table 13). One-hundred-four patients were included in study part 2.

| Variable | % (n) |
|---|---|
| Age, years (median, IQR) | 71 (65-75) |
| Gender (male) | 42% (55/130) |
| **Symptoms** | 28% (36/130) |
| - Jaundice | 2% (3/130) |
| - Weight loss | 4% (5/130) |
| - Abdominal pain | 11% (15/130) |
| - Acute pancreatitis | 12% (16/130) |
| - Diabetes (recent onset) | 0 |
| **Serum Ca19-9** (U/mL) | |
| - Median, IQR | 13 (6.4-29) |
| - Min-max | 0.3-30359 |
| Ca19-9 >37 U/mL | 18% (24/130) |
| **Imaging features BD-IPMN** | |
| Maximum diameter (mm) | Median 32 (IQR 24-43) |
| Diameter ≥ 30 mm | 62% (81/130) |
| Diameter ≥ 40 mm | 36% (47/130) |
| Volume ($cm^3$) | Median 9.7 (IQR 4.2-19.6) |
| Contrast-enhancing MN | 15% (20/130) |
| Multifocality | 64% (84/130) |
| Cyst location | |
| - Head/uncinate process | 53% (69/130) |
| MPD diameter (mm) (median, IQR) | Median 5.2 (IQR 3.1-7.4) (range 1.5-19) |
| MPD ≥ 5mm | 55% (72/130) |
| MPD ≥ 10mm | 11% (15/130) |
| **Cystic grade of dysplasia** | |
| Low-grade | 78% (102/130) |
| High-grade/Invasive cancer | 22% (28/130) |
| **Histological cell subtypes** | |
| Pancreatobiliary (PB) | 5% (6/130) |
| Gastric | 73% (95/130) |
| Intestinal | 6% (8/130) |
| PB+gastric | 3% (4/130) |
| Gastric+intestinal | 11% (15/130) |
| PB+gastric+intestinal | 2% (2/130) |
| **MRI equipment** | |
| - 1.5 Tesla | 80% (104/130) |
| - 3 Tesla | 20% (26/130) |
| Siemens Healthineers | 69% (90/130) |
| Philips Healthcare | 25% (32/130) |
| GE Healthcare | 6% (8/130) |
| Abbreviations: IQR, interquartile range; MN, mural nodules; MPD, main pancreatic duct | |

***Table 13.*** *Patient's characteristics (study 3).*

Twenty-nine percent (38/130) of the cases were malignant at final histopathology. However, after radiologic-pathological revision of the cases with HGD/INV, only 22% (28/130) of the selected BD-IPMN were confirmed malignant, implying that in ten cases, the malignant focus was located elsewhere than the segmented BD-IPMN (i.e., the largest or most suspicious at preoperative MRI).

*Spatial and Cross-vendor Stability of Radiomics Features*

In total, 95% (987/1037) of the extracted features had ICC > 0.75 and, therefore were considered spatially stable (Figure 10a). The percentage of stable features was relatively high across feature classes and image filters. Regarding image filters, the features calculated with a local binary pattern were the least stable (with only 79.6% of lbp-2D features considered stable).

In total, 78% (805/1037) of the features were considered cross-vendor stable (Figure 10b). Shape was the most stable feature type. The remaining feature classes had similar proportions of stable features, ranging between 68-85%. Regarding image filters, the highest proportion of stable features was found among those calculated with gradient or wavelet filters (over 90% of features considered stable), in contrast with the exponential, logarithm, and square filters, which produced the lowest proportion of stable features (23%, 46%, and 47%, respectively).

Overall, 74% (767/1037) of the features were both spatially and cross-vendor stable (Figure 10c). Gradient and wavelet filters produced the highest percentage of stable features, in contrast to exponential, logarithm and square filters that generated the least stable features. Once more, the shape features were the most stable feature type. Regarding feature classes, the same pattern arose with shape as the most stable feature type.

a

| Percentage of stable features (Spatial Stability) | | | | | | | | |
|---|---|---|---|---|---|---|---|---|
| | firstorder | shape | glcm | glrlm | glszm | gldm | ngtdm | total |
| original | 100 | 92.86 | 100 | 100 | 100 | 100 | 100 | 99.07 |
| exponential | 88.89 | NaN | 100 | 100 | 81.25 | 100 | 100 | 94.62 |
| gradient | 94.44 | NaN | 100 | 100 | 93.75 | 100 | 80 | 96.77 |
| logarithm | 88.89 | NaN | 95.83 | 87.5 | 87.5 | 92.86 | 100 | 91.4 |
| lbp-2D | 88.89 | NaN | 87.5 | 68.75 | 50 | 100 | 80 | 79.57 |
| square_ | 88.89 | NaN | 100 | 100 | 100 | 100 | 100 | 97.85 |
| squareroot | 100 | NaN | 100 | 100 | 100 | 92.86 | 100 | 98.92 |
| wavelet-LH_ | 100 | NaN | 100 | 100 | 100 | 100 | 100 | 100 |
| wavelet-HL_ | 100 | NaN | 100 | 100 | 100 | 100 | 100 | 100 |
| wavelet-HH_ | 83.33 | NaN | 91.67 | 87.5 | 87.5 | 92.86 | 100 | 89.25 |
| wavelet-LL_ | 100 | NaN | 100 | 100 | 100 | 92.86 | 100 | 98.92 |
| total | 93.94 | 92.86 | 97.73 | 94.89 | 90.91 | 97.4 | 96.36 | 95.18 |

b

| Percentage of stable features (Vendor Stability) | | | | | | | | |
|---|---|---|---|---|---|---|---|---|
| | firstorder | shape | glcm | glrlm | glszm | gldm | ngtdm | total |
| original | 61.11 | 100 | 91.67 | 100 | 100 | 100 | 100 | 91.59 |
| exponential | 11.11 | NaN | 12.5 | 25 | 25 | 35.71 | 60 | 22.58 |
| gradient | 100 | NaN | 100 | 100 | 100 | 92.86 | 100 | 98.92 |
| logarithm | 44.44 | NaN | 41.67 | 62.5 | 43.75 | 50 | 20 | 46.24 |
| lbp-2D | 83.33 | NaN | 87.5 | 75 | 100 | 85.71 | 100 | 87.1 |
| square_ | 27.78 | NaN | 58.33 | 43.75 | 43.75 | 50 | 80 | 47.31 |
| squareroot | 55.56 | NaN | 83.33 | 81.25 | 81.25 | 78.57 | 80 | 76.34 |
| wavelet-LH_ | 100 | NaN | 91.67 | 100 | 100 | 100 | 100 | 97.85 |
| wavelet-HL_ | 100 | NaN | 87.5 | 100 | 100 | 100 | 100 | 96.77 |
| wavelet-HH_ | 100 | NaN | 95.83 | 100 | 87.5 | 100 | 100 | 96.77 |
| wavelet-LL_ | 61.11 | NaN | 91.67 | 100 | 100 | 100 | 100 | 90.32 |
| total | 67.68 | 100 | 76.52 | 80.68 | 80.11 | 81.17 | 85.45 | 77.63 |

c

| Percentage of stable features | | | | | | | | |
|---|---|---|---|---|---|---|---|---|
| | firstorder | shape | glcm | glrlm | glszm | gldm | ngtdm | total |
| original | 61.11 | 92.86 | 91.67 | 100 | 100 | 100 | 100 | 90.65 |
| exponential | 11.11 | NaN | 12.5 | 25 | 18.75 | 35.71 | 60 | 21.51 |
| gradient | 94.44 | NaN | 100 | 100 | 93.75 | 92.86 | 80 | 95.7 |
| logarithm | 44.44 | NaN | 37.5 | 56.25 | 31.25 | 42.86 | 20 | 40.86 |
| lbp-2D | 77.78 | NaN | 87.5 | 43.75 | 50 | 85.71 | 80 | 70.97 |
| square_ | 22.22 | NaN | 58.33 | 43.75 | 43.75 | 50 | 80 | 46.24 |
| squareroot | 55.56 | NaN | 83.33 | 81.25 | 81.25 | 71.43 | 80 | 75.27 |
| wavelet-LH_ | 100 | NaN | 91.67 | 100 | 100 | 100 | 100 | 97.85 |
| wavelet-HL_ | 100 | NaN | 87.5 | 100 | 100 | 100 | 100 | 96.77 |
| wavelet-HH_ | 83.33 | NaN | 87.5 | 87.5 | 75 | 92.86 | 100 | 86.02 |
| wavelet-LL_ | 61.11 | NaN | 91.67 | 100 | 100 | 92.86 | 100 | 89.25 |
| total | 64.65 | 92.86 | 75.38 | 76.14 | 72.16 | 78.57 | 81.82 | 73.96 |

***Figure 10.*** *Spatial (a), vendor (b) and overall (c) stability of extracted radiomics features by feature class and image filter. Filters are listed in the first column, feature classes in the second row. Abbreviation: NaN, Not a Number (i.e., no features of that type).*

*Pipeline selection*

All the selected pipelines included the full set of features (stable and unstable), tree-based feature selection, and they were all Logistic Regressions. The type of penalty (Ridge or Lasso) and the C parameter, for the degree of penalty, were hyperparameters optimized during model training with nested cross-validation (Table 14).

| Classifier | Radiologist | Number of features | Pre-processing | Penalty | C |
|---|---|---|---|---|---|
| **Clin** | None | 11 | Removal of correlated variables | l2 | 1000 |
| **Rad1** | Radiologist1 | 13 | Removal of correlated variables. Tree-based feature selection. | l1 | 10 |
| **RadClin1** | Radiologist1 | 40 | Removal of correlated variables. Tree-based feature selection. | l1 | 1000 |

***Table 14.*** *Pipeline selection.*

*Classifier Performance*

The results of the DeLong test for comparing the classifiers' AUC are shown in Table 15. Only Rad1 and RadClin1, classifiers trained with radiomics features extracted from the segmentations drawn by radiologist 1, resulted significantly different from the dummy classifier (i.e., trained to detect the majority class, corresponding to LGD).

Only the radiomics classifier Rad1 was statistically significant different compared to the clinical classifier.

Comparing the two radiologists' performances, no significant differences were found between Rad and RadClin classifiers after FDR correction (p=0.12 and 0.38, respectively). Finally, there was no significant improvement in the performance of RadClin1 classifiers compared to the Rad1 classifier.

Upon these findings, the focus was directed towards the results obtained by the radiologist 1 classifiers.

| DeLong test* | Dummy classifier | Clinical Classifier | Rad1 Classifier | RadClin2 Classifier |
|---|---|---|---|---|
| **Rad1 classifier** | **8.65E-17** | **0.0002** | | |
| **Rad2 classifier** | 0.42 | 0.50 | 0.12 | 0.98 |
| **RadClin1 classifier** | **0.005** | 0.12 | 0.42 | 0.38 |
| **RadClin2 classifier** | 0.42 | 0.50 | | |
| *Corrected for multiple comparisons (FDR correction) | | | | |

***Table 15.*** *Comparison of the areas under the correlated receiver operating characteristic curves (AUC) of the clinical (Clin), radiomics (Rad) and combined clinical-radiomics (RadClin) models calculated after segmentation performed by two radiologists (i.e., Rad1 and Rad2; RadClin1 and RadClin2 respectively). Figures correspond to p-values calculated with the DeLong test.*

Table 16 shows the performance of the classifiers Clin, Rad1 and RadClin1 after 3-fold internal cross-validation. The classifiers using radiomics data (Rad1 and RadClin1) outperformed the clinical classifier, although there was no statistically significant difference between Clin and RadClin1 classifiers (DeLong test, p=0.12, Table 15). Together with a strong statistically significant difference compared to the Clin performance, the Rad1 classifier needed significantly fewer extracted features than the RadClin1. Moreover, the RadClin1 classifier automatically extracted only one clinical variable (serum levels of CA19-9).

| Classifier | 3-fold cross-validation performance (95% CI) | | | | | Nr. of features |
|---|---|---|---|---|---|---|
| | F2-score | Cohen's Kappa | AUC | Sensitivity | Specificity | |
| **Clin** | 0.53 (0.19-0.77) | 0.31 (0-0.56) | 0.67 (0.43-0.83) | 0.57 (0.21-0.85) | 0.77 (0.60-0.87) | 11 |
| **Rad1** | 0.63 (0.38-0.80) | 0.43 (0.09-0.64) | 0.75 (0.55-0.86) | 0.68 (0.42-0.87) | 0.81 (0.65-0.91) | 13 |
| **RadClin1** | 0.63 (0.30-0.82) | 0.42 (0.13-0.70) | 0.75 (0.57-0.87) | 0.69 (0.31- 0.87) | 0.81 (0.74-0.94) | 40 |

***Table 16.*** *Performance of the Clinical (Clin), pure Radiomics (Rad1) and combined Clinical and Radiomics (RadClin1) classifiers in differentiating high-grade dysplasia/invasive cancer from low-grade dysplasia in branch-duct IPMN. Figures within brackets are 95% confidence intervals (CI).*

Concerning the stability of the included features, out of the 13 used by the Rad1 classifier, two were spatially unstable to segmentation, nine were unstable across vendors, and one was unstable to both. Out of 40 features used by the RadClin1 classifier, eleven were spatially unstable to segmentation, ten were unstable across vendors, and two were unstable to both.

*SHAP analysis*

In Figure 11, we present the results of the SHAP analysis performed on the Rad1 and RadClin1 classifiers from radiologist 1. The plots display the features ordered according to their impact on the model output. For the Rad1 classifier, the variables with the highest impact were Sphericity and Elongation. Sphericity was negatively correlated to the presence of HGD/INV, while Elongation was positively correlated to it.

Other features positively correlated to the outcome HGD/INV were:

- wavelet-LL_firstorder_Kurtosis
- lbp-2D_glszm_ZoneEntropy
- logarithm_glcm_Correlation
- wavelet-LH_firstorder_RootMeanSquared
- logarithm_gldm_DependenceNonUniformityNormalized

Negatively correlated features to the outcome were:

- wavelet-LH_firstorder_Skewness

- wavelet-HH_gldm_DependenceVariance
- exponential_ngtdm_Busyness
- exponential_gldm_DependenceNonUniformityNormalized
- exponential_glszm_SizeZoneNonUniformityNormalized
- wavelet-HL_firstorder_RootMeanSquared

Regarding the RadClin1 classifier, the feature with the highest impact on the model output was the variable "serum levels of CA19-9", whose value was positively correlated to the HGD/INV output. Shape features, such as Sphericity and Elongation, were still used by the model, although with a lower impact.

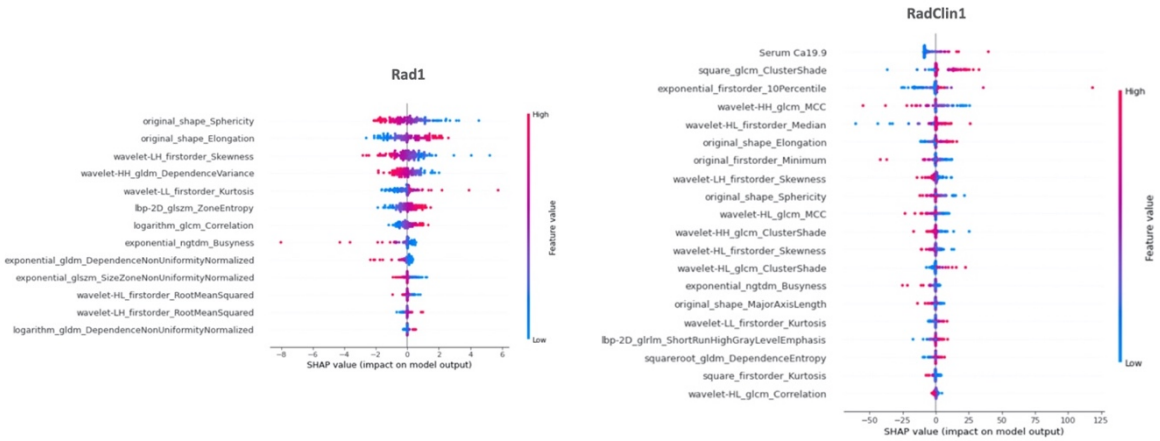


***Figure 11.*** *SHAP analysis for Rad1 and RadClin1 classifiers, showing the contribution of the extracted radiomics features. Features are ranked in descending order based on their importance and contribution to the model. The dots in the plot correspond to the feature's SHAP values; their position along the x-axis indicates whether the variable is associated with a positive or negative prediction. The red colour indicates higher values of a feature; the blue colour means lower values. A threshold of 20 features was set. For this reason, only the first best 20 out of 40 radiomics features are displayed for RadClin1.*

## *Volatility analysis*

Figure 12 displays the results of the volatility analysis for the AUC performed on the Rad1 and RadClin1 classifiers. The Rad1 train set showed a better performance than the test set, with some degree of overlap between the two distributions. On the other hand, the RadClin1 train performed even better than the test set, without any distributions' overlap, indicating a greater overfitting.

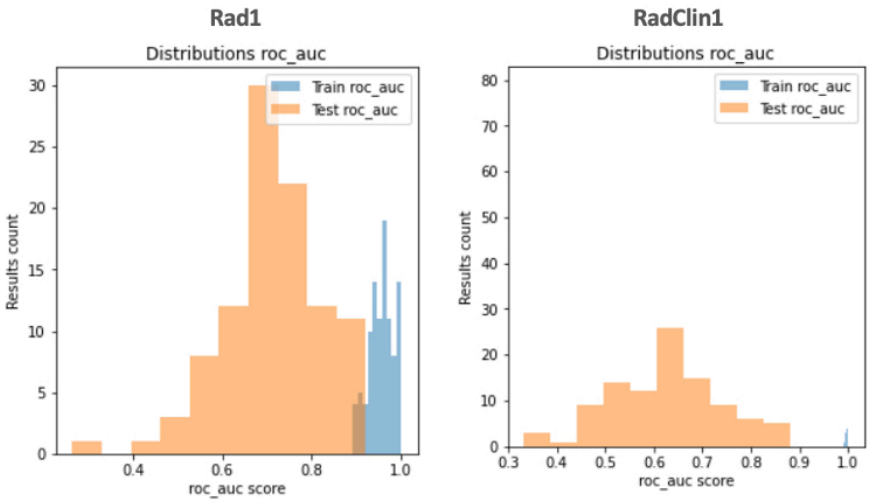


***Figure 12.*** *The volatility analysis shows the distribution of the areas under the correlated receiver operating characteristic curves (AUC) for the Rad1 and RadClin1 classifiers. The blue histograms represent the performances on the train set. The orange histograms represent the performances on the test set. The performances on the train sets are higher in both Rad1 and RadClin1. However, both classifiers are very overfitted although the grade of overfitting is higher for RadClin1.*

## 5.4 STUDY IV

Study 4 included 278 patients with a median age of 53 years (IQR 45-61; range, 23-86). Patients were followed for a median time of 4.5 years (IQR 2.5-8.3 years). The longest follow-up was 19 years. The follow-up was shorter than 12 months in only 16 cases (6%). The patient's characteristics are shown in Table 17.

MRI was the only surveillance imaging method for 69% of the cases, with a median of 5 examinations per patient (IQR 3-7) (Table 17).

| Variable | % (n) |
|---|---|
| **Age** | Median 53 (IQR 45-61) |
| - ≥ 50 years | 60% (167/278) |
| **Gender** | |
| - Females | 63.3% (176/278) |
| - Males | 36.7% (102/278) |
| **Body Mass Index (BMI)*** | Median 25 (IQR 22.7-28.1) |
| - BMI 25-29.9 | 36.5% (73/200) |
| - BMI ≥ 30 | 14% (28/200) |
| **Alcohol overconsumption*** | 2.7% (6/223) |
| **Diabetes mellitus*** | 11.72% (32/272) |
| **Chronic pancreatitis*** | 9.1% (25/273) |
| **Smoking*** | 24.9% (62/249) |
| **CA 19-9 (U/mL)*** | Median 7.8 (IQR 5.4-14; range 0.3-4410) |
| **CA 19-9 ≥ 37 U/mL** | 6% (14/232) |
| **Subcategories of IAR** | |
| *Familial pancreatic cancer* | 72.3% (201/278) |
| - ≥ 3 relatives with ≥ 1 FDR | 52.7% (106/201) |
| - ≥ 2 FDR | 27.8% (56/201) |
| - No predisposing mutations at genetic test | 52% (104/201) |
| - Genetic test not performed | 48% (97/201) |
| *Hereditary pancreatic cancer* | 27.7% (77/278) |
| - Peutz-Jeghers syndrome (PJS) | 2.6% (2/77) |
| - FAMMM | 15.6% (12/77) |
| - HBOC | 66.2% (51/77) |
| - Lynch syndrome | 14.3% (11/77) |
| - AT (ataxia telangiectasia) | 1.3% (1/77) |
| **Imaging method** | |
| - MRI | 69.4% (193/278) |
| - CT | 1.8% (4/278) |
| - Combination of MRI and CT | 29.1% (81/278) |
| **Treatment** | |
| - Surgery | 2.9% (8/278) |
| - Palliative chemotherapy | 0.7% (2/278) |
| **Histopathology** | |
| (10 available: 8 after pancreatic surgery; 2 after liver biopsy) | |
| - Pancreatic adenocarcinoma | 40% (4/10) |
| - Mixed-type IPMN with microinvasive carcinoma and PanIn high-grade dysplasia | 10% (1/10) |
| - Mixed-type IPMN low-grade dysplasia | 20% (2/10) |
| - PanIn low-grade dysplasia | 10% (1/10) |
| - Other benign lesions | 20% (2/10) |

Abbreviations: FDR, First-degree Relative; FAMMM, Familial Atypical Multiple Mole Melanoma (CDKN2A/p16); HBOC, Hereditary Breast and Ovarian Cancer syndrome (BRCA1, BRCA2, PALB2).

*BMI was unavailable in 78/279 (28%) patients. Alcohol consumption history was missing in 55/278 (20%) patients. Data on diabetes mellitus were unavailable in 6/278 (2%) patients. Information on chronic pancreatitis was unavailable in 5/278 (2%) patients. Smoking status was missing in 29/278 (10%). Serum level of Ca 19-9 was unavailable in 46/278 patients (16%).

***Table 17.*** *Characteristics of the 278 patients included in study 4.*

*Imaging findings*

The types of lesions detected by imaging screening are summarized in Figure 13.

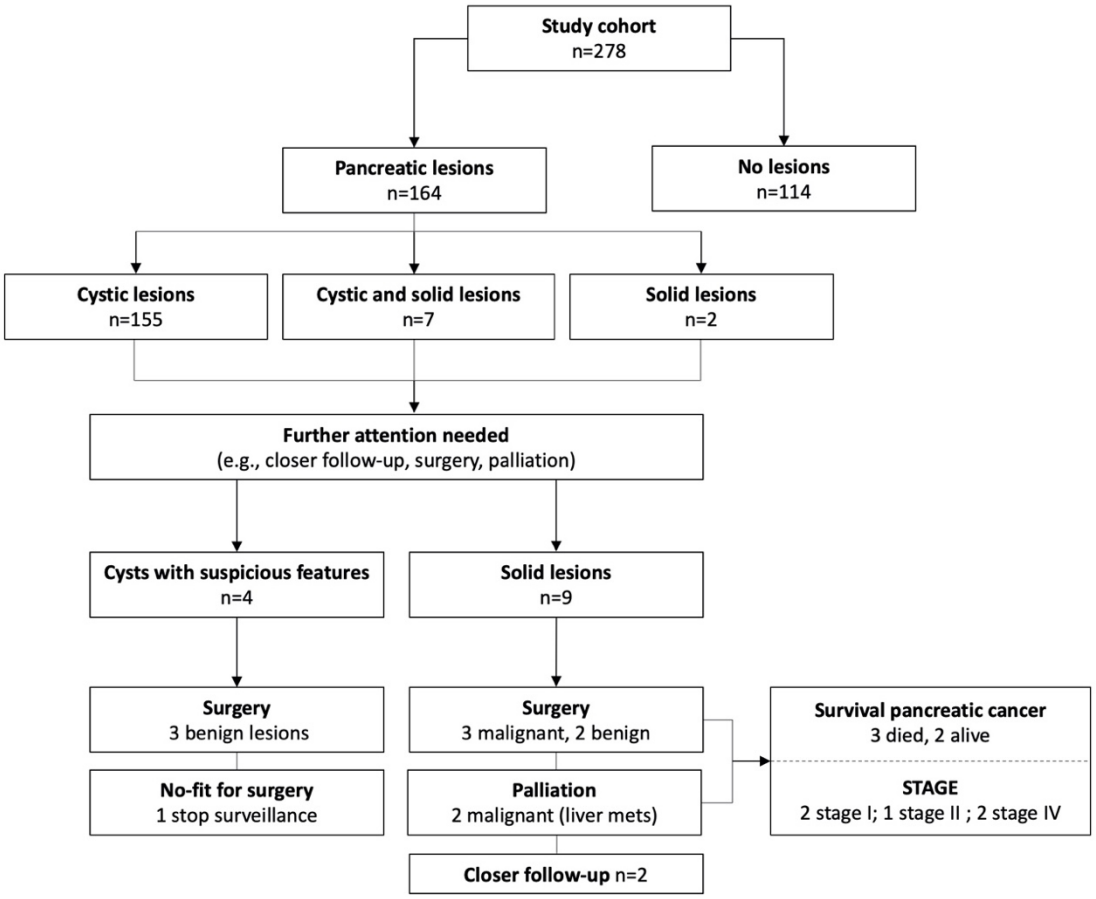


***Figure 13.*** *Flowchart displaying the detected pancreatic lesions in study 4.*

In 59% of the patients (164/278), imaging surveillance detected one (or more) focal lesion. Cystic lesions were either the only finding in 56% (155/278) of the cases or coexisted with a solid lesion in 2.5% (7/278) of the cases. Only two patients (0.7%, 2/278) were diagnosed with an isolated solid lesion without a coexisting pancreatic cyst.

Tables 18 and 19 show the prevalence of patients and lesions per encountered clinical scenarios and subcategory of IAR (FPC versus HPC).

Most of the detected pancreatic cysts were either identified at a baseline examination (scenario 8, 37% of the cases) or appeared after a negative baseline (scenario 5, 17%). Scenario 5 was significantly more often encountered in FPC than HPC (21% versus 6%, p=0.002) (Table 18).

Very seldom patients with cystic lesions developed imaging risk factors (solid masses included) during surveillance (scenario 7, 1.4%; scenario 4, 1.1%) or at baseline (scenario 10, 0.3%). In only 3 cases (1.1%), a solid lesion was detected at baseline (scenario 6) in patients with FPC.

| Scenario | Description (in short) | % (n) | Prevalence among IAR % (n) | |
|---|---|---|---|---|
| | | | FPC (n=201) | HPC (n=77) |
| 1 | No findings at baseline | 41% (114/278) | 39.8% (80/201) | 44.2% (34/77) |
| 2 | No findings at baseline → onset of solid lesion | 0 | 0 | 0 |
| 3 | No findings at baseline → onset of a cystic lesion with iRF | 0 | 0 | 0 |
| 4 | No findings at baseline → onset of a cystic lesion without iRF → F/U → onset of iRF | 1.1% (3/278) | 1% (2/201) | 1.3% (1/77) |
| 5 | No findings at baseline → onset of a cystic lesion without iRF → unchanged during F/U | 17.3% (48/278) | 21.4% (43/201)* | 6.5% (5/77)* |
| 6 | Solid lesion at baseline | 1.1% (3/278) | 1.5% (3/201) | 0 |
| 7 | Cystic lesion without iRF at baseline → onset of iRF or solid mass | 1.4% (4/278) | 1% (2/201) | 2.6% (2/77) |
| 8 | Cystic lesion without iRF at baseline→ unchanged during F/U | 37% (103/278) | 33.8% (68/201) | 45.4% (35/77) |
| 9 | No findings/cyst without iRF at baseline → onset of "interval cancer" during F/U | 0.7% (2/278) | 1% (2/201) | 0 |
| 10 | Cystic lesion(s) with iRF at baseline | 0.3% (1/278) | 0.5% (1/201) | 0 |
| Abbreviations: iRF, imaging Risk Factors; F/U, follow-up<br>*Statistically significant difference (p=0.002) (Fisher's exact test) | | | | |

***Table 18.*** *Prevalence of clinical scenarios among individuals with familial pancreatic cancer (FPC) and hereditary pancreatic cancer (HPC).*

| IAR subcategory | Nr. | Type of lesions at imaging | | | | Malignancy at histology |
|---|---|---|---|---|---|---|
| | | No lesions | Cystic | Solid | Cystic + solid | |
| **Familial PC** | 201 | 40% (80/201) | 57% (114/201) | 1% (2/201) | 2% (5/201) | 2% (4/201) |
| **Hereditary PC** | 77 | 44% (34/77) | 53% (41/77) | 0 | 3% (2/77) | 1.3% (1/77) |
| - Peutz-Jeghers | 2 | 0 | 100% (2/2) | 0 | 0 | 0 |
| - FAMMM | 12 | 58.3% (7/12) | 41.7% (5/12) | 0 | 0 | 0 |
| - HBOC | 51 | 51% (26/51) | 45% (23/51) | 0 | 4% (2/51) | 1.9% (1/51) |
| - Lynch syndrome | 11 | 9% (1/11)* | 91% (10/11)* | 0 | 0 | 0 |
| - AT | 1 | 0 | 100% (1/1) | 0 | 0 | 0 |
| Abbreviations: PC, pancreatic cancer; FAMMM, Familial Atypical Multiple Mole Melanoma; HBOC, Hereditary Breast and Ovarian Cancer syndrome; AT, Ataxia telangiectasia<br>*Statistically significant difference (p=0.03, Fisher's exact test). | | | | | | |

***Table 19.*** *Prevalence of imaging findings and malignancy among subcategories of Individuals at Risk.*

The features of cystic lesions are reported in Table 20. IPMN and undefined cysts were the most common diagnosis, with a significantly higher proportion of IPMN (58% and 42%, respectively, p=0.04). Their prevalence was not statistically significantly different among IAR subtypes (p=0.8), neither the cystic features were significantly different among IAR categories. Almost 65% of the cases (91/162) had multifocal cysts, the majority with less than five cysts (80%, 84/105).

Only four patients with cystic lesions (2.5%, 4/162) showed imaging risk factors (solid masses excluded), which led to surgery in three patients (Table 20). The median time-interval

between the baseline examination and the onset of imaging risk factors was 4.3 years (IQR 3.2-5.3 years). In only 1 FPC patient, the imaging risk factors were present at baseline (scenario 10).

| Imaging features | % (n) | FPC | HPC | p-value |
|---|---|---|---|---|
| **Diameter (mm)** | Median 5.5 (IQR 3-10)<br>Range 1-36 mm | 6 (4-10) | 5 (3-8) | 0.41 |
| **Hypothetical working diagnosis**<br>- BD-IPMN<br>- Mixed-type IPMN<br>- Undefined | <br>56% (91/162)<br>2% (3/162)<br>42% (68/162) | <br>72.5% (66/91)<br>100% (3/3)<br>73.5% (50/68) | <br>27.5% (25/91)<br>0<br>26.5% (18/68) | 0.8 |
| **Multifocal cysts**<br>- < 5 cysts<br>- 5 ≤ cysts <10<br>- ≥ 10 cysts | 64.8% (105/162)<br>80% (84/105)<br>15.2% (16/105)<br>4.8% (5/105) | 68.5% (72/105)<br>67.8% (57/84)<br>86.7% (11/16)<br>80% (4/5) | 31.5% (33/105)<br>32.2% (/84)<br>31.3% (5/16)<br>20% (1/5) | 0.06 |
| **Location**<br>- Head/uncinate process<br>- Body/tail<br>- Diffusely spread | <br>22.8% (37/162)<br>38.3% (62/162)<br>38.9% (63/162) | <br>86.5% (32/37)<br>66.1% (41/62)<br>73.1% (46/63) | <br>13.5% (5/37)<br>33.9% (21/62)<br>26.9% (17/63) | 0.08 |
| **Imaging risk factors***<br>- MPD ≥5 mm<br><br>- Contrast-enhancing MN<br>- Growth rate (≥ 5 mm/year) | 2.5% (4/162)<br>75% (3/4)<br>(range 6.2-7.7 mm)<br>0<br>25% (1/4) | 75% (3/4)<br>100% (3/3)<br><br>-<br>0 | 25% (1/4)<br>0<br><br>-<br>100% (1/1) | 1 |
| **Treatment**<br>- Surgery<br>- Stop surveillance (not fit) | <br>75% (3/4)<br>25% (1/4) | <br>66.7% (2/3)<br>100% (1/1) | <br>33.3% (1/3)<br>0 | 1 |
| **Histopathology**<br>- IPMN ± PanIn LGD<br>- Pancreatitis + retentions cysts<br>- IPMN ± PanIn HGD | <br>66.7% (2/3)<br>33.3% (1/3)<br>0 | <br>50% (1/2)<br>100% (1/1)<br>- | <br>50% (1/2)<br><br>- | |
| Abbreviations: MPD, main pancreatic duct; MN, mural nodule; PanIn, pancreatic intraepithelial neoplasia; LGD, low-grade dysplasia; HGD, high-grade dysplasia.<br>*Solid masses were not included among cystic imaging risk factors in this table and were reported in Table 21. | | | | |

***Table 20.*** *Characteristics of cystic lesions detected at imaging surveillance, overall and subdivided by familial (FPC) and hereditary pancreatic cancer (FPC). The reported p-values derive from testing differences among FPC and HPC with Wilcoxon rank-sum test (numerical variables) and Fisher's exact test (categorical variables).*

Solid lesions were recorded in only 9 cases (3%, 9/278; 7 FPC and 2 HPC), of whom seven were concomitant to cysts (Table 21).

In 33% (3/9) of the patients, solid lesions were present at the first examination (scenario 6), although all were benign. In the remaining 67% (6/9), lesions were encountered at follow-up with a median time-delay from baseline of 4.9 years (IQR 3.7-6.1 years; range, 1.1-7.1 years). Unfortunately, among those patients diagnosed with a solid lesion, two (22%, 2/9) developed symptoms between controls (abdominal pain and jaundice, which occurred 6 and 11 months after the last examination) with a final diagnosis of PC. In only one case, we could re-evaluate the previous MRI, finding restricted signal at DWI in a focal area in the pancreatic head without a corresponding mass on T2-weighted images. In another patient, the last two MRIs were not archived in our PACS system and thus not accessible for re-evaluation.

Histopathology showed benign findings in all three patients with pancreatic cysts and suspicious imaging risk factors (Table 20). Among those with a solid mass, histopathology was available for seven patients, showing malignancy in 71% (5/7) of the cases (4 PDAC; 1 mixed-type IPMN with microinvasive cancer and PanIN HGD) (Table 21). The stage of the

5 PCs is reported in Table 21. Two patients with solid lesions were still under closer follow-up.

| Imaging features | % (n) | FPC | HPC | p-value |
|---|---|---|---|---|
| **Diameter (mm)** | Mean 13.8±5.4<br>Range 6-30 mm | 14±6.1<br>(6-20) | 13±6.1<br>(11-15) | 0.76 |
| **Location**<br>- Head and/or uncinate process<br>- Body and/or tail | <br>66.7% (6/9)<br>33.3% (3/9) | <br>83.3% (5/6)<br>66.7% (2/3) | <br>16.7% (1/6)<br>33.3% (1/3) | 1 |
| **Coexistent cysts**<br>Cyst mean diameter (mm)<br>- BD-IPMN<br>- Undefined | 77.7% (7/9)<br>9.1± 5.3 (range 3-16)<br>71.4%% (5/7)<br>28.6% (2/7) | 71.4% (5/7)<br>8.6±5<br>60% (3/5)<br>100% (2/2) | 28.6% (2/7)<br>10.5±7.7<br>40% (2/5)<br>0 | 1 |
| MPD diameter (mm)<br>MPD ≥ 5 mm | Median 2.3 (IQR 2-2.7)<br>20% (2/10) | 2.3 (IQR 2-2.7)<br>100% (2/2) | 2.3 (IQR 2-2.6) | 0.46 |
| **Treatment**<br>- Upfront surgery<br>- Palliative CHT<br>- Only surveillance | <br>55.6% (5/9)<br>22.2% (2/9)<br>22.2% (2/9) | <br>42.8% (3/7)<br>28.6% (2/7)<br>28.6% (2/7) | <br>100% (2/2) | |
| **Histopathology**<br>- PDAC<br>- Mixed-type IPMN + microinvasive cancer + PanIN HGD<br>- PanIN LGD<br>- Intrapancreatic accessory spleen | (available in 7 patients)<br>57.1% (4/7)<br>14.3% (1/7)<br>14.3% (1/7)<br>14.3% (1/7) | (5 patients)<br>60% (3/5)<br>20% (1/5)<br><br>20% (1/5) | (2 patients)<br>50% (1/2)<br><br>50% (1/2) | |
| **Stage**<br>Stage IA<br>Stage IB<br>Stage IIA<br>Stage IV | <br>20% (1/5)<br>20% (1/5)<br>20% (1/5)<br>40% (2/5) | <br>1<br><br>1<br>2 | <br><br>1 | |
| Abbreviations: BD-IPMN, branch-duct IPMN; MPD, main pancreatic duct; CHT, chemotherapy; PDAC, pancreatic adenocarcinoma; PanIN, pancreatic intraepithelial neoplasia; HGD, high-grade dysplasia; LGD, low-grade dysplasia<br>N.B.: all cases of PDAC and IPMN with invasive cancer were associated or concomitant to cystic lesions. | | | | |

***Table 21.*** *Features of the solid lesions detected at imaging surveillance. The reported p-values derive from testing differences among FPC and HPC using the rank-sum test (numerical variables) and Fisher's exact test (categorical variables).*

We observed an overall prevalence of PC of 2% (5/278), similar among FPC and HCP (1.9% and 1.3%, respectively, p=1). The proportion of patients with stage I (stage IA and IB) was equal to that of patients in stage IV (0.7%, 2/278) (Table 21). At the time of writing, three out of the five patients with PC died (60%), with a median overall survival-time of 1.4 years (IQR 0.95-4.97). The individual survival for the three patients was 0.9, 1.4 and 4.9 years, respectively.

The only imaging feature associated with PC and solid lesions was the MPD ≥ 5 mm (OR 44; 95% C.I 5.7-339; p=0.000; Table 22).

The diagnostic accuracy metrics for the imaging screening were as follow: sensitivity 60% (95% C.I. 15-95%), specificity 98% (95%C.I. 95-99%), PPV 37% (95%C.I. 16-65%), NPV 99% (95%C.I. 97-99%) (Table 23). The characteristics of the patients with solid and cystic lesions with imaging risk factors are shown in Table 24.

*Clinical features*

Age was not associated with a higher probability of malignant or solid lesions (p=0.63 and p=0.87 respectively) (Table 22). However, the probability of having a pancreatic cystic lesion increased by increasing age at baseline (p=0.000). Indeed, the proportion of patients with cysts and age ≥ 50 years with cysts was statistically significantly higher compared with younger patients [112/162 (69%) versus 50/162 (30%) respectively; (p=0.000)], with an OR of 2.5 (95% C.I. 1.5-4.1; p=0.000) for having a cystic lesion being older than 50 years old.

The odds of cystic, solid, or malignant lesions were not associated with other clinical features (gender, body mass index, smoking status, alcohol overconsumption, diabetes mellitus, and chronic pancreatitis) (Table 22). We did not observe any case of new-onset diabetes before the diagnosis of PC. Only elevated serum levels of CA19-9 (>37 U/mL) were positive predictors of malignant lesions (OR 11.9, 95% C.I. 1.8-78.4; p=0.01) and cystic lesions (OR 8.9, 95% C.I. 1.14-69, p=0.04).

| **Predictor** | **Cystic lesions (n=162)** | | **Solid lesions (n=9)** | | **Malignant lesions (n=5)** | |
|---|---|---|---|---|---|---|
| | OR (95% C.I.) | p-value | OR (95% C.I.) | p-value | OR (95% C.I.) | p-value |
| **Clinical features** | | | | | | |
| Age (years) | 1.06 (1.04-1.09) | **0.000** | 1 (0.94-1.06) | 0.87 | 1 (0.9-1.1) | 0.63 |
| Age ≥50 years | 2.5 (1.5-4.1) | **0.000** | 1.3 (0.3-5.48) | 0.68 | 0.9 (0.2-6.1) | 0.99 |
| Gender (female) | 1.03 (0.6-1.7) | 0.9 | 1.2 (0.3-4.7) | 0.83 | 0.8 (0.1-5.2) | 0.87 |
| BMI | 1.05(0.9-1.1) | 0.17 | 0.9 (0.8-1.1) | 0.76 | 1.02 (0.8-1.3) | 0.79 |
| BMI ≥25 | 1.4 (0.8-2.4) | 0.24 | 0.7 (0.2-2.9) | 0.7 | 1.5 (0.2-8.9) | 0.67 |
| Alcohol | 1.5 (0.2-8.3) | 0.6 | 0 | - | 0 | - |
| Diabetes mellitus | 1.05 (0.5-2.2) | 0.91 | 2.2 (0.4-11.2) | 0.33 | 5.3 (0.8-32.8) | 0.07 |
| Chronic pancreatitis | 1.05 (0.4-2.4) | 0.91 | 0 | - | 0 | - |
| Smoking | 0.9 (0.5-1.5) | 0.63 | 1 (0.2-5.1) | 0.99 | 2 (0.3-12.5) | 0.44 |
| CA19-9 ≥37 U/mL | 8.9 (1.14-68.5) | **0.04** | 5 (0.9-26.8) | 0.06 | 11.9 (1.8-78.4) | **0.01** |
| **Imaging features** | | | | | | |
| Presence of solid lesion | - | - | - | - | (present in 5/5) | |
| Presence of cystic lesion | | | | | | |
| - IPMN | - | - | 2.5 (0.6-9.6) | 0.17 | 8.1 (0.8-73.8) | 0.06 |
| - Undetermined cyst | - | - | 0.8 (0.2-4.3) | 0.87 | 0.8 (0.1-6.9) | 0.81 |
| - Multifocal cysts | - | - | 0.4 (0.08-1.8) | 0.23 | 0.13 (0.01-1.1) | 0.06 |
| Cyst diameter, mm | - | - | 1.06 (0.9-1.2) | 0.26 | 1.1 (0.9-1.24) | 0.07 |
| Mural nodules | - | - | 0 | - | 0 | - |
| Cyst growth (≥5mm/year) | - | - | 0 | - | 0 | - |
| MPD diameter, mm | - | - | 1.9 (1.3-2.9) | **0.002** | 2.4 (1.5-3.8) | **0.000** |
| MPD ≥5 mm | - | - | 18.6 (2.9-118) | **0.002** | 44 (5.7-339) | **0.000** |
| Abbreviations: BMI, body mass index; MPD, main pancreatic duct | | | | | | |

***Table 22.*** *Clinical and imaging features associated with the presence of cystic, solid and malignant lesions at univariate logistic regression analysis.*

| | | Outcome (HGD/invasive cancer) | | |
|---|---|---|---|---|
| | | **Positive** | **Negative** | **(total)** |
| **Imaging screening** | **Positive** | 3 (TP) | 5 (FP) | 8 |
| | **Negative** | 2 (FN) | 252 (TN) | 254 |
| | **(total)** | 5 | 257 | 262 |
| Abbreviations: HGD, high-grade dysplasia; TP, true positive; FP, false positive; FN, false negative; TN, true negative. For definitions of TP, FP, FN and TN, please refer to section 4.7 (study 4). Sensitivity: TP/(TP+FN)=3/5; specificity: TN/(FP+TN)=252/257. PPV:TP/(TP+FP)=3/8; NPV:TN/(FN+TN)=252/254. | | | | |

***Table 23.*** *Contingency table for calculating the diagnostic accuracy metrics for the surveillance program in study 4.*

| Patient/gender /age | Type of IAR | Suspected lesion | Imaging and clinical findings | Intervention | Histology | Stage/survival |
|---|---|---|---|---|---|---|
| 1, F, 45 | FPC<br>1FDR + 2 SDR | Solid lesion, onset at F/U | Hypervascular + MPD stricture<br>+ unchanged unspecific cysts<br>Symptoms: no. Ca19-9: 5.6 U/mL | Surgery | Mixed-type IPMN with microinvasive carcinoma + high-grade PanIN | IA<br>(Alive, 3.8 years) |
| 2, F, 53 | FPC<br>2FDR | Solid lesion at baseline | Hypervascular (spleen-like)<br>$^{Ga68}$DOTATOC PET/CT: positive<br>$^{99m}$TC-DRBC SPECT/CT: negative | Surgery | Intrapancreatic accessory spleen | - |
| 3, M, 42 | HPC (BRCA1)<br>1 FDR + 2 SDR | Solid lesion, onset at F/U | Isovascular, restricted signal at DWI<br>+ unchanged multifocal BD-IPMN | Surgery | Low-grade PanIn | - |
| 4, M, 64 | FPC<br>3FDR + 1SDR | Solid lesion,<br>interval cancer | Hypovascular + unchanged multifocal BD-IPMN<br>Symptoms: yes. Ca19-9: 4410 U/mL | Palliation<br>(liver metastases) | PDAC | IV<br>(Dead, 0.9 years) |
| 5, M, 61 | FPC<br>2FDR + 1SDR | Solid lesion,<br>interval cancer | Hypovascular + unchanged solitary BD-IPMN<br>Symptoms: yes. Ca19-9: 1990 U/mL | Palliation<br>(liver metastases) | PDAC | IV<br>(Dead, 1.4 years) |
| 6, F, 54 | FPC<br>1FDR + 1SDR | Solid lesion at baseline | Isovascular (6 mm), no restricted signal at DWI, unchanged over 22 months. Ca19-9 < 5 U/mL | MRI in 6 months | - | - |
| 7, F, 58 | FPC<br>1FDR + 1SDR | Solid lesion at baseline | Hypovascular (7 mm), restricted signal at DWI.<br>EUS: negative; Ca19-9 10 U/mL<br>CT+MRI: lesion regress | MRI in 6 months | - | |
| 8, F, 62 | FPC<br>3FDR + 1SDR | Solid lesion, onset at F/U | Hypovascular + unchanged solitary BD-IPMN<br>Symptoms: no. Ca19-9: 0.5 U/mL | Surgery | PDAC | IIA<br>(Dead, 4.9 years) |
| 9, F, 48 | HPC (BRCA2)<br>2SDR | Solid lesion, onset at F/U | Hypovascular + unchanged solitary BD-IPMN<br>Symptoms: no. Ca19-9: 24 U/mL | Surgery | PDAC | IB<br>(Alive, 0.7 years) |

***Table 24.*** *Characteristics of patients with solid and cystic lesions with imaging risk factors in study 4.*

*Table 24. (continue).*

| Patient/gender /age | Type of IAR | Suspected lesion | Imaging and clinical findings | Intervention | Histology | Stage/survival |
|---|---|---|---|---|---|---|
| 10, F, 86 | FPC<br>3FDR | Mixed-type IPMN | onset MPD dilatation (6-7mm) at F/U | Stop surveillance (no fit for surgery) | - | - |
| 11, M, 76 | FPC<br>1FDR + 3SDR | Mixed-type IPMN | onset MPD dilatation (6mm) at F/U<br>Pancreatoscopy: no suspicious findings<br>Ca19-9 5.2 U/mL | Surgery | Pancreatitis with retention cysts | - |
| 12, M, 73 | FPC<br>2FDR | Mixed-type IPMN | MPD dilatation at baseline (7-8 mm)<br>Ca19-9 5.8 U/mL | Surgery | Mixed-type IPMN LGD | - |
| 13, F, 30 | HPC (PJS)<br>1FDR | BD-IPMN | progress in size (10→15mm in 1 year).<br>Ca19-9 17 U/mL | Surgery | Mixed-type IPMN LGD | - |

Abbreviations: IAR, individual at risk. FPC, familial pancreatic cancer. HPC, hereditary pancreatic cancer. FDR, first-degree relative. SDR, second-degree relative. PDAC, pancreatic ductal adenocarcinoma. F/U, follow-up. MPD, main pancreatic duct. LGD, low-grade dysplasia. PJS, Peutz-Jeghers syndrome.

# 6 DISCUSSION

## 6.1 STUDY I

In this study, comparing a short versus a comprehensive MRI protocol, we demonstrated an almost complete equivalence in the assessment of relevant imaging features needed for the management of patients undergoing surveillance for pancreatic cystic neoplasms. Indeed, our three readers showed a very strong inter-observer agreement in the evaluation of the MPD and the cystic lesion's diameters, which are features included among the resection criteria for suspected IPMN both in the previous guidelines followed at our institution at the time this study was performed [81] and the current EG and ICG [6, 7]. In particular, the overall difference of the $D_C$ measured with the SP and CP was only 0.3 mm, which can be deemed as not clinically relevant (although statistically significant) as it corresponds to less than 1.5% of the mean $D_C$. Moreover, also the $D_{MPD}$ measured with the two protocols was almost equivalent with a difference of 0.06 mm. These results imply that the SP can be reliably applied for the assessment of such dimensional features.

Interestingly, the three readers showed an almost perfect agreement for the $D_C$ and $D_{MPD}$ even without any recommendation on measurements' standardization. Standardization may improve measurements' variability and inter-observer agreement, especially with less experienced fellow radiologists [94]. However, in our study, the three readers were staff abdominal radiologists with similar experience, which may have impacted on the very good inter-observer agreement.

Very important is also the assessment of MN, as it is a predictor factor for malignancy in IPMN. We observed that – overall - the evaluation with the SP and CP of the presence or absence of MNs coincided in 93% and 98% of the cases for $MN_C$ and $MN_{MPD}$, respectively, with a very high concordance between readers.

These findings suggest that the detection of relevant cystic features may be effective even without the acquisition of time-consuming sequences such as 3D-MRCP, DWI, and dynamic contrast-enhanced series.

In the past literature, some attempts have been made for evaluating shorter MRI protocols without contrast-enhanced sequences in the follow-up of PCNs. For instance, it has been shown that the assessment of cystic lesions (in terms of benign/indeterminate/malignant) coincided in 95.5% of the cases, when reading MRI examinations with and without contrast-enhanced sequences. In the remaining 4.5% of the cases with disagreement, a consensus retrospective revision did not find any relationship between the absence of contrast-enhanced series and the discordant evaluation [95]. In a larger study on 301 patients by Nougaret et al. [57], assessing the risk of malignancy as in the previous cited work, the overall intra-observer agreement for the image evaluation with and without contrast agent was 0.93 (95% C.I. 0.88-0.96) [57].

Compared to the two aforementioned studies, our work tried to assess an even shorter protocol, that did only include two respiratory-triggered T2-weighted sequences acquired in the axial and coronal plan as well as a breath-hold T1-weighted gradient-echo sequence, with

an estimated acquisition time of approximately 8 minutes, against about 35 minutes for the CP.

However, there may be some issues with the SP in the daily clinical praxis. First, not acquiring sequences after gadolinium-based contrast agents may affect the ability of differentiating a "true" contrast-enhancing MN from a "false" MN such as mucin plugs. However, the overestimation of the malignancy risk in IPMN, due to a false positive MN at unenhanced MRI, occurred in only three cases in Nougaret et al. [57]. Nevertheless, in case of development of a "filling defect" within the cyst or the MPD during surveillance, leading to the suspicion of a MN, the patient can either be recalled for completing the MRI examination with contrast agent, or the case can be discussed at the multidisciplinary team conference for further decision, also in relation to the size of the detected MN. Indeed, the assessment of contrast-enhancement in smaller (< 5 mm) MN may be challenging with MRI. Thus, in case of high suspicion, the collegial decisions might be to perform a contrast-enhanced EUS with or without biopsy, as recommended by guidelines [6, 7]. Second, the SP as proposed in our study does not include DWI. Interestingly, DWI was not part of the MRI protocol neither in the study of Macari et al. [95], nor in Nougaret's at al. [57]. Nonetheless, DWI is considered a valuable tool for the detection of PC, especially in case of solid masses located in the pancreatic tail or not affecting the MPD [59, 60]. Indeed, it might be more challenging to identify an associated or concomitant solid PC without DWI, and it should be underlined that our study did not include the detection of solid tumours among the variables, which should be seen as a limitation. However, a recently published study, that in a very similar manner compared an ultrashort MRI protocol (consisting of an axial T2-weighted and a 3D-MRCP sequences) with longer MRI protocols, showed that the ultrashort and longer protocols agreed in 99% of the cases in the assessment of solid PC [96].

Our study showed also an important economic advantage in substituting the CP with the SP, as the cost of the SP was estimated as circa 25% of the CP. For instance, we simulated the cost reduction for the follow-up of a 45-years old patient until the age of 80, obtaining a cost reduction of about 50,000 EUR. The economic benefit is even more evident when looking at the cost reduction for our study cohort of 154 patients over a ten-year period, that corresponded to circa 550,000 EUR. Assuming to apply the SP to the entire cohort of 498 patients under surveillance for the presence of pancreatic cystic lesions until 2015, the estimated cost reduction would be approximately 1,6 million EUR. This cost reduction is not negligible considering, on the one hand, the very high prevalence of pancreatic cystic lesions in the healthy population, and, on the other hand, the impelling need of rationalize the health-costs. Moreover, the advantage of applying the SP in the surveillance of pancreatic cystic lesions is not only economical. Indeed, the shorter acquisition time of the SP allows to schedule more patients per MRI suite and may improve patients' experience by decreasing stress and anxiety, often felt by patients during long MRI examinations. Finally, the absence of contrast agent in the SP eliminates the risk of gadolinium deposition in the body and nephrogenic systemic fibrosis, an important advantage on an ethical point of view, particularly in the setting of a screening performed on healthy people.

There are some limitations in our study. First, this was a retrospective analysis of a cohort of patients with PCNs, where only a few had a histopathologically proven lesion. For this reason, we could not calculate and compare the diagnostic accuracy metrics for the SP and

the CP in detecting concerning imaging features and malignancy. However, our study aimed to assess whether the SP might have missed relevant clinical information compared to the standard CP. Second, we included MRIs performed over a ten-year time interval. Thus, minor differences in the technical parameters - such as interslice gap or slice thickness – may partially affect our results. Third, the cost of the CP and SP was calculated from our institution's Department of Economics. Hence, different costs and billing may apply in other institutions. Fourth, we simulated the individual cost reduction for a hypothetical patient of 45 years old, younger than the median age of our cohort, being aware that usually pancreatic cystic neoplasms most often are encountered in patients in their sixties. However, we aimed to test the "worst case scenario" of an extended follow-up, thus, to better highlight the individual benefit.

## 6.2 STUDY II

In the second study, we demonstrated that neither new features such as volume and elongation value nor well-known standard imaging criteria (cystic diameter, wall thickness, multifocality or size progression) were able to preoperatively predict malignancy in patients with BD- and mixed type IPMN.

The role of volume as a predictor of malignancy in IPMN was previously assessed in another study, that, in contrast to our results, demonstrated that an intraductal volume ≥10 $cm^3$ could identify malignancy with a sensitivity and specificity of approximately 70% [97]. However, the authors included both CT and MRI images, analysed the volume of the whole ductal system (i.e., including the MPD), and performed a manual segmentation by pen-drawing, scanning and thereafter digitalizing the IPMN volumetry, which was complicated and not feasible in the daily routine. Although not correlated to malignancy - similarly though to cystic diameter - automatic or semiautomatic volumetry might still be a useful tool for assessing size progression due to its high reproducibility [98], as it may potentially be obtained with any segmentation tool implemented in any PACS workstation.

According to our hypothesis, malignancy might be related to BD-IPMN's shape, expressed by the elongation value. For instance, we supposed that more spheric BD-IPMN with an EV closer to zero might produce more mucin, due to its mucin immunophenotype (MUC) and grade of dysplasia. We observed that the EV tended to be inversely associated to malignancy, i.e., the lower the EV value the higher the probability of HDG/INV. However, this association was not statistically significant. Hence, our hypothesis of an association between cyst morphology and risk of malignancy was not supported by sufficient evidence.

In line with previously published papers, the presence of contrast-enhancing mural nodules was associated to malignancy [25, 28].

Noteworthy, the dilatation of the MPD resulted a positive predictive factor for malignancy in IPMN, even after excluding all the cases with solid mass-forming PC. The choice of not to include solid masses was motivated by the need to explore the real effect of the MPD dilatation in IPMN, thus, without lesions causing stricture and upstream dilatation of the MPD. For this reason, our results reenforce the role of a dilated MPD in a surgical series in

predicting malignancy, in line with previously published papers which also included solid masses [18, 20, 99]. Indeed, particularly if associated with other findings (e.g., MN and/or elevated CA19-), the dilatation of the MPD is associated to a higher risk of malignancy. Nonetheless, when the MPD dilation was the only surgical indication (15 cases), we observed low sensitivity and PPV (11% and 20%, respectively). Presumably, the MPD may get dilated not only because of disseminated epithelial malignant changes along the entire ductal system, but also due to mucin distension produced by solitary or multifocal BD-IPMNs. Hence, the decision upon surgery based on the only finding of a dilated MPD in a patient with suspected IPMN should be carefully weighted.

Elevated serum levels of CA19-9 were the only "clinical" concerning feature associated with a higher risk of malignancy, which is well consistent with data from the literature [22, 23, 99, 100]. On the contrary, we could not demonstrate any association between the presence of symptoms and malignancy, probably because of the small sample and the exclusion of mass-forming PC, which are the most often cause of symptoms.

We believe that excluding solid PC from our analysis represents a strength of the study. First, the onset of a solid mass probably corresponds to the latest form of IPMN malignant transformation, and it always represents an absolute indication for surgery (assuming that the patient is fit for surgery and the tumour is technically resectable). Second, merging cases with associated or concomitant PC, causing a stenosis of the MPD and its upstream dilatation, together with cases with "pure" IPMN may induce an overestimation of the impact of the "MPD dilatation" on the risk of malignancy. Indeed, at our multidisciplinary team conferences, it is much more common to debate about "to operate or not" a patient on the only basis of a dilated MPD, rather than a solid mass. The risk versus benefit assessment in such cases, based on current guidelines, may be biased by previous published literature that also included solid tumours causing stenosis and dilatation of the MPD.

Our study has several limitations. It is based on a retrospectively collected cohort of surgically resected IPMNs with slight variation of surgical resection criterion over time, which may limit the generalization of our results on a "population-level basis". However, this is a common and inevitable issue of all similar and previously published papers on this topic. Furthermore, the study population was small, although it still allowed us to reach statistically significant results. Larger cohorts are probably needed to better assess volume and elongation value. Regarding the role of MN as a malignancy predictor, we did not perform a radiologic-pathologic correlation of the malignant focus location in relation to the MN. Moreover, on a technical point of view, segmenting the BD-IPMN on T2-weighted axial images, performed with different vendors and slightly different technical parameters, might have caused less accurate measurements. However, not all cases included a 3D-MRCP sequence since it is not a requirement according to guidelines [7]. When 3D-MRCP were available, artifacts affected the image quality in several cases not allowing any reliable analysis. Additionally, two radiologists assessed the MR-images in consensus; thus, we could not calculate the inter-rater agreement for the collected variables.

## 6.3 STUDY III

In the third study, we trained, internally validated, and compared five different models for the preoperative differentiation of malignant BD-IPMN using MRI images: one model based on standard clinical and imaging features only (Clin), two models based on extracted radiomics features only (Rad), and two hybrid models, comprising standard and radiomics features (RadClin) for the discrimination of malignant (HGD/INV) BD-IPMN after segmentation of pre-operative MRIs. We found that the Rad1 model, built with only 13 pure radiomics features after images segmentation from radiologist 1, outperformed the Clin model, although with an expected high degree of overfitting. The radiomics features that mostly concurred were shape-related features (Sphericity and Elongation).

The main challenge in this study was represented by the adoption of MRI images for the radiomics' modelling. Indeed, operating on MRI images and radiomics implies some issue, due to the inherent variability of MRI images. This variability depends on both patient- (e.g., motion or respiratory artefacts) and technique-related factors (field strength inhomogeneities, different acquisition parameters within the same sequence and vendor, but also linked to different vendors), not to mention the intra- and interrater segmentation variability. All these factors accounted for a great amount of heterogenicity of our data. For this reason, we were compelled to assess the spatial (i.e., stability to slight variations in segmentation) and cross-vendor stability before starting to build and select the radiomics models.

Although we observed an overall very high spatial stability, the Local Binary Pattern filter generated the lowest proportion of stable features, probably because of its dependence on neighbouring voxels in determining the binary value of each voxel, which would make it more sensible to slight differences in segmentation margins.

As expected, the cross-vendor stability showed different outcomes. On the one hand, filters that amplified intensity differences between vendors (i.e., exponential, logarithm, and square filters) produced the highest percentage of unstable features. On the other hand, filters that did not place as much weight on the image intensities (i.e., gradient or wavelet), returned the highest percentage of stable features. We also considered a subanalysis for comparing the radiomics performances across vendors and assessing possible biases. However, we did not have enough patients in the "General Electric Healthcare" group to generalize to the source population.

Another issue was represented by the imbalanced nature of the dataset, with a greater proportion of patients with benign (LGD) than malignant (HGD/INV) BD-IPMN. To overcome this issue, we optimized the models applying an F-score with *beta* equal to 2, which overweighted recall (i.e., sensitivity), placing a higher performance cost on false negatives and counteracting the natural tendency of the models toward making a "negative" prediction [101].

The results of our performance analysis are interesting. The Clin model was surpassed by the Rad1 and RadClin1 models, which had similar performances. However, the Rad1 needed only 13 features compared to the RadClin1 (40 features, with automatically selection of only one standard clinical feature – CA19-9). To reduce the risk of overfitting, it is recommended to have a ratio of approximately 10-15 patients per included radiomics features [71, 102].

Thus, the Rad1 model appears more robust than RadClin1 for our small cohort of 130 cases, as demonstrated in the volatility analysis. The fact that malignancy in BD-IPMN might be predicted by a pure radiomics signature, i.e., without any standard imaging/clinical feature, is intriguing, although it must be underlined that our model should be first externally validated in a large multicentre cohort.

Noteworthy, shape-related radiomics features as Sphericity and Elongation were those which contributed the most to the Rad1 model (with negative and positive relation with malignancy outcome, respectively), suggesting that BD-IPMN morphology may play a role in malignancy prediction. However, Elongation in PiRadiomics is measured differently compared to our elongation value in study 2 (i.e., "the inverse of true elongation" according to the PiRadiomics package's description).

An original aspect of this study is the comparison of radionics models' performances after segmentation by two separate radiologists, which was the first attempt of its kind in the setting of the IPMN malignancy prediction at pre-operative imaging. Indeed, in previous publications, the segmentations were either performed by one experienced radiologist [74, 76, 77, 103], or by one radiologist and verified by a second radiologist [78]. The Rad and RadClin models did not perform differently among the two radiologists, although Rad2 and RadClin2 did not show any difference compared to the Clin model or the dummy classifier. The reason for this incongruence is not fully understood. It might be related to broader confidence intervals of the AUCs for radiologist 2 compared to radiologist 1 (results not shown), presumably due to less consistent segmentations, even though the spatial stability was very high.

Interestingly, compared to other internally cross-validated studies, our MRI-based radiomics models showed similar good performance [76, 103]. However, these studies had even smaller sample sized (38 and 103 cases, respectively), with the inherent risk of high degree of overfitting. To the best of our knowledge, only two diagnostic accuracy studies, including an internal and external validating cohort, assessed radiomics models in predicting IPMN malignancy [77, 78]. In Tobaly et al. [77], the CT-based radiomics model had an AUC of 0.84 and 0.71 in the training and external validating cohort, respectively. In Cui et al. [78], the MRI-based radiomics model showed AUC of 0.81-0.82 in the two external validation groups, versus an AUC of 0.84 in the internal training set. Moreover, the authors proposed a nomogram for the prediction of IPMN malignancy, which included radiomics and clinical features, such as CA19-9 and the diameter of the MPD.

Although our work is a proof-of-concept study aiming at the evaluation of a prediction model in a pre-clinical stage, our promising results suggest that radiomics models are worth further exploration with multicentre diagnostic accuracy studies and much larger sample sizes.

Some limitations are present in this study. First, our results should be treated with caution, due to the small sample size and the only internal cross-validation. Our radiomics models may still overfit even in an external validating cohort. Second, we retrospectively included MRI examinations performed with different magnetic field strength, vendors, and T2-weighted sequences' parameters, introducing large heterogenicity. However, 77% of the extracted radiomics features were considered cross-vendor stable. Third, we could not assess

the temporal stability of the radiomics features, as we analysed only one set of MRI sequences per patient. Fourth, although most of the MRI examinations were performed with one vendor, we did not address the imbalanced nature of the distribution of the MRI scanners.

## 6.4 STUDY IV

Study 4 represents the largest single-centre cohort of IAR in Scandinavia, including 278 asymptomatic patients with a median follow-up of 4.5 years.

We observed a very high prevalence of focal pancreatic lesions (59%). Most of them were very small cysts with a median size of only 5.5 mm. Almost 60% of these cystic lesions corresponded to suspected IPMN. The prevalence of pancreatic cysts in our cohort was higher than in a previously published study performed on IAR (48%) [104] or in the "*population-based Study of Health in Pomerania (SHIP)*" (49%) [15], and even higher compared to the overall weighted pooled proportion of 0.15 at baseline reported in a recent meta-analysis [105]. However, our prevalence of 59% includes cysts detected both at baseline and under surveillance, while others' proportions derived from baseline controls only [15, 105]. The proportion of patients with cysts at baseline (scenarios 7, 8 and 10) was 38%, similar to the range of 40-43% reported by the CAPS Consortium [50, 51].

Only a minority of patients with imaging findings (5%, 13 patients with cysts with imaging risk factors and/or solid lesions) required further attention (surgery, palliation, or closer follow-up).

None of the three cysts with concerning features that underwent surgery were malignant at final histology. In contrast, data from the "CAPS 1-5 studies", including 732 patients, showed that 7% of the entire cohort (24/732) were operated because of cysts with concerning features detected at baseline/follow-up; 20% of them (5 cases) were diagnosed with IPMN with HGD or associated PDAC [104].

In our cohort, the overall prevalence of preneoplastic lesions and early PC was 0.7% (2/278), compared with 3.4% (12/354) in the "CAPS 1-4" study [51], and 0.9% (13/1461) in the "CAPS 5" study [52].

Besides the absence of preneoplastic lesions, another noteworthy finding in our cohort is the presence of only two patients with PC stage I (one stage IA and one stage IB) among the 5 PC cases. In the "CAPS 1-4" study, in a series of 354 IAR, two patients had PC in stage IA, and ten IPMN/PanIn with HGD (thus, 22% among 54 patients with imaging risk factors and solid lesions) [51]. In the recent "CAPS 5" study, of the nine PC detected under surveillance, seven were in stage I, and further 3 HGD were correctly diagnosed [52]. Interestingly, in our cohort, 40% (2/5) of the patients with PC had symptoms and 40% (2/5) had unresectable/metastatic disease, a slightly higher proportion compared to a rate of 26-28% in previous studies [51, 106]. In Dbouk et al. and Klatte et al., only 16-20% of the cases were considered unresectable/metastatic [52, 107].

Considering all the facts presented above, the results of our screening appear disappointing at first sight, if the main aim of IAR screening is detecting preneoplastic lesions or early PC

in stage I [49, 105], since we did not observe any preneoplastic lesion and we had a high rate of symptomatic and advanced/metastatic PC. However, recently published multicentre studies showed analogous issues. Overbeek et al. found that more than 70% (out of 2552 patients) of the screening-detected PC were diagnosed in an advanced stage [53]. Similarly, a recent meta-analysis showed that the incidence of target lesions (HGD or T1N0M0 tumours) was lower than that of advanced PC [54].

It is not simple to address the causes of the absence of HGD and the low prevalence of early asymptomatic PC in our cohort. Cohorts' different sizes and composition, or the lengths of the follow-up may have affected the results. Furthermore, in some patients the MRI follow-up examinations were delayed. At our institution, IAR with cystic lesions are controlled with MRI every six months. In three patients with "trivial" cysts that developed PC (one stage IB, one stage IIA and one stage IV), the examinations were performed 7-13 months later than the due time for various patient-related issues. However, although the MRI controls were punctual in two cases, one patient still developed a PC stage IA, and another had a PC stage IV (missed at MRI and eventually became symptomatic). This seems in line with Overbeek K at al., where almost half of PC in IAR occurred as new lesions after barely one year [53]. Another explanation may rely on the imaging modalities chosen for the screening. Our program is mainly MRI-based, unlikely other programs that use a combination of EUS and MRI as in CAPS Consortium [51, 52, 104] or in European multicentre studies [106, 107]. Only a few publications reported the yield of an MRI-based screening on high-risk individuals [108–110]. Interestingly, also in Ludwig et al., the prevalence of preneoplastic lesions (HGD) or early PC was low (0.9%, 1/109 - PanIn with HGD), although they only encountered one T3N0 PC [108]. At our institution, EUS is not routinely performed as a screening test. It is reserved for selected cases after discussion at the multidisciplinary conference. However, this might only partly explain the low prevalence of early PC or preneoplastic lesions. Indeed, although EUS appears superior in the detection of solid lesions [111], some authors showed poor or no agreement between MRI and EUS in the detection of "high-risk stigmata", such as enhanced solid component and dilated MPD >10 mm [67], while others found a very high concordance in detecting pancreatic changes, such as cystic lesions or dilated MPD [68]. Moreover, no difference in the detection of early PC or preneoplastic lesions was found between MRI and EUS at baseline examinations in high-risk individuals [105]. This may imply that a similar good performance can be observed even during follow-up controls. Further, it must be highlighted that no agreement was found in the CAPS Consortium's recommendation on whether EUS and MRI should be alternated [49].

Another issue of imaging-based screenings for IAR is represented by the low sensitivity and PPV in detecting malignancy. Our program achieved a sensitivity of 60% and a PPV of 37%, in line with the ICG [6] and the CAPS Recommendations [49], that reached a sensitivity of 40% and 60%, and a PPV of 40% and 50% respectively in IAR screening [104]. Clearly, imaging features alone are not sufficient for the early identification of PC and its precursors in individuals at risk.

In IAR surveillance, serum biomarkers capable of predicting malignancy are need. For instance, fasting blood glucose or Haemoglobin A1c (HbA1c) is recommended by the CAPS Consortium for the early detection of new-onset diabetes [49], since progressive metabolic changes characterize the development of PC, the earliest being the onset of hyperglycaemia

starting about three years before the diagnosis of PC [112, 113]. In our centre, CA19-9 was used in the follow-up, although affected by low sensitivity and specificity [114, 115]. Additionally, HbA1c and faecal elastase-1 have been included in the routine laboratory panel. Liquid biopsy and circulating biomarkers may represent the future direction for the diagnosis of PC [114]. Interestingly, some data suggests the role of faecal "microbiota-based" biomarkers [116].

Our study has some limitations. First, it is a retrospective study based on the database of IAR followed up by medical gastroenterologists over a 19-year long period. Thus, some clinical and laboratory data (such as chronic pancreatitis, diabetes, smoke, and alcohol overconsumption) were not available for all the patients. Additionally, although most patients were screened with MRI only, in almost 30% of the cases, CT and MRI were both used, particularly in the first years until 2010. Third, our study population is relatively small, with a low prevalence of some categories of patients (e.g., FAMMM - CDKN2A/p16 mutation; or Lynch syndrome). Given the rarity of constitutional genetic mutations, multicentre studies involving several Scandinavian centres will be needed in the future.

# 7 CONCLUSIONS

**Study I**

A short MRI protocol for the surveillance of patients with pancreatic cystic neoplasms was faster, less expensive and provided equal clinically relevant information compared to a comprehensive MRI protocol.

**Study II**

Novel imaging features, such as volumetry and elongation value, were not able to predict malignancy in BD-IPMN. However, the dilatation of the main pancreatic duct, particularly if associated with contrast-enhancing mural nodules and elevated serum levels of CA19-9, represented a predictor of malignancy in BD-IPMN even excluding solid mass-forming pancreatic cancers.

**Study III**

In this feasibility study, the MRI-based radiomics models with and without the inclusion of "standard" clinical/imaging features were able to predict malignancy in BD-IPMN with good performance metrics. A pure radiomics model appeared more robust than a hybrid radiomics model, including also "standard" clinical features. It is worthwhile to proceed with further studies with external cross-validation for corroborating the validity of the radiomic models.

**Study IV**

The MRI-based screening of individuals at risk for pancreatic cancer showed a very high prevalence of lesions, most of them represented by "trivial" cysts. No precursors of pancreatic cancer, such as IPMN or PanIn with high-grade dysplasia, were identified. The prevalence of pancreatic cancer was low, with an equal proportion of cases in stage I and IV. Sensitivity and positive predictive values were low. Thus, in line with the recent literature, the early diagnosis of pancreatic cancer and its precursors in individuals at risk represents a challenge for an MRI-based screening program.

# 8 POINTS OF PERSPECTIVE

**Study I**

Being able to demonstrate the equality of a short compared to a "traditional" comprehensive MRI protocol in the surveillance of pancreatic cystic neoplasms led to its implementation in the clinical practice at our institution, allowing shorter examination times and more available slots in the daily practice. However, since we did not compare the ability to detect solid masses in our study, we decided to include DWI with two b-values in our clinical protocol, thus, not to risk overlooking the onset of associated or concomitant tumours. Interestingly, our paper encouraged further research in this field, that has been recently published, supporting our results [96, 117].

Considering that our short protocol (although in its slightly "extended" version, including DWI) has been currently used since 2017, we have gained enough data to assess its performance over these years, in terms of diagnostic accuracy metrics.

**Study II and III**

In study II, we did not achieve sufficient evidence to prove that BD-IPMN's volume and morphology, expressed by the elongation value, may predict malignancy. We also observed that standard imaging concerning features, except for contrast-enhancing mural nodules and dilated main pancreatic duct, are associated with a low risk of malignancy. Nonetheless, a MRI radiomics-based model could predict BD-IPMN malignancy with better performance than standard clinical and imaging features.

Our results have an important clinical impact. On the one hand, study II once more highlights the challenge of correctly identifying suspicious BD-IPMN with standard imaging criteria, which it is extremely relevant to reduce the proportion of unnecessary surgery. On the other hand, study III demonstrated that other methods, such as an MRI-based radiomics models, are feasible and potentially able to assist radiologists and clinicians in correctly define patients at risk. However, before we can routinely apply machine learning and radiomics models in the clinical praxis, larger multicentre studies are needed, thus, to assess their ability in discriminating malignant IPMN by means of external validation.

**Study IV**

The aforementioned limits of "traditional" imaging features for the detection of potentially malignant lesions are evident also from the results of study IV. Indeed, a prevalently MRI-based screening on individuals at risk for pancreatic cancer showed low sensitivity and positive predictive value. As mentioned before, addressing the reasons of this unsuccess is difficult, although it has important implications. It might depend on demographic characteristics of our cohort or the chosen surveillance modality. Hence, it would be beneficial to compare two different screening approaches in the setting of a multicentre study, an MRI-based screening versus the combined MRI-EUS screening as proposed and analysed in the multiple CAPS Consortium's publications. Moreover, more research is needed for better understanding not only the economic impact of the MRI screening, but also its

epidemiological impact in terms of lives saved – a cornerstone in other screening programs such as breast cancer screening - by means of prospective randomized trials.

# 9 ACKNOWLEDGEMENTS

This thesis represents the end of a long, extraordinary - often challenging - journey that would not have been possible without the help and support from my colleagues, friends, and family.

In particular, I would like to express my greatest gratitude to:

My principal supervisor **Nikolaos Kartalis**. Yours was the idea to drag me into this adventure, which I will never regret. Thank you for your encouragement, inspiration, and guidance. We worked incredibly well together.

My co-supervisor **Marco del Chiaro**. You were one of the first colleagues I met when I started my working experience at Karolinska University Hospital. Your charisma and cleverness have always been fascinating and inspiring. Thank you for teaching me all I know about pancreatic surgery.

My co-supervisor **Caroline Verbeke**. Thank you for being so supportive, kind, and patient during all these years and for sharing your extraordinary knowledge and experience in pancreatic pathology.

My co-supervisor **Lennart Blomqvist**. You were always there for me when I needed you the most. Your thoughtful wisdom and kindness helped me through the toughest decisions of my life.

My professor **Torkel Brismar**, for creating such a good and stimulating research environment, and my former professor **Peter Aspelin**, for your vision and insight, your warmness and dedication.

My coauthors **Nikolaos Papanikolaou**, **Ana Carolina Rodrigues**, **Matthias Löhr** and **Miroslav Vujasinovic**. It would not have been possible to realize my studies without your patience, knowledge, and advice.

My coauthor **Carlos Fernández Moro**. We literally spent hours and hours at the microscope. Thank you for your great availability and dedication and for everything you taught me about IPMN.

My co-author and dearest friend **Roberto Valente**, for your invaluable help and support, but especially for all the happy moments, we spent with our families. I miss you and **Chiara** so much.

All my co-authors, **Irina Rinta-Kiikka**, **Katharina Wünsche**, **Johanna Laukkarinen**, **Knut Jørgen Labori**, **Kim Ånonsen**, **Ingrid Pettersson**, **Ana Farah-Mwais**, **Peter Gustavsson**, **Poya Ghorbani**, for your efforts and kind suggestions.

Our statistician **Per Näsman**, for your excellent work and prompt availability every time I got confused.

Our statistician and my great friend **Nicola Orsini**, for firmly believing in me being capable of understanding statistics. You pushed me hard and spent countless hours trying to make the

impossible possible. My great friend and epidemiologist, **Debora Rizzuto**, for supporting me when I did not dare to ask (her husband) Nicola.

My chief of the Abdominal Radiology section and dear friend **Louiza Loizou**, for your encouragement, but particularly for your patience (or – better- resilience) during the last two toughest years.

My former chiefs, **Maria Kristoffersen Wiberg**, **Elisabet Axelsson**, **Jan Carlson**, **Katarina Fredriksson** and **Natalia Luotsinen**, for your trust and support during all the years we spent working together.

My mentor and former chief **Giovanni Morana**. You are the reason why I love abdominal imaging so much. You instilled this unshakable passion in me and taught me how to fly. Ad maiora semper.

My precious colleague **Katharina Brehmer**. You have been so kind, caring and supportive by helping me in preparing my thesis.

My dear colleague **Aristeidis Grigoriadis**, for all the fantastic brainstorming on MRI and research over the last decade (sic!).

All my amazing colleagues for the Abdominal Radiology section, in rigorous alphabetic order: **Mats Andersson**, **Konstantinos Arvanitis**, **Harout Bakkalian**, **Maria Blomberg**, **Stefan Hamma**, **Gunnar Herlin**, **Nafsika Korsavidou Hult**, **Gunnar Juliusson, Klaus Lange**, **Trevor Peters**, **Andrej Saletic**, **Chen Tamm**, **Carlos Valls**, **Nikolaos Voulgarakis**. You are all very special to me. With most of you, I professionally grew up in the last ten years, and with some of you, this fantastic journey has just started.

My research fellows **Antonios Tzortzakakis** and **Ola Kvist**, for all the good, funny times together during our PhDs.

My dearest friends from my broad Italian family here in Stockholm, **Elisabetta Bari** and **Massimiliano Sacco**, **Nadia Battain** and **Giuseppe Dreossi**. Without you, life here would not have been so easy and enjoyable.

My dear friend **Lara Simonova**, for making my life more colourful.

All my parents-in-law, **Cristiana** and **Mario**, **Annie** and **Augusto**. Thank you for welcoming me into your families and always being so supportive.

Lastly, I would like to thank the most special people in my life.

My parents, **Riccardo** and **Emanuela**, and my brother **Andrea**. I am what I am thanks to everything I have learnt from you. Thank you from the deepest of my heart for your unconditional support and caring love.

My husband **Marco** and our sweetest girls **Chiara** and **Sofia**. Marco, you are my Pole star. I would have never made it without you. Chiara and Sofia, thank you for motivating me with all your love, laughs, screams, and cries. There is nothing stronger than my love for you.

# 10 REFERENCES


1. Siegel RL, Miller KD, Fuchs HE, Jemal A (2022) Cancer statistics, 2022. CA Cancer J Clin 72:7–33. https://doi.org/10.3322/CAAC.21708
2. American Cancer Society (2022) Cancer Facts & Figures 2022. Atlanta: American Cancer Society
3. Nationell kvalitetsregistergrupp bukspottkörtelcancer (2022) Kvalitetsregister för tumörer i pankreas och periampullärt Årsrapport nationellt kvalitetsregister
4. Mizrahi JD, Surana R, Valle JW, Shroff RT (2020) Pancreatic cancer. The Lancet 395:2008–2020. https://doi.org/10.1016/S0140-6736(20)30974-0
5. Grossberg AJ, Chu LC, Deig CR, et al (2020) Multidisciplinary standards of care and recent progress in pancreatic ductal adenocarcinoma. CA Cancer J Clin caac.21626. https://doi.org/10.3322/caac.21626
6. Tanaka M, Fernandez-Del Castillo C, Kamisawa T, et al (2017) Revisions of international consensus Fukuoka guidelines for the management of IPMN of the pancreas. Pancreatology 17:738–753. https://doi.org/10.1016/j.pan.2017.07.007
7. The European Study Group on Cystic Tumours of the Pancreas (2018) European evidence-based guidelines on pancreatic cystic neoplasms. Gut 67:789–804. https://doi.org/10.1136/gutjnl-2018-316027
8. Crippa S, Fogliati A, Valente R, et al (2021) A tug-of-war in intraductal papillary mucinous neoplasms management: Comparison between 2017 International and 2018 European guidelines. Digestive and Liver Disease 53:998–1003. https://doi.org/10.1016/J.DLD.2021.03.009
9. Rosenthal MH, Wolpin BM, Yurgelun MB (2022) Surveillance Imaging in Individuals at High Risk for Pancreatic Cancer: Not a Ceiling, but Rather a Floor Upon Which to Build. Gastroenterology 162:700–702. https://doi.org/10.1053/j.gastro.2021.12.259
10. Nagtegaal ID, Odze RD, Klimstra D, et al (2020) The 2019 WHO classification of tumours of the digestive system. Histopathology 76:182–188. https://doi.org/10.1111/his.13975
11. Ren B, Liu X, Suriawinata AA (2019) Pancreatic Ductal Adenocarcinoma and Its Precursor Lesions: Histopathology, Cytopathology, and Molecular Pathology. American Journal of Pathology 189:9–21. https://doi.org/10.1016/j.ajpath.2018.10.004
12. Maire F, Couvelard A, Palazzo L, et al (2013) Pancreatic Intraepithelial Neoplasia in Patients With Intraductal Papillary Mucinous Neoplasms. Pancreas 42:1262–1266. https://doi.org/10.1097/MPA.0b013e3182962723
13. Leblanc JK, Chen JH, Al-Haddad M, et al (2014) Can endoscopic ultrasound predict pancreatic intraepithelial neoplasia lesions in chronic pancreatitis?: A retrospective study of pathologic correlation. Pancreas 43:849–854. https://doi.org/10.1097/MPA.0000000000000142
14. Vullierme MP, Menassa L, Couvelard A, et al (2019) Non-branched microcysts of the pancreas on MR imaging of patients with pancreatic tumors who had pancreatectomy may predict the presence of pancreatic intraepithelial neoplasia (PanIN): a preliminary study. Eur Radiol 29:5731–5741. https://doi.org/10.1007/s00330-019-06154-3
15. Kromrey ML, Bülow R, Hübner J, et al (2018) Prospective study on the incidence, prevalence and 5-year pancreatic-related mortality of pancreatic cysts in a population-based study. Gut 67:138–145. https://doi.org/10.1136/GUTJNL-2016-313127

16. Valsangkar NP, Morales-Oyarvide V, Thayer SP, et al (2012) 851 resected cystic tumors of the pancreas: A 33-year experience at the Massachusetts General Hospital. https://doi.org/10.1016/j.surg.2012.05.033
17. Marchegiani G, Andrianello S, Pollini T, et al (2019) "Trivial" Cysts Redefine the Risk of Cancer in Presumed Branch-Duct Intraductal Papillary Mucinous Neoplasms of the Pancreas: A Potential Target for Follow-Up Discontinuation? Am J Gastroenterol 114:1678–1684. https://doi.org/10.14309/ajg.0000000000000378
18. del Chiaro M, Beckman R, Ateeb Z, et al (2019) Main Duct Dilatation Is the Best Predictor of High-grade Dysplasia or Invasion in Intraductal Papillary Mucinous Neoplasms of the Pancreas. Ann Surg. https://doi.org/10.1097/sla.0000000000003174
19. Hackert T, Fritz S, Klauss M, et al (2015) Main-duct Intraductal Papillary Mucinous Neoplasm: High Cancer Risk in Duct Diameter of 5 to 9 mm. Ann Surg 262:871–875. https://doi.org/10.1097/sla.0000000000001462
20. Marchegiani G, Andrianello S, Morbin G, et al (2018) Importance of main pancreatic duct dilatation in IPMN undergoing surveillance. British Journal of Surgery 105:1825–1834. https://doi.org/10.1002/bjs.10948
21. Sahora K, Mino-Kenudson M, Brugge W, et al (2013) Branch duct intraductal papillary mucinous neoplasms: does cyst size change the tip of the scale? A critical analysis of the revised international consensus guidelines in a large single-institutional series. Ann Surg 258:466–475. https://doi.org/10.1097/SLA.0b013e3182a18f48
22. Jang J-Y, Park T, Lee S, et al (2017) Proposed Nomogram Predicting the Individual Risk of Malignancy in the Patients With Branch Duct Type Intraductal Papillary Mucinous Neoplasms of the Pancreas. Ann Surg 266:1062–1068. https://doi.org/10.1097/SLA.0000000000001985
23. Kim HS, Song W, Choo W, et al (2021) Development, validation, and comparison of a nomogram based on radiologic findings for predicting malignancy in intraductal papillary mucinous neoplasms of the pancreas: An international multicenter study. J Hepatobiliary Pancreat Sci. https://doi.org/10.1002/jhbp.962
24. Jung W, Park T, Kim Y, et al (2019) Validation of a nomogram to predict the risk of cancer in patients with intraductal papillary mucinous neoplasm and main duct dilatation of 10 mm or less. British Journal of Surgery 106:1829–1836. https://doi.org/10.1002/bjs.11293
25. Zhao W, Liu S, Cong L, Zhao Y (2022) Imaging Features for Predicting High-Grade Dysplasia or Malignancy in Branch Duct Type Intraductal Papillary Mucinous Neoplasm of the Pancreas: A Systematic Review and Meta-Analysis. Ann Surg Oncol 29:1297–1312. https://doi.org/10.1245/S10434-021-10662-2/FIGURES/3
26. Wong J, Weber J, Centeno BA, et al (2013) High-Grade Dysplasia and Adenocarcinoma Are Frequent in Side-Branch Intraductal Papillary Mucinous Neoplasm Measuring Less than 3 cm on Endoscopic Ultrasound. Journal of Gastrointestinal Surgery 17:78–85. https://doi.org/10.1007/s11605-012-2017-0
27. Ciprani D, Weniger M, Qadan M, et al (2020) Risk of malignancy in small pancreatic cysts decreases over time. Pancreatology 20:1213–1217. https://doi.org/10.1016/j.pan.2020.08.003
28. Marchegiani G, Andrianello S, Borin A, et al (2018) Systematic review, meta-analysis, and a high-volume center experience supporting the new role of mural nodules proposed by the updated 2017 international guidelines on IPMN of the pancreas. Surgery 163:1272–1279. https://doi.org/10.1016/j.surg.2018.01.009
29. Wang W, Zhang L, Chen L, et al (2015) Serum carcinoembryonic antigen and carbohydrate antigen 19-9 for prediction of malignancy and invasiveness in

intraductal papillary mucinous neoplasms of the pancreas: A meta-analysis. Biomed Rep 3:43. https://doi.org/10.3892/BR.2014.376
30. Ciprani D, Morales-Oyarvide V, Qadan M, et al (2020) An elevated CA 19-9 is associated with invasive cancer and worse survival in IPMN. https://doi.org/10.1016/j.pan.2020.04.002
31. Kaiser J, Scheifele C, Hinz U, et al (2021) IPMN-associated pancreatic cancer: Survival, prognostic staging and impact of adjuvant chemotherapy. https://doi.org/10.1016/j.ejso.2021.12.009
32. Nilsson LN, Keane MG, Shamali A, et al (2016) Nature and management of pancreatic mucinous cystic neoplasm (MCN): A systematic review of the literature. Pancreatology 16:1028–1036. https://doi.org/10.1016/j.pan.2016.09.011
33. Park JW, Jang JY, Kang MJ, et al (2014) Mucinous cystic neoplasm of the pancreas: Is surgical resection recommended for all surgically fit patients? Pancreatology 14:131–136. https://doi.org/10.1016/j.pan.2013.12.006
34. Llach J, Carballal S, Moreira L (2020) Familial pancreatic cancer: Current perspectives. Cancer Manag Res 12:743–758. https://doi.org/10.2147/CMAR.S172421
35. Canto MI, Harinck F, Hruban RH, et al (2013) International cancer of the pancreas screening (CAPS) consortium summit on the management of patients with increased risk for familial pancreatic cancer. Gut 62:339–347. https://doi.org/10.1136/gutjnl-2012-303108
36. Klatte DCF, Wallace MB, Löhr M, et al (2022) Hereditary pancreatic cancer. Best Pract Res Clin Gastroenterol. https://doi.org/10.1016/J.BPG.2021.101783
37. Giardiello FM, Brensinger JD, Tersmette AC, et al (2000) Very high risk of cancer in familial Peutz-Jeghers syndrome. Gastroenterology 119:1447–1453. https://doi.org/10.1053/gast.2000.20228
38. Matsubayashi H, Takaori K, Morizane C, Kiyozumi Y (2019) Familial pancreatic cancer and surveillance of high-risk individuals. Gut Liver 13:498–505
39. Klein AP, Brune KA, Petersen GM, et al (2004) Prospective Risk of Pancreatic Cancer in Familial Pancreatic Cancer Kindreds. Cancer Res 64:2634–2638. https://doi.org/10.1158/0008-5472.CAN-03-3823
40. Oyama H, Tada M, Takagi K, et al (2020) Long-term Risk of Malignancy in Branch-Duct Intraductal Papillary Mucinous Neoplasms. Gastroenterology 158:226-237.e5. https://doi.org/10.1053/j.gastro.2019.08.032
41. Choi SH, Park SH, Kim KW, et al (2017) Progression of Unresected Intraductal Papillary Mucinous Neoplasms of the Pancreas to Cancer: A Systematic Review and Meta-analysis. Clinical Gastroenterology and Hepatology 15:1509-1520.e4. https://doi.org/10.1016/j.cgh.2017.03.020
42. Kang MJ, Jang JY, Lee KB, et al (2014) Long-term prospective cohort study of patients undergoing pancreatectomy for intraductal papillary mucinous neoplasm of the pancreas: Implications for postoperative surveillance. Ann Surg 260:356–363. https://doi.org/10.1097/SLA.0000000000000470
43. del Chiaro M, Ateeb Z, Hansson MR, et al (2017) Survival Analysis and Risk for Progression of Intraductal Papillary Mucinous Neoplasia of the Pancreas (IPMN) Under Surveillance: A Single-Institution Experience. Ann Surg Oncol 24:1120–1126. https://doi.org/10.1245/s10434-016-5661-x
44. Yamaguchi K, Kanemitsu S, Hatori T, et al (2011) Pancreatic ductal adenocarcinoma derived from IPMN and pancreatic ductal adenocarcinoma concomitant with ipmn. Pancreas 40:571–580. https://doi.org/10.1097/MPA.0b013e318215010c
45. Felsenstein M, Noë M, Masica DL, et al (2018) IPMNs with co-occurring invasive cancers: Neighbours but not always relatives. Gut 67:1652–1662. https://doi.org/10.1136/gutjnl-2017-315062

46. Sharib JM, Fonseca AL, Swords DS, et al (2018) Surgical overtreatment of pancreatic intraductal papillary mucinous neoplasms: Do the 2017 International Consensus Guidelines improve clinical decision making? Surgery (United States) 164:1178–1184. https://doi.org/10.1016/j.surg.2018.07.014
47. Jan I-S, Chang M-C, Yang C-Y, et al (2020) Validation of Indications for Surgery of European Evidence-Based Guidelines for Patients with Pancreatic Intraductal Papillary Mucinous Neoplasms. Journal of Gastrointestinal Surgery 24:2536–2543. https://doi.org/10.1007/s11605-019-04420-9
48. Springer S, Masica DL, Dal Molin M, et al (2019) A multimodality test to guide the management of patients with a pancreatic cyst. Sci Transl Med 11:eaav4772. https://doi.org/10.1126/scitranslmed.aav4772
49. Goggins M, Overbeek KA, Brand R, et al (2020) Management of patients with increased risk for familial pancreatic cancer: updated recommendations from the International Cancer of the Pancreas Screening (CAPS) Consortium. Gut 69:7–17. https://doi.org/10.1136/gutjnl-2019-319352
50. Canto MI, Hruban RH, Fishman EK, et al (2012) Frequent detection of pancreatic lesions in asymptomatic high-risk individuals. Gastroenterology 142:796–804. https://doi.org/10.1053/j.gastro.2012.01.005
51. Canto MI, Almario JA, Schulick RD, et al (2018) Risk of Neoplastic Progression in Individuals at High Risk for Pancreatic Cancer Undergoing Long-term Surveillance. Gastroenterology 155:740-751.e2. https://doi.org/10.1053/j.gastro.2018.05.035
52. Dbouk M, Katona BW, Brand RE, et al (2022) The Multicenter Cancer of Pancreas Screening Study: Impact on Stage and Survival. Journal of Clinical Oncology. https://doi.org/10.1200/JCO.22.00298
53. Overbeek KA, Goggins MG, Dbouk M, et al (2022) Timeline of Development of Pancreatic Cancer and Implications for Successful Early Detection in High-Risk Individuals. Gastroenterology 162:772-785.e4. https://doi.org/10.1053/j.gastro.2021.10.014
54. Chhoda A, Vodusek Z, Wattamwar K, et al (2022) Late-Stage Pancreatic Cancer Detected During High-Risk Individual Surveillance: A Systematic Review and Meta-Analysis. Gastroenterology 162:786–798. https://doi.org/10.1053/j.gastro.2021.11.021
55. Sainani NI, Saokar A, Deshpande V, et al (2009) Comparative performance of MDCT and MRI with MR cholangiopancreatography in characterizing small pancreatic cysts. American Journal of Roentgenology 193:722–731. https://doi.org/10.2214/AJR.08.1253
56. Waters JA, Schmidt CM, Pinchot JW, et al (2008) CT vs MRCP: Optimal classification of IPMN type and extent. In: Journal of Gastrointestinal Surgery. J Gastrointest Surg, pp 101–109
57. Nougaret S, Reinhold C, Chong J, et al (2014) Incidental pancreatic cysts: natural history and diagnostic accuracy of a limited serial pancreatic cyst MRI protocol. Eur Radiol 24:1020–9. https://doi.org/10.1007/s00330-014-3112-2
58. McDonald RJ, Levine D, Weinreb J, et al (2018) Gadolinium Retention: A Research Roadmap from the 2018 NIH/ACR/RSNA Workshop on Gadolinium Chelates. Radiology 289:517–534. https://doi.org/10.1148/radiol.2018181151
59. Kartalis N, Lindholm TL, Aspelin P, et al (2009) Diffusion-weighted magnetic resonance imaging of pancreas tumours. Eur Radiol 19:1981–1990. https://doi.org/10.1007/s00330-009-1384-8
60. Kawakami S, Fukasawa M, Shimizu T, et al (2019) Diffusion-weighted image improves detectability of magnetic resonance cholangiopancreatography for pancreatic ductal adenocarcinoma concomitant with intraductal papillary mucinous

neoplasm. Medicine (United States) 98:. https://doi.org/10.1097/MD.0000000000018039
61. Donati F, Casini C, Cervelli R, et al (2021) Diffusion-weighted MRI of solid pancreatic lesions: Comparison between reduced field-of-view and large field-of-view sequences. Eur J Radiol 143:109936. https://doi.org/10.1016/j.ejrad.2021.109936
62. Corral JE, Das A, Bruno MJ, Wallace MB (2019) Cost-effectiveness of Pancreatic Cancer Surveillance in High-Risk Individuals: An Economic Analysis. Pancreas 48:526–536. https://doi.org/10.1097/MPA.0000000000001268
63. Correa-Gallego C, Ferrone CR, Thayer SP, et al (2010) Incidental pancreatic cysts: do we really know what we are watching? Pancreatology 10:144–150. https://doi.org/10.1159/000243733
64. Salvia R, Malleo G, Marchegiani G, et al (2012) Pancreatic resections for cystic neoplasms: from the surgeon's presumption to the pathologist's reality. Surgery 152:S135-42. https://doi.org/10.1016/j.surg.2012.05.019
65. del Chiaro M, Segersvärd R, Pozzi Mucelli R, et al (2014) Comparison of preoperative conference-based diagnosis with histology of cystic tumors of the pancreas. Ann Surg Oncol 21:1539–44. https://doi.org/10.1245/s10434-013-3465-9
66. Choi SY, Kim JH, Yu MH, et al (2017) Diagnostic performance and imaging features for predicting the malignant potential of intraductal papillary mucinous neoplasm of the pancreas: a comparison of EUS, contrast-enhanced CT and MRI. Abdominal Radiology 42:1449–1458. https://doi.org/10.1007/S00261-017-1053-3/TABLES/4
67. Uribarri-Gonzalez L, Keane MG, Pereira SP, et al (2018) Agreement among Magnetic Resonance Imaging/Magnetic Resonance Cholangiopancreatography (MRI-MRCP) and Endoscopic Ultrasound (EUS) in the evaluation of morphological features of Branch Duct Intraductal Papillary Mucinous Neoplasm (BD-IPMN). Pancreatology. https://doi.org/10.1016/j.pan.2018.01.002
68. Siegel A, Friedman M, Feldman D, et al (2022) Concordance of EUS and MRI/MRCP findings among high-risk individuals undergoing pancreatic cancer screening. Pancreatology. https://doi.org/10.1016/J.PAN.2022.07.015
69. Aghaei Lasboo A, Rezai P, Yaghmai V (2010) Morphological analysis of pancreatic cystic masses. Acad Radiol 17:348–351. https://doi.org/10.1016/j.acra.2009.09.013
70. Smith MT, Vermeulen R, Li G, et al (2005) Use of "Omic" technologies to study humans exposed to benzene. Chem Biol Interact 153–154:123–127. https://doi.org/10.1016/J.CBI.2005.03.017
71. Papanikolaou N, Matos C, Koh DM (2020) How to develop a meaningful radiomic signature for clinical use in oncologic patients. Cancer Imaging 20:1–10. https://doi.org/10.1186/s40644-020-00311-4
72. Shur JD, Doran SJ, Kumar S, et al (2021) Radiomics in oncology: A practical guide. Radiographics 41:1717–1732. https://doi.org/10.1148/RG.2021210037/SUPPL_FILE/RG210037SUPPA1.PDF
73. Xie H, Ma S, Guo X, et al (2020) Preoperative differentiation of pancreatic mucinous cystic neoplasm from macrocystic serous cystic adenoma using radiomics: Preliminary findings and comparison with radiological model. Eur J Radiol 122:. https://doi.org/10.1016/j.ejrad.2019.108747
74. Polk SL, Choi JW, McGettigan MJ, et al (2020) Multiphase computed tomography radiomics of pancreatic intraductal papillary mucinous neoplasms to predict malignancy. World J Gastroenterol 26:3458–3471. https://doi.org/10.3748/wjg.v26.i24.3458
75. Shen X, Yang F, Yang P, et al (2020) A Contrast-Enhanced Computed Tomography Based Radiomics Approach for Preoperative Differentiation of Pancreatic Cystic

Neoplasm Subtypes: A Feasibility Study. Front Oncol 10:248. https://doi.org/10.3389/fonc.2020.00248
76. Chakraborty J, Midya A, Gazit L, et al (2018) CT Radiomics to Predict High Risk Intraductal Papillary Mucinous Neoplasms of the Pancreas HHS Public Access. Med Phys 45:5019–5029. https://doi.org/10.1002/mp.13159
77. Tobaly D, Santinha J, Sartoris R, et al (2020) CT-based radiomics analysis to predict malignancy in patients with intraductal papillary mucinous neoplasm (IPMN) of the pancreas. Cancers (Basel) 12:1–19. https://doi.org/10.3390/cancers12113089
78. Cui S, Tang T, Su Q, et al (2021) Radiomic nomogram based on MRI to predict grade of branching type intraductal papillary mucinous neoplasms of the pancreas: a multicenter study. Cancer Imaging 21:. https://doi.org/10.1186/s40644-021-00395-6
79. Horton J (2002) Principles of biomedical ethics: Fifth edition. T. L. Beauchamp & J. F. Childress. New York: Oxford University Press, 2001. xiv+454pp. Price £19.95. ISBN 0-19-514332-9. Trans R Soc Trop Med Hyg 96:107
80. Tanaka M, Chari S, Adsay V, et al (2006) International consensus guidelines for management of intraductal papillary mucinous neoplasms and mucinous cystic neoplasms of the pancreas. Pancreatology 6:17–32. https://doi.org/10.1159/000090023
81. del Chiaro M, Verbeke C, Salvia R, et al (2013) European experts consensus statement on cystic tumours of the pancreas. Dig Liver Dis 45:703–711. https://doi.org/10.1016/j.dld.2013.01.010
82. Pozzi Mucelli RM, Moro CF, del Chiaro M, et al (2022) Branch-duct intraductal papillary mucinous neoplasm (IPMN): Are cyst volumetry and other novel imaging features able to improve malignancy prediction compared to well-established resection criteria? Eur Radiol. https://doi.org/10.1007/s00330-022-08650-5
83. MedSeg Free Medical Segmentation Online. https://www.medseg.ai/
84. World Health Organization (2014) World Health Statistics 2014. Geneva. Available via http://apps.who.int/iris/bitstream/handle/10665/112738/9789240692671_eng.pdf?sequence=1)
85. Cronbach LJ (1951) Coefficient alpha and the internal structure of tests. Psychometrika 1951 16:3 16:297–334. https://doi.org/10.1007/BF02310555
86. Shrout PE, Fleiss JL (1979) Intraclass correlations: uses in assessing rater reliability. Psychol Bull 86:420–428. https://doi.org/10.1037//0033-2909.86.2.420
87. Knoke D, Bohrnstedt G (1991) Basic Social Statistics. F E Peacock Publishers, Inc
88. Yu CH (2005) Test–Retest Reliability. Encyclopedia of Social Measurement 777–784. https://doi.org/10.1016/B0-12-369398-5/00094-3
89. van Griethuysen JJM, Fedorov A, Parmar C, et al (2017) Computational radiomics system to decode the radiographic phenotype. Cancer Res 77:e104–e107. https://doi.org/10.1158/0008-5472.CAN-17-0339
90. Sun X, Xu W (2014) Fast implementation of DeLong's algorithm for comparing the areas under correlated receiver operating characteristic curves. IEEE Signal Process Lett 21:1389–1393. https://doi.org/10.1109/LSP.2014.2337313
91. Jafari M, Ansari-Pour N (2019) Why, When and How to Adjust Your P Values? Citation: Jafari M, Ansari-Pour N. Why, When and how to adjust your P values? Cell Journal(Yakhteh) 20:604–607. https://doi.org/10.22074/cellj.2019.5992
92. Benjamini Y, Hochberg Y (1995) Controlling the False Discovery Rate - a Practical and Powerful Approach to Multiple Testing. Journal of The Royal Statistical Society Series B-Statistical Methodology 57:289–300. https://doi.org/10.1111/j.2517-6161.1995.tb02031.x
93. Lundberg SM, Allen PG, Lee S-I (2017) A Unified Approach to Interpreting Model Predictions. ArXiv 1–10. https://doi.org/10.48550/ARXIV.1705.07874

94. Dunn DP, Brook OR, Brook A, et al (2016) Measurement of pancreatic cystic lesions on magnetic resonance imaging: efficacy of standards in reducing inter-observer variability. Abdominal Radiology 41:500–507. https://doi.org/10.1007/s00261-015-0588-4
95. Macari M, Lee T, Kim S, et al (2009) Is gadolinium necessary for MRI follow-up evaluation of cystic lesions in the pancreas? Preliminary results. AJR Am J Roentgenol 192:159–64. https://doi.org/10.2214/AJR.08.1068
96. Johansson K, Mustonen H, Nieminen · Heini, et al (2022) MRI follow-up for pancreatic intraductal papillary mucinous neoplasm: an ultrashort versus long protocol Graphical abstract Keywords Pancreatic intraductal neoplasms · IPMN · MRI · Abbreviated protocol. 47:727–737. https://doi.org/10.1007/s00261-021-03382-4
97. Murayama S, Kimura W, Hirai I, et al (2011) Volumetric and morphological analysis of intraductal papillary mucinous neoplasm of the pancreas using computed tomography and magnetic resonance imaging. Pancreas 40:876–882. https://doi.org/10.1097/MPA.0b013e31821fdcff
98. Pandey P, Pandey A, Varzaneh FN, et al (2018) Are pancreatic IPMN volumes measured on MRI images more reproducible than diameters? An assessment in a large single-institution cohort. Eur Radiol 28:2790–2800. https://doi.org/10.1007/s00330-017-5268-z
99. Ateeb Z, Valente R, Pozzi-Mucelli RM, et al (2019) Main pancreatic duct dilation greater than 6 mm is associated with an increased risk of high-grade dysplasia and cancer in IPMN patients. Langenbecks Arch Surg 404:. https://doi.org/10.1007/s00423-018-1740-8
100. Ricci C, Casadei R, Taffurelli G, et al (2016) Risk factors for malignancy of branch-duct intraductal papillary mucinous neoplasms a critical evaluation of the fukuoka guidelines with a systematic review and meta-analysis. Pancreas 45:1243–1254. https://doi.org/10.1097/MPA.0000000000000642
101. Sun Y, Wong AKC, Kamel MS (2009) Classification of Imbalanced Data: a Review. Intern J Pattern Recognit Artif Intell 23:687–719. https://doi.org/10.1142/S0218001409007326
102. Chalkidou A, O'doherty MJ, Marsden PK (2015) False Discovery Rates in PET and CT Studies with Texture Features: A Systematic Review. https://doi.org/10.1371/journal.pone.0124165
103. Permuth JB, Choi J, Balarunathan Y, et al (2016) Combining radiomic features with a miRNA classifier may improve prediction of malignant pathology for pancreatic intraductal papillary mucinous neoplasms. Oncotarget 7:85785–85797. https://doi.org/10.18632/oncotarget.11768
104. Dbouk M, Brewer Gutierrez OI, Lennon AM, et al (2021) Guidelines on management of pancreatic cysts detected in high-risk individuals: An evaluation of the 2017 Fukuoka guidelines and the 2020 International Cancer of the Pancreas Screening (CAPS) consortium statements. Pancreatology 21:613–621. https://doi.org/10.1016/j.pan.2021.01.017
105. Kogekar N, Diaz KE, Weinberg AD, Lucas AL (2020) Surveillance of high-risk individuals for pancreatic cancer with EUS and MRI: A meta-analysis: Pancreatic Cancer Surveillance Meta-Analysis. Pancreatology 20:1739–1746. https://doi.org/10.1016/j.pan.2020.10.025
106. Vasen H, Ibrahim I, Robbers K, et al (2016) Benefit of surveillance for pancreatic cancer in high-risk individuals: Outcome of long-term prospective follow-up studies from three European expert centers. Journal of Clinical Oncology 34:2010–2019. https://doi.org/10.1200/JCO.2015.64.0730

107. Klatte DCF, Boekestijn B, Wasser MNJM, et al (2022) Pancreatic Cancer Surveillance in Carriers of a Germline CDKN2A Pathogenic Variant: Yield and Outcomes of a 20-Year Prospective Follow-Up . Journal of Clinical Oncology. https://doi.org/10.1200/JCO.22.00194
108. Ludwig E, Olson SH, Bayuga S, et al (2011) Feasibility and yield of screening in relatives from familial pancreatic cancer families. Am J Gastroenterol 106:946–954. https://doi.org/10.1038/ajg.2011.65
109. Potjer TP, Schot I, Langer P, et al (2013) Variation in precursor lesions of pancreatic cancer among high-risk groups. Clinical Cancer Research 19:442–449. https://doi.org/10.1158/1078-0432.CCR-12-2730
110. del Chiaro M, Verbeke CS, Kartalis N, et al (2015) Short-term results of a magnetic resonance imaging-based Swedish screening program for individuals at risk for pancreatic cancer. JAMA Surg 150:512–518. https://doi.org/10.1001/jamasurg.2014.3852
111. Harinck F, Konings ICAW, Kluijt I, et al (2016) A multicentre comparative prospective blinded analysis of EUS and MRI for screening of pancreatic cancer in high-risk individuals. Gut 65:1505–1513. https://doi.org/10.1136/gutjnl-2014-308008
112. Sah RP, Sharma A, Nagpal S, et al (2019) Phases of Metabolic and Soft Tissue Changes in Months Preceding a Diagnosis of Pancreatic Ductal Adenocarcinoma. Gastroenterology 156:1742–1752. https://doi.org/10.1053/j.gastro.2019.01.039
113. Chari ST, Leibson CL, Rabe KG, et al (2008) Pancreatic Cancer-Associated Diabetes Mellitus: Prevalence and Temporal Association With Diagnosis of Cancer. Gastroenterology 134:95–101. https://doi.org/10.1053/j.gastro.2007.10.040
114. O'neill RS, Stoita A (2021) Biomarkers in the diagnosis of pancreatic cancer: Are we closer to finding the golden ticket? World J Gastroenterol 27:4045–4087. https://doi.org/10.3748/wjg.v27.i26.4045
115. Yang M, Zhang C-Y, Fellow P (2021) Diagnostic biomarkers for pancreatic cancer: An update. World J Gastroenterol 27:7862–7865. https://doi.org/10.3748/wjg.v27.i45.7862
116. Kartal E, Schmidt TSB, Molina-Montes E, et al (2022) A faecal microbiota signature with high specificity for pancreatic cancer. Gut 71:1359–1372. https://doi.org/10.1136/gutjnl-2021-324755
117. Kierans AS, Gavlin · Alexander, Wehrli N, et al (2022) Utility of gadolinium for identifying the malignant potential of pancreatic cystic lesions. Abdominal Radiology 47:1351–1359. https://doi.org/10.1007/s00261-022-03446-z